The Role of Endothelial Cell Metabolic Reprogramming in Diabetes-impaired Angiogenesis

KHALIA PRIMER

A thesis submitted to fulfil requirements for the degree of

Doctor of Philosophy

Faculty of Health and Medical Sciences

Adelaide Medical School

The University of Adelaide

December, 2022

THE UNIVERSITY
of ADELAIDE

Table of Contents

Abstract

An impairment to ischaemia-driven angiogenesis underpins the development of many vascular complications in patients with diabetes. Angiogenesis is driven by endothelial cells, and to develop new therapies that can effectively support endothelial cell function and stimulate angiogenesis in the diabetic context, we need to understand more about how diabetes affects these cells and identify new essential pathways that can be therapeutically targeted. The role of mitochondrial respiration in diabetes-impaired angiogenesis has not previously been examined, and may play an important role in endothelial cell function. The PDK4/PDC axis represents one critical point at which mitochondrial respiration can be regulated, but little is known about its role in angiogenesis.

The overarching aim of this thesis is to characterise the role of the PDK4/PDC axis in endothelial cell angiogenesis, determine the effect of diabetes upon the axis, and assess the efficacy of targeting the axis as a potential therapeutic strategy for diabetic vascular complications.

The studies conducted in this thesis have characterised, for the first time, a highly context-specific and essential role for the PDK4/PDC axis and mitochondrial respiration in diabetes-impaired angiogenesis. Disruption of the axis by siRNA-mediated PDK4 knockdown impaired endothelial cell function including angiogenesis and migration, and high glucose exposure *in vitro* and hyperglycaemia *in vivo* impaired the induction of the PDK4/PDC axis in response to hypoxia. Overexpression of PDK4 and suppression of mitochondrial respiration rescued high glucose-impaired endothelial cell angiogenesis. rHDL also rescued diabetes-impaired angiogenesis in parallel with correction of the PDK4 response to hypoxia, and using siRNA knockdown the PDK4/PDC axis was found to be essential for these pro-angiogenic effects. Consistent with the effects of PDK4 overexpression *in vitro*, endothelial-specific, inducible overexpression of PDK4 by lentiviral gene transfer *in vivo* significantly enhanced wound

angiogenesis and healing. Collectively, these data support our hypothesis that the PDK4/PDC axis plays a critical role in endothelial cell angiogenesis, and that diabetes impairs the integrity of the axis. Restoration of the PDK4/PDC axis, using either rHDL treatment or PDK4 overexpression, improved endothelial cell angiogenesis under high glucose conditions *in vitro*, and improved wound angiogenesis and healing in diabetic mice.

In conclusion, endothelial cell metabolic reprogramming through the PDK4/PDC axis plays a critical role in endothelial cell angiogenic function, and shows promise as a novel therapeutic target in the treatment of diabetic vascular complications.

Declaration of Originality

I certify that this work contains no material which has been accepted for the award of any other degree or diploma in my name in any university or other tertiary institution and, to the best of my knowledge and belief, contains no material previously published or written by another person, except where due reference has been made in the text. In addition, I certify that no part of this work will, in the future, be used in a submission in my name for any other degree or diploma in any university or other tertiary institution without the prior approval of the University of Adelaide and where applicable, any partner institution responsible for the joint award of this degree.

The author acknowledges that copyright of published works contained within this thesis resides with the copyright holder(s) of those works.

I give permission for the digital version of my thesis to be made available on the web, via the University's digital research repository, the Library Search and also through web search engines, unless permission has been granted by the University to restrict access for a period of time.

I acknowledge the support I have received for my research through the provision of an Australian Government Research Training Program Scholarship.

Khalia Primer

29th December, 2022

Statement of Authorship

Parts of Chapter 1 of this thesis have been published as a review article: Primer, KR, Psaltis, PJ, Tan, JTM, Bursill, CA 2020, 'The Role of High-density Lipoproteins in Endothelial Cell Metabolism and Diabetes-impaired Angiogenesis', *International Journal of Molecular Sciences,* vol. 21, no. 10, pp. 3633. I completed the literature review and wrote this manuscript.

Chapter 4 of this thesis has been prepared for publication as an original research article and is currently in submission: Primer KR, Tan JTM, Psaltis PJ, and Bursill CA, "Diabetes impairs endothelial cell metabolic reprogramming and angiogenic responses to hypoxia, which are rescued by reconstituted high-density lipoproteins (rHDL)". I completed all the experimental work, performed all the data analysis, and wrote the manuscript.

Acknowledgements

When I started this PhD, I wondered how I would feel at the end. Would I feel burnt out, disillusioned, or frustrated with research? Would I still feel that ping of excitement at having connected two new ideas? Find joy in designing and completing experiments? Would I want to leave research? Stay? I remember feeling annoyed that I couldn't peer into the future and just *know* how it was all going to pan out so I could keep making plans for what might come next. Well, I'm here, in the future, and the one thing I can tell you is that I now know that this isn't the "end" (obviously!).

Over the last four years I've learnt a lot about being a scientist, but I've also learnt a lot about being a person. I've spent some of my most formative early-adult years working on this PhD at SAHMRI, and it's strange to reflect on how much has happened in that short time. This PhD and the people I've worked with over its course have taught me patience, resilience, and to value the responsibility that comes with seeking new knowledge about our world.

My primary supervisor Associate Professor Christina Bursill has taught me how to think creatively about problems, and has trusted me to try new ideas and techniques. She's helped me stick to deadlines, encouraged me to step outside my comfort zone, and been a consistent, supportive presence. My secondary supervisor Dr Joanne Tan, among many other things, has taught me to inspect my work with a fine-toothed comb, though I don't think I'll ever be as good at it as her! Both Chris and Jo have given me valuable examples of what it means to be a scientist, and have given me the tools and knowledge I need for the next stage of my career.

When I started my Honours year, there were a few senior PhD students in the lab who made me think, "I want to be just like them when I grow up!". Emma, Sanuja, Jocelyne, and Anna – you all approached your work differently but each of you made a big impression on me, and I feel so lucky to have had you around in those early months.

To my fellow PhD students: Jake, Sanuri, Victoria, Ben, Zahra, and Emma – what an experience these last few years have been. I don't think I could have gotten through this without all of you there to debrief, vent, ask silly questions of, etc. I'm so proud of how each of you has approached the unique challenges that came with your projects, and so excited to see what each of you does next.

Emma, you'd started with Chris and Jo as a research assistant only a few months before I started my Honours year in 2018, but it seemed like you knew the answer to every question I had (and I had a lot!). Thank you for teaching me so much, and for being a wonderful example of a fantastic scientist and an amazing person.

Thalia and Lauren – the lab would literally not be functioning today without you. You're both so thoughtful and competent, and we have been incredibly lucky to have you both. Special mention to Lauren (my next-door desk neighbour) for happily listening to whatever random thoughts I was having at any given time, even though you were certainly very busy.

To all the members of the Vascular Research Centre family past, and present: I could not have done this without you.

Conference Presentations

Oral Presentations

Primer KR, Psaltis PJ, Tan JTM, Bursill CA, "Pyruvate Dehydrogenase Kinase 4 Is A Novel Regulator of Endothelial Cell Mitochondrial Respiration in Diabetes-impaired Angiogenesis: Implications For Preventing Diabetic Vascular Complications", *American Heart Association Scientific Sessions, Chicago IL, 2022*

Primer KR, Psaltis PJ, Tan JTM, Bursill CA, *"*Diabetes impairs endothelial cell metabolic reprogramming and angiogenic responses to hypoxia, which are rescued by reconstituted high-density lipoproteins (rHDL)", *Cardiac Society of Australia and NZ Annual Scientific Meeting, Gold Coast QLD, 2022*

Primer KR, Psaltis PJ, Tan JTM, Bursill CA, "Targeting endothelial cell metabolic reprogramming to enhance new blood vessel growth in diabetes.", *SAHMRI Research Showcase, Adelaide SA, 2021*

Primer KR, Psaltis PJ, Tan JTM, Bursill CA, "Investigating pyruvate dehydrogenase kinase 4 as a novel regulator of endothelial cell mitochondrial respiration in diabetes-impaired angiogenesis.", *Australasian Diabetes Congress, Virtual, 2021*

Primer KR, Psaltis PJ, Tan JTM, Bursill CA, "Investigating pyruvate dehydrogenase kinase 4 as a novel regulator of endothelial cell mitochondrial respiration in diabetes-impaired angiogenesis.", *Cardiac Society of Australia and NZ Annual Scientific Meeting, Virtual, 2020*

Primer KR, Tan JTM, Bursill CA, "The "Good Cholesterol" Rescues Diabetes-impaired Wound Healing via Improved Responses to Hypoxia", *CNBP Annual Scientific Meeting, Virtual, 2020*

Primer KR, Solly E, Psaltis PJ, Tan JTM, Bursill CA, "High-density lipoproteins rescue diabetes-impaired angiogenesis by restoring cellular metabolic reprogramming responses to hypoxia.", *SAHMRI Annual Research Showcase, Adelaide SA, 2019*

Primer KR, Solly E, Psaltis PJ, Tan JTM, Bursill CA, "High-density lipoproteins rescue diabetes-impaired angiogenesis by restoring cellular metabolic reprogramming responses to hypoxia.", *Cardiac Society of Australia and NZ Annual Scientific Meeting, Adelaide SA, 2019*

Primer KR, Solly E, Psaltis PJ, Tan JTM, Bursill CA, "High-density lipoproteins rescue diabetes-impaired angiogenesis by restoring cellular metabolic reprogramming responses to hypoxia.", *Australian Society for Medical Research Annual Scientific Meeting, Adelaide SA, 2019*

Primer KR, Solly E, Psaltis PJ, Tan JTM, Bursill CA, "High-density lipoproteins rescue diabetes-impaired angiogenesis by restoring cellular metabolic reprogramming responses to hypoxia.", *Australian Atherosclerosis Society Annual Scientific Meeting, Melbourne VIC, 2019*

Poster Presentations

Primer KR, Psaltis PJ, Tan JTM, Bursill CA, "Investigating pyruvate dehydrogenase kinase 4 as a novel regulator of endothelial cell mitochondrial respiration in diabetes-impaired angiogenesis.", *Florey Postgraduate Conference, Virtual, 2020*

Primer KR, Solly E, Psaltis PJ, Tan JTM, Bursill CA, "High-density lipoproteins rescue diabetes-impaired angiogenesis by restoring cellular metabolic reprogramming responses to hypoxia.", *Australian Atherosclerosis Society Annual Scientific Meeting, Melbourne VIC, 2019*

Publications Arising from this Thesis

Primer, KR, Psaltis, PJ, Tan, JTM, Bursill, CA 2022, 'rHDL Rescues Diabetes-impaired Regulation of the PDK4/PDC axis, a Mechanism of Endothelial Cell Metabolic Reprogramming', *in submission.*

Primer, KR, Psaltis, PJ, Tan, JTM, Bursill, CA 2020, 'The Role of High-density Lipoproteins in Endothelial Cell Metabolism and Diabetes-impaired Angiogenesis', *International Journal of Molecular Sciences,* vol. 21, no. 10, pp. 3633.

Awards

Finalist – ATVB Elaine W. Raines Early Career Investigator Award, *American Heart Association Scientific Sessions, Chicago IL, 2022*

Finalist – Ralph Reader Basic & Translational Science Prize, *Cardiac Society of Australia & NZ Annual Scientific Meeting, Gold Coast QLD, 2022*

Finalist – Best Early-Career Researcher Presentation Award, *SAHMRI Annual Research Showcase, Adelaide SA, 2021*

Winner – Australian Diabetes Society Pincus Taft Young Investigator Award, *Australasian Diabetes Congress, Virtual, 2021*

Finalist – ISHR Student Investigator Prize, *Cardiac Society of Australia and NZ/International Society for Heart Research Annual Scientific Meeting, Virtual, 2020*

Winner – First Place Award, Student's Choice Award, and People's Choice Award, *University of Adelaide 3MT Final, Virtual, 2020*

Winner – First Place Award, *Faculty of Health and Medical Sciences 3MT Competition, University of Adelaide, Virtual, 2020*

Winner – Best Presenter Prize for the "Cardiovascular to Wound" Session, *CNBP Annual Scientific Meeting, Virtual, 2020*

Winner – Best 3 Minute Thesis Presentation Award, *SAHMRI Annual Research Showcase, Adelaide SA, 2019*

Winner – Best Mini-Oral Presentation Award, *Cardiac Society of Australia and NZ/International Society for Heart Research Annual Scientific Meeting, Adelaide SA, 2019*

Winner – Most Outstanding PhD Oral Presentation Award, *Australian Society of Medical Research Annual Scientific Meeting, Adelaide SA, 2019*

1. Introduction

1.1. Diabetes and its Vascular Complications

1.1.1. Diabetes mellitus

Diabetes mellitus (DM) is one of the most debilitating and prevalent diseases in the world and imposes a significant health and economic burden upon the global community. In 2017, diabetes was reported to affect 425 million people worldwide. This number is expected to reach 629 million by 2045 [1]. Worldwide healthcare expenditure on diabetes tops 850 billion USD, and this is predicted to leap to 958 billion USD by 2045. DM is a metabolic disorder characterised by insulin insufficiency or insensitivity, and a dysregulation of blood glucose levels.

DM is strongly associated with a diverse range of vascular complications, which are pathologies that are caused by dysfunctional blood vessels. These complications are broadly divided into two categories: micro- and macrovascular complications. The microvascular complications of diabetes include retinopathy, nephropathy, and neuropathy, while the macrovascular complications include ischaemic heart disease, peripheral artery disease, and cerebrovascular disease. Impaired cutaneous wound healing and the development of diabetic foot ulcers can also be considered a vascular complication of diabetes due to its close association with neuropathy, peripheral artery disease, and microvascular dysfunction in the wound environment. Cardiovascular disease, which encompasses ischaemic heart disease and the associated complications such as myocardial infarction and stroke, is the leading cause of death in people with DM.

1.1.2. Type 1 diabetes

Type 1 diabetes is primarily caused by autoimmune-induced destruction of pancreatic B-cell islets, leading to an impairment to insulin production. The associated insulin deficiency means

that people with T1D experience potentially life-threatening dysregulation of their blood glucose levels, and must administer exogenous insulin to prevent ketoacidosis [2]. The exact cause of type 1 diabetes has yet to be fully elucidated, but the consensus is that both genetic and environmental factors play a role. It is commonly diagnosed during adolescence, and is the most common chronic disease in children [2]. Treatment strategies for type 1 diabetes focus on glucose monitoring and insulin administration.

Although the underlying cause of blood glucose level disturbance is predominantly genetic rather than environmental, people with type 1 diabetes experience similar microvascular and macrovascular complications to people with type 2 diabetes.

1.1.3. Type 2 diabetes

In contrast to type 1 diabetes, type 2 diabetes is caused by a progressive impairment to insulin production and a desensitisation of key metabolic tissues to insulin. This leads to a decrease in glucose utilisation which eventually causes chronic hyperglycaemia. These effects develop slowly over time, and most people with type 2 diabetes are diagnosed in their mid-life, though the prevalence of diabetes in children and adolescents is rising [3].

The increasing rates of type 2 diabetes are closely tied to increasing rates of obesity in adults and children [3]. Being overweight or obese is the single strongest predictor of developing type 2 diabetes, though there are many other established risk factors. Established non-modifiable risk factors for type 2 diabetes include age, sex, ethnicity, and a family history of type 2 diabetes [3]. Modifiable risk factors include being overweight or obese, physical inactivity, dietary factors, smoking, elevated triglyceride levels, and hypertension. Any or all of these risk factors can contribute to the development of type 2 diabetes.

Management of type 2 diabetes primarily involves modification of risk factors, with a focus on diet and exercise. If a patient is unable to achieve glycaemic targets with lifestyle modification alone, these methods of primary prevention can be accompanied by pharmacotherapy with medications such as Metformin which aid in controlling blood glucose levels.

Because cardiovascular disease is the leading cause of death for diabetic patients, assessing cardiovascular disease risk and managing this with lifestyle modification or pharmacotherapy is also a central goal for healthcare practitioners.

If a patient is deemed to be at risk of developing cardiovascular disease or any other diabetes-related vascular complications, there are various strategies that can be employed by the healthcare practitioner. Some of these strategies, such as the use of lipid-lowering medications to address the development of atherosclerosis, are well-established in clinical practice and are extremely effective in reducing a patient's risk of cardiac events. However, there are still significant gaps in the treatment of pathologies such as chronic wounds, and there exists an unmet clinical need for new therapies that address novel aspects of these complications to fully eliminate the burden they place on patients with diabetes.

1.1.4. Ischaemic heart disease

Ischaemic heart disease occurs when the coronary arteries develop atherosclerotic plaque that restricts blood flow and oxygen delivery to the myocardium (Figure 1.1). Atherosclerotic plaque develops through deposition of excess cholesterol, carried in low-density lipoproteins (LDL), in the vascular wall [4]. Macrophages attempt to remove the excess modified LDL from the vessel wall, but uncontrolled uptake causes the macrophages to become lipid-laden foam cells, which remain in the vessel wall and are inflammatory, exacerbating plaque development. Foam cells ultimately undergo apoptosis, leaving behind extracellular cholesterol and cellular debris in the plaque that coalesce to form a necrotic core that is unstable [4]. As the plaque

increases in size, smooth muscle cells migrate from the vessel wall to the top of the plaque and secrete collagen to form a stabilising fibrous cap. Over time the fibrous cap may be digested by metalloproteinases and become thinner, making it more vulnerable to rupture by mechanical forces in the vessel [5]. If an atherosclerotic plaque ruptures and releases the necrotic core contents into the bloodstream, it can induce arterial thrombosis, and the resultant thrombus may block the coronary artery completely [5]. Complete blockage of a coronary artery and starvation of the myocardium of oxygen in this way causes tissue death, which is called a myocardial infarction (MI).

To prevent an MI, patients are commonly placed on lipid-lowering medications such as statins (e.g., atorvastatin and rosuvastatin), to slow the progression of atherosclerosis. Statins lower a patient's low-density lipoprotein cholesterol (LDL-C) and therefore lower the risk of excess deposition of cholesterol that becomes occlusive in the coronary arteries. Metal scaffolds called stents are also used to prevent MI if a patient has been identified through intravascular imaging to have a significant occlusion in one or more major vessels. The stent is deployed at the site of the atherosclerotic occlusion and expanded to re-open the artery and restore blood flow to the myocardium [6]. Once a stent has been placed, patients will also be prescribed an anti-thrombotic medication such as aspirin or clopidogrel.

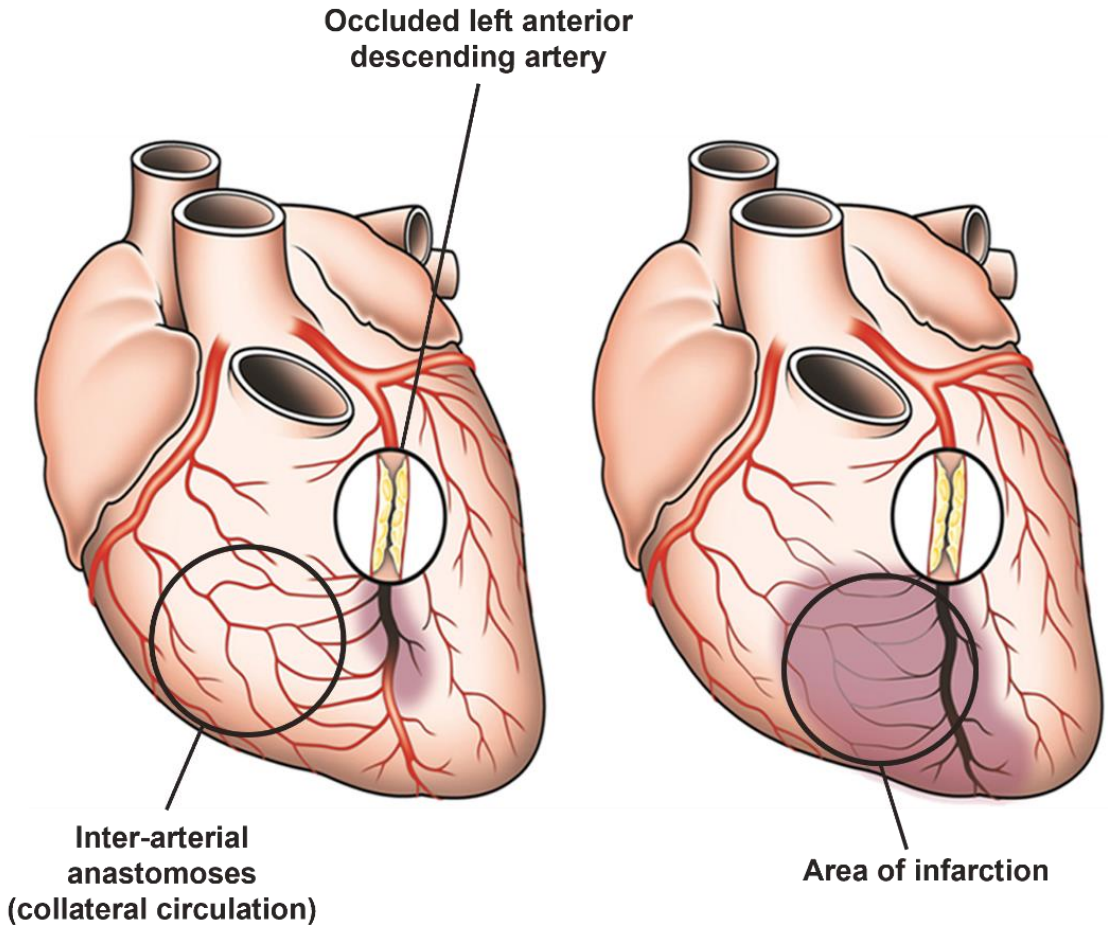

Figure 1.1. Ischaemic heart disease. Schematic of the coronary artery circulation with (left panel) and without (right panel) inter-arterial anastomoses between the right coronary artery and the occluded left anterior descending artery (LAD). The grey area indicates the area at risk for myocardial infarction in case of the LAD occlusion and in the absence of collaterals (corresponding to the infarct size in the example on the right side). (Figure adapted from Meier *et al.* 2013, illustration by Anne Wadmore, Medical Illustrations Ltd, London, UK).

Many patients will experience recurrent periods of myocardial ischaemia before an MI occurs, caused by the atherosclerotic occlusions that restrict blood flow to regions of the myocardium [7]. In response, there is an opportunity for the body to stimulate new blood vessel growth and maturation to circumvent the vessel blockage and supply extra oxygen to the myocardium. Coronary collateral vessel development in the heart is a controversial topic of discussion, as experts have yet to come to a consensus on how the vessels develop and to what extent they are clinically relevant [8]. It is generally agreed that endothelial shear stress from increased blood flow and increased monocyte recruitment are the primary stimulators of collateral expansion through arteriogenesis [8]. However, a very recent study has challenged this idea by providing key evidence that sprouting angiogenesis does contribute to coronary collateralisation. Juguilon *et al.* used a ROSA mT/mG reporter mice with an Apln-CreERT2 transgene to trace the lineage of sprouting endothelial cells, and when they induced coronary collateral formation, found that the newly formed capillaries were comprised of the $Apelin^{+}$, green fluorescent protein $(GFP)^{+}$ endothelial cells, while the pre-existing arteries and arterioles did not share this lineage [9]. This suggests that the new vessels formed through angiogenesis rather than arteriogenic expansion of existing vessels. Regardless, numerous clinical studies have reported positive associations between the extent of coronary collateral circulation and better cardiovascular outcomes. For example, a 2011 meta-analysis of 123 studies assessing the impact of coronary collateral circulation on mortality found that patients with a high degree of collateralisation showed a significantly reduced mortality rate compared to patients with low collateralisation [7].

Patients with diabetes consistently exhibit a less extensive collateral circulation than their non-diabetic counterparts. Abaci *et al.* identified this in the late 1990s, with a study of 306 diabetic patients showing that they had significantly poorer coronary collateral vessel development than non-diabetic patients [10]. In the mid-2000s, Mouquet *et al.* demonstrated that patients who

had metabolic syndrome, including key markers of insulin resistance, exhibited less developed collateral vessels [11].

There are currently no therapies routinely used in clinical practice that stimulate the growth of coronary collateral vessels, though a number have been assessed in clinical trials. Some examples of these treatments include the pharmacological activation of monocytes [12], or stimulation of shear stress using external counterpulsation [13]. Several clinical trials were conducted in the early 2000s which aimed to use recombinant VEGF protein to stimulate coronary collateral formation in patients [14]. For example, the VIVA trial (Vascular endothelial growth factor in Ischemia for Vascular Angiogenesis) administered recombinant human VEGF (rhVEGF) or a placebo to 178 patients with stable exertional angina, and performed exercise treadmill tests (ETT), angina class assessments, and quality of life assessments. They found that a high dose of rhVEGF was associated with a significant improvement in angina class 120 days after rhVEGF injection but no significant change in ETT time or angina frequency [15]. These findings were considered to be very promising, and yet many years later VEGF-based therapeutics for coronary collateral development still have not been successfully translated to clinical practice. Whilst the underlying reasons for the failure of these strategies to translate is unclear, it nevertheless highlights the continued unmet need for new approaches that stimulate blood vessel growth in the context of ischaemic heart disease to prevent MI.

1.1.5. Peripheral artery disease

PAD occurs when atherosclerotic plaque develops in the blood vessels of the lower limb. This restricts blood flow and oxygen delivery to the downstream tissues and manifests symptomatically as lower limb pain - or intermittent claudication - either with exercise or at rest depending on the severity of the occlusion [16]. If the disease progresses, it can be

associated with limb ulceration and gangrene and may ultimately lead to lower limb amputation [16, 17]. Diabetes is one of the strongest risk factors for developing PAD, and amputation associated with PAD is the leading cause of disability for people with diabetes [18].

Similar to ischaemic heart disease, management of PAD is also focused on modification of lifestyle factors, but a special emphasis is placed upon exercise and walking, since extending a patient's walking distance is strongly associated with an improvement in overall wellbeing and fewer cardiovascular events [16, 19]. In addition to lifestyle modification, lipid-lowering and anti-hypertensive medications may also be employed similarly as in the treatment of ischaemic heart disease.

PAD may be associated with more instances of intermittent ischaemia than ischaemic heart disease, since a patient is experiencing limb ischaemia every time they feel lower limb pain caused by oxygen insufficiency [16, 20]. However, although the growth of new blood vessels in response to ischaemia and their compensation for arterial occlusion is more clinically apparent in PAD than MI, there is still some debate about the origins of the collateral circulation. Similar to the coronary collateral vessels, some researchers maintain that the lower limb collateral vessels are pre-existing and simply expand via arteriogenesis in response to shear stress, yet others report that vessels form *de novo* through angiogenesis in response to ischaemia [21].

Regardless, there is once again clear evidence that a more extensive collateral circulation is protective against lower limb ischaemia. McDermott *et al.* reported that PAD patients with fewer collateral vessels performed poorly in a walking test compared to patients with more numerous collateral vessels [22]. Comparatively, an additional study by McDermott *et al.* which included 457 participants showed that more numerous collateral vessels, as identified

by magnetic resonance angiography, was associated with better performance in a walking test [23].

Not only do patients with diabetes experience higher rates of PAD than non-diabetic patients, they also develop a less extensive collateral circulation in the lower limb. A study by De Vivo *et al.* demonstrated that type 2 diabetes was significantly associated with fewer collateral vessels [20], and this effect has been replicated in preclinical studies, with diabetic mice exhibiting poorer revascularisation than non-diabetic mice in surgical models of lower-limb ischaemia [24, 25].

Therefore, PAD is another diabetic vascular complication in which there is a clear need for novel therapeutic agents that stimulate blood vessel growth to prevent further complications.

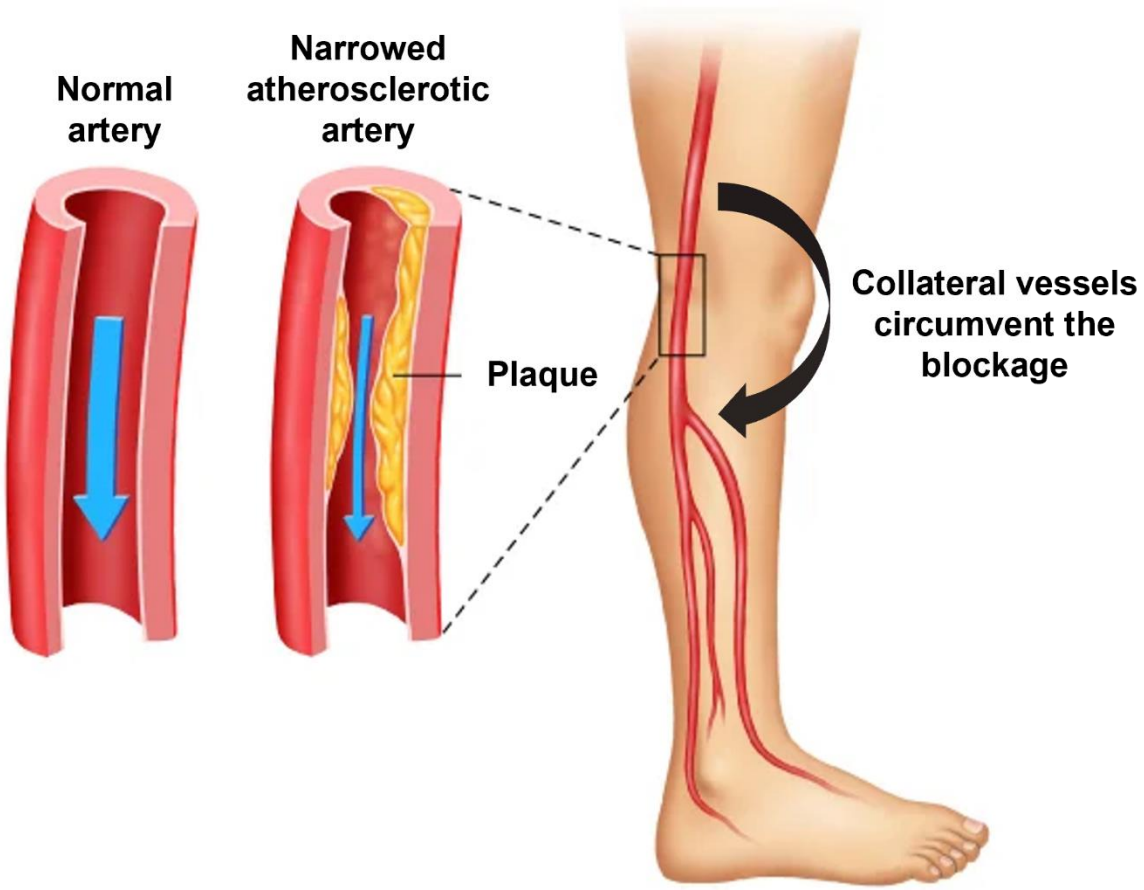

Figure 1.2. Peripheral artery disease. Schematic of a normal lower limb artery (left) and an artery containing atherosclerotic plaque which is causing narrowing (right) and reducing oxygen delivery to the distal tissue. The black arrow represents where collateral vessels may form through angiogenesis and arteriogenesis to circumvent the atherosclerotic blockage and restore blood flow to the limb.

1.1.6. Diabetic wound healing

Diabetic patients are particularly susceptible to developing persistent wounds that heal slowly and expose the patient to infection and further harm [26]. Combined with other diabetic complications, such as PAD which reduces blood flow to the lower limb and can cause peripheral neuropathy, impaired wound healing can lead to the development of diabetic foot ulcers (DFU). DFU may ultimately lead to limb necrosis and ischaemia so extensive that amputation is required [27].

The current treatment strategy for DFU primarily involves the management of the patient's co-morbidities that may contribute to ulcer development, such as glycaemic status or physical fitness. Additionally, regular dressing changes, management of infection, offloading, and debridement of the wound tissue are employed to enhance the likelihood of a DFU healing in a timely manner [28, 29]. Hyperbaric oxygen therapy may be attempted in eligible patients, and can be effective in reducing tissue hypoxia, but requires further study to fully delineate its effects [30]. Outside of these approaches, there are few effective therapies that actively improve the wound healing process.

In healthy tissue, wound healing occurs in progressive and distinct, yet overlapping stages [31] (Figure 1.3).

The first stage involves rapid haemostasis of the wound, wherein local blood vessels undergo vasoconstriction and platelets accumulate in order to stop blood flow [31]. This process is controlled by both extrinsic and intrinsic coagulation pathways, and the vasoconstriction is short-lived as it is quickly followed by inflammation-induced vasodilation which allows immune cells to more readily infiltrate the damaged tissue [31]. This influx of immune cells such as neutrophils, macrophages, and monocytes signals the beginning of the inflammatory stage.

The inflammatory stage is characterised by this influx of immune cells, which release pro-inflammatory cytokines to promote the recruitment and activation of other leukocytes [26]. Critically, neutrophils clear cellular debris and bacteria from the wound site, while macrophages clear apoptotic cells and begin to secrete factors which promote the transition into the proliferative phase of healing [26, 32].

The proliferative phase is the third and most important stage of wound healing. This stage involves regrowth of healthy epithelium and the development of new blood vessels through angiogenesis to ensure adequate oxygen and nutrient delivery to the healing tissue [33]. Signalling factors released by macrophages stimulate keratinocytes, fibroblasts, and endothelial cells [32, 34]. Keratinocytes and fibroblasts contribute to processes such as collagen deposition and re-epithelialisation, while endothelial cells undergo angiogenesis to form new capillaries. Unlike the development of collateral vessels in atherosclerotic pathologies, it is well established that wound neovessels develop through ischaemia-induced angiogenesis rather than shear stress-induced arteriogenesis [27, 35-38].

The final stage of healing is the maturation stage, which generally begins around three weeks post-wounding and can last up to twelve months [31]. Excess collagen deposited by fibroblasts begins to degrade, and the remaining collagen aligns along tension lines. Importantly, excess immature blood vessels are pruned during this stage to leave a mature vascular network. The wound also undergoes a degree of physical contraction, which is believed to be mediated by myofibroblasts [26, 31].

Patients with diabetes experience major disruptions to this normal sequence of wound healing. Most significantly, the inflammatory stage is prolonged, and the proliferative and maturation phases are stunted [35]. While the pathophysiology of DFU is complex and multifactorial, the progression of the wound to a non-healing state is closely linked to an insufficient vascular

network. This means the wounds of patients with diabetes may be more hypoxic than those of non-diabetic patients, and experience elevated levels of oxidative stress.

Diabetic wounds exhibit decreased capillary density and vascularity due to insufficient angiogenesis during the proliferative phase of healing [27, 29]. Specifically, it has been shown that in chronic diabetic wounds, the angiogenic response normally induced by tissue hypoxia is dysregulated [27, 39]. Consistent with this, pharmacological agents that inhibit angiogenesis, such as TNP-470 and SU5416, have been shown to inhibit wound repair [37, 40]. Therefore, promoting wound angiogenesis is a promising strategy for the acceleration of wound healing. This has been addressed in murine wound healing studies using pro-angiogenic agents such as vascular endothelial growth factor A (VEGFA) [36]. The promotion of angiogenesis in a chronic non-healing wound would allow for enhanced delivery of oxygen to the tissue and may mitigate the effects of oxidative stress.

Though the exact developmental origin and process of expansion of the collateral blood vessels varies across ischaemic heart disease, PAD, and wound healing, enhancement of new blood vessel growth in each of these pathologies could elicit a significant clinical benefit. In order to develop a strategy to achieve this, we must first understand the underlying mechanisms of new blood vessel growth and angiogenesis in response to ischaemia and how diabetes impairs them.

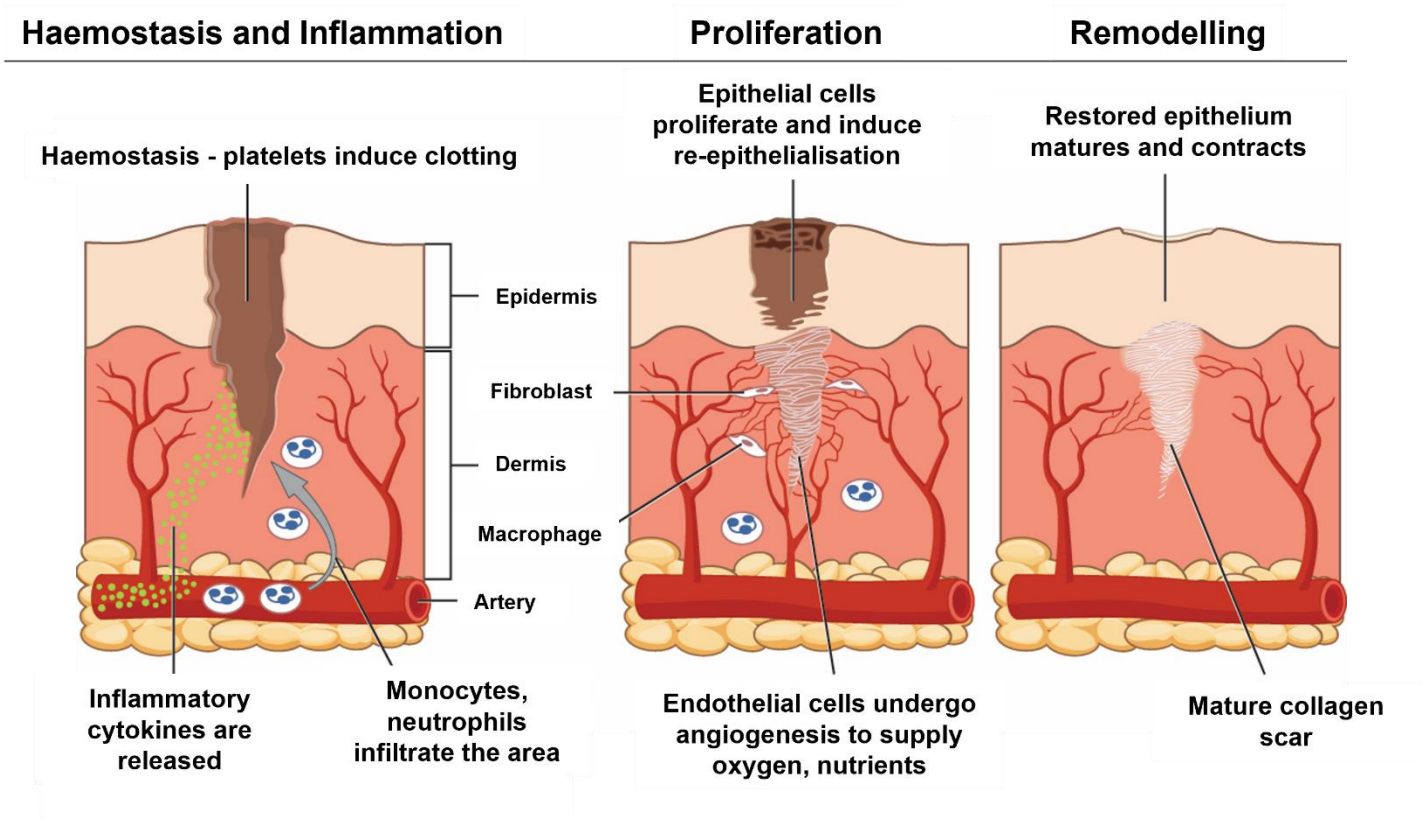

Figure 1.3. The stages of normal wound healing. Haemostasis occurs first, with platelets inducing clotting in the open wound. The inflammatory stage is initiated by the release of inflammatory cytokines, and the infiltration of immune cells like monocytes and neutrophils which clear bacteria and debris. The proliferation stage follows, where re-epithelialisation and angiogenesis occur. Finally, the remodelling stage involves the pruning and maturation of the vascular network, and maturation of the newly-deposited collagen. Figure adapted from OpenStax College.

1.2. Ischaemia-driven Angiogenesis

Physiological ischaemia-driven angiogenesis is complex and regulated by many different factors. It is the process by which new blood vessels are formed from pre-existing ones, and is initially driven by endothelial cells.

Endothelial cells are the main vessel-forming cells in angiogenesis and exist in three sub-types; migratory tip cells, proliferative stalk cells, and quiescent phalanx cells [41]. These sub-types are influenced by signalling molecules in a dynamic fashion to regulate cellular metabolism and behaviour, such as migration and proliferation.

Under normal conditions, endothelial cells are quiescent, remaining dormant in the vascular wall. This quiescence can be interrupted by a number of physiological factors to induce the shift to the migratory and proliferative phenotype that is critical for angiogenesis. One of these factors is hypoxia, and the signalling pathways that are triggered by a lack of oxygen (Figure 1.4). Hypoxia signalling is characterised by an initial decrease in the activity of the prolyl hydroxylase domain (PHD) proteins, which ordinarily utilise oxygen to target the hypoxia-inducible factors (HIF) for degradation [42]. To achieve this under normal oxygen conditions, the PHD proteins hydroxylate HIF subunits, which are then recognised by the von Hippel–Lindau (VHL) protein of the E3 ubiquitin ligase complex. The HIF subunits are then quickly degraded through the proteasomal degradation pathway [42]. Under conditions of low oxygen, the decrease in PHD protein activity allows for the HIF subunit HIF-1α to accumulate, rather than be degraded. HIF-1α then translocates from the cytosol of a cell to the nucleus and, in combination with other HIF subunits, initiates transcription of key angiogenic genes [43, 44]. Potentially the most important of these is VEGFA, which is secreted by local cells such as endothelial cells and macrophages to create a signalling molecule concentration gradient. This gradient serves to induce endothelial cell proliferation and migration and leads them to the

origin of hypoxia, and they form new blood vessels as they travel [45, 46]. In addition to this, fibroblast growth factors (FGFs) are also increased in response to hypoxia and contribute to increased endothelial cell proliferation in a similar way [47, 48].

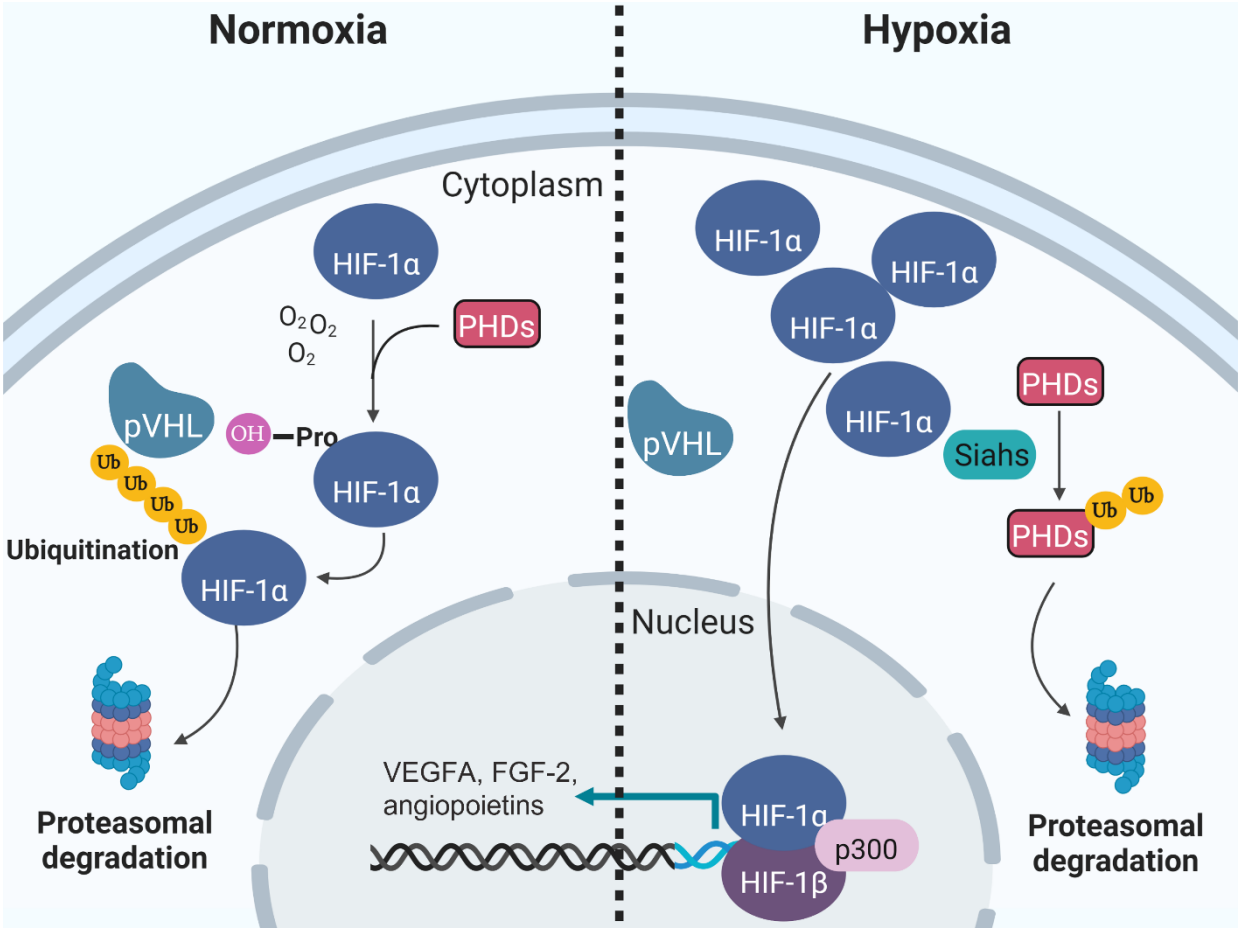

Figure 1.4. Mechanisms that drive physiological angiogenesis in hypoxia. Hypoxia-inducible factor (HIF)-1α is the central regulator of ischaemia-driven angiogenesis. In normoxia, HIF-1α is inhibited by the prolyl hydroxylase domain (PHD) proteins, which use oxygen to hydroxylate proline residues on HIF-1α, targeting it for ubiquitination and proteasomal degradation by the von Hippel-Lindau (VHL) protein complex. In hypoxia, activation of the ubiquitin ligases Siah1/2 leads to degradation of the PHDs and subsequent stabilisation of HIF-1α. This allows it to accumulate and translocate to the nucleus where it dimerises with the HIF-1β subunit, and binds to hypoxia-response elements along with the transcriptional co-factor p300. This HIF complex can upregulate numerous pro-angiogenic genes including VEGFA.

While hypoxia signalling may be the most important initiator of angiogenesis, there are many HIF-1α-independent pathways and transcription factors have also been found to be critically important in angiogenesis. These pathways alter endothelial cell function to ensure their survival in challenging environments such as ischaemic tissue.

One of these pathways involves the forkhead box O (FOXO) transcription factor, FOXO1. FOXO1 is an effector of the PI3K/Akt pathway, and its nuclear activity can be inhibited by Akt-mediated phosphorylation. Wilhelm *et al.* demonstrated that FOXO1 acts as an enforcer of endothelial cell quiescence and that its deletion in mice causes an uncontrolled increase in vessel sprouting. Contrastingly, its overexpression severely restricted angiogenesis and led to vessel thinning [49].

Another important factor is peroxisome proliferator-activated receptor gamma coactivator 1-alpha (PGC-1α). PGC-1α is well-recognised as a central modulator of cellular metabolism and mitochondrial biogenesis. In muscle cells, PGC-1α has also been shown to potently upregulate VEGF under hypoxic conditions in a mechanism that is independent of HIF-1α. Arany *et al.* demonstrated this by exposing cultured muscle cells to a low oxygen environment. This induced the expression of PGC-1α, which then coactivated oestrogen-related receptor-α (ERR-α) on the VEGF promoter, leading to increased expression of VEGF and promotion of capillary density in skeletal muscle. This identified a role for PGC-1α in the regulation of angiogenic signalling, potentially in connection with its role in metabolism [50].

FOXO1 and PGC-1α are predominantly recognised as modulators of metabolism, but are also clearly associated with angiogenesis.

This dual relationship between metabolic regulation and angiogenesis highlights that even though hypoxia signalling is critically important for angiogenesis, endothelial cells must adjust many other aspects of their phenotype to ensure they can perform angiogenic functions

adequately. Many of these adjustments to an endothelial cell's phenotype are disturbed by diabetes, which fundamentally contributes to the impaired angiogenesis that we observe in patients with diabetes.

1.2.1. Impaired angiogenic signalling in diabetes

It is well-established that hyperglycaemia or *in vitro* high glucose treatment destabilises the HIF-1α protein and therefore reduces its translocation to the nucleus and upregulation of pro-angiogenic genes [45]. This effect is due to a high glucose-induced increase in the PHD proteins, which tag HIF-1α for degradation. Increased degradation of HIF-1α means it cannot travel to the nucleus and induce transcription of pro-angiogenic genes. This therefore also impairs hypoxia-induced expression of VEGFA and is subsequently associated with the impairment of angiogenesis under high glucose conditions [45].

Another important factor that is significantly affected by diabetes is PGC-1α. Sawada *et al.* aimed to fully characterize the effect of diabetes on PGC-1α and determine how this affected endothelial cell function and angiogenesis. They demonstrated that PGC-1α was significantly elevated in endothelial cells from the heart or lung tissue from several different diabetic mouse models [51]. This effect was replicated *in vitro* with cultured primary endothelial cells exposed to high glucose. Furthermore, endothelial cells overexpressing PGC-1α exhibited significantly impaired migration as demonstrated with a transwell assay. This study identified a strong link between modulation of metabolism and control of angiogenesis, as well as highlighting the negative effects of diabetes upon this mechanism.

1.3. Endothelial Cell Metabolism

1.3.1. Glycolysis

Glycolysis describes a chain of reactions by which one molecule of glucose is broken down into two molecules of pyruvate (Figure 1.5). Glycolysis occurs in the cytosol and does not require oxygen, meaning that it can occur in the presence or absence of oxygen. There are many steps in this chain of reactions, one of which is ATP-producing. Glycolysis produces 2 molecules of ATP for every molecule of glucose. There are also many metabolic intermediates produced as glycolysis progresses, and these have their own roles in the regulation of endothelial cell function which will be discussed later.

Active endothelial cells rely on glycolysis for the bulk of their ATP production, though this may seem counter-intuitive given their ordinarily easy access to oxygen from the bloodstream [41]. However, the sheer quantity of oxygen that endothelial cells are exposed to could easily lead the cells to experience severe oxidative stress if they did not restrict flux through pathways that consume oxygen. Furthermore, reducing reliance on oxygen-consuming pathways ensures that endothelial cells are always primed to function in hypoxia, which is useful for re-vascularisation of ischaemic tissues. This is unique and in contrast to many other cell types for which full oxidation of glucose through mitochondrial respiration is the most efficient method of ATP production.

Upon encountering hypoxia, endothelial cells undergo a substantial metabolic shift. It is essential that endothelial cells further upregulate glycolysis to account for the increased energy demands of proliferation and migration, while simultaneously keeping oxygen consumption low to avoid oxidative stress. To achieve this, VEGF and FGF signalling support an increase in glycolytic flux [41, 48]. This means that the rate of glucose breakdown through glycolysis

increases, producing more ATP, more glycolytic intermediates, and more pyruvate. This section will discuss the key roles of VEGF and FGFs in regulating glycolytic flux.

Firstly, the increase in glycolytic flux has been found to be mediated, at least in part, by an interaction between VEGF and 6-phosphofructo-2-kinase/fructose-2,6-biphosphatase 3 (PFKFB3) [41]. An important rate-limiting step in glycolysis is the conversion of fructose-6-phosphate (F6P) to fructose-1,6-bisphosphate ($F1,6P_2$) by 6-phosphofructo-1-kinase (PFK-1). PFKFB3 synthesises fructose-2,6-bisphosphate ($F2,6P_2$), a strong activator of PFK-1. Therefore, activity of PFKFB3 represents an avenue for potent upregulation of glycolysis. De Bock *et al.* have shown that PFKFB3 knockdown using short hairpin RNA (shRNA) reduced glycolytic flux by 35% in both microvascular and arterial endothelial cells, indicating that PFKFB3 is important for maintaining adequate levels of glycolytic flux in endothelial cells. Importantly, it was shown that VEGF increases both PFKFB3 expression and glycolysis. With respect to the effect on angiogenesis, knockdown of PFKFB3 decreased vessel sprouting in endothelial cell spheroids. Further investigation of this *in vivo* revealed that mice with endothelial cells deficient in PFKFB3 displayed significant defects in retinal blood vessel development as well as decreased vascular area in the hindbrain [41].

Other glycolytic enzymes have also been implicated in the regulation of endothelial cell angiogenic functions. One of these is hexokinase 2 (HK2), which phosphorylates a molecule of glucose to produce glucose-6-phosphate. This is the first step in glycolysis and is also rate-limiting. Yu *et al.* investigated the relationship between FGF2 and HK2 in endothelial cells with the aim of delineating the mechanism by which FGF2 stimulates angiogenesis. This group found that mouse embryos deficient in endothelial FGF receptor 1 (FGFR1) exhibited reduced vessel branching in the skin. To elucidate this mechanism, human umbilical vein endothelial cells (HUVECs) were treated with FGF, which significantly enhanced glycolysis and HK2

expression. Knockdown of HK2 significantly reduced glycolysis, while adenoviral-mediated overexpression of HK2 increased glycolysis. This study identified a relationship between FGF and HK2 in endothelial cells and determined that HK2-mediated glycolysis was essential for angiogenesis [48].

Pyruvate kinase (PK) catalyses the conversion of phospho-enol-pyruvate to pyruvate, which is the final rate-limiting step in glycolysis. When PK activity is low, upstream glycolytic intermediates may accumulate and be shunted to various side-pathways. Endothelial cells predominantly express the PKM2 isoform of this enzyme, and this was examined in the context of angiogenesis by Kim *et al.*, who knocked down PKM2 using siRNA and observed significant suppression of cell proliferation, migration, and tubule formation *in vitro*. This was associated with a decrease in extracellular acidification which represents completion of the glycolytic pathway through lactate export. Furthermore, endothelial cell-specific deletion of PKM2 in mice was associated with significant reduction of retinal vessel density and branching. Finally, PKM2 was found to achieve its effects on proliferation via inhibition of p53, causing a blockade of the cell cycle. Although this role of PKM2 was found to be independent of its specific role in glycolysis, this study nevertheless highlights the close relationship between the integrity of metabolic pathways and the angiogenic capacity of endothelial cells [52].

Together, this research highlights the importance of glycolysis in angiogenesis and identifies key regulatory mechanisms that may be implicated in diabetes-impaired angiogenesis.

1.3.2. Glycolytic side-pathways

Glycolytic side pathways are also critical for endothelial cell function. These pathways involve various glycolytic intermediates and have a wide range of functions that can have either positive or negative consequences for an active endothelial cell, if affected by disease. Thus

far, the pentose phosphate pathway (PPP) has been the most extensively studied, and has been demonstrated to be of great importance to endothelial cell function. The PPP utilises glucose-6-phosphate from glycolysis in two different branching pathways. The oxidative branch (oxPPP) comprises an irreversible reaction which generates NADPH and ribose-5-phosphate (R5P), while the non-oxidative branch produces only R5P [53]. NADPH is critical for redox homeostasis as it allows for the conversion of oxidised glutathione (GSSG) to its reduced form (GSH). Reduced glutathione is an essential antioxidant which neutralises reactive oxygen species [54]. Therefore, this mechanism is likely to play an important role in maintaining the redox balance of an endothelial cell during hypoxia-driven angiogenesis. Additionally, the R5P produced by this pathway is essential for the synthesis of nucleotides, which likely supports the increased proliferation required during vessel sprouting [53, 55]. The rate of the oxPPP is determined by glucose-6-phosphate dehydrogenase (G6PD). The importance of this pathway and its close relationship with the rate of glycolysis implicate it in diabetes-impaired angiogenesis.

1.3.3. Mitochondrial respiration

It has been shown that endothelial cells maintain very low levels of mitochondrial respiration relative to their rate of glycolysis [41]. Mitochondrial respiration, which encompasses both the tricarboxylic acid (TCA) cycle and the electron transport chain (ETC), ordinarily consumes a high quantity of oxygen and subsequently contributes to production of reactive oxygen species (ROS). Suppressing oxidative phosphorylation may be necessary for endothelial cells to reduce ROS production and maintain redox homeostasis, but may also be important for production of macromolecules like amino acids for cell proliferation.

Because of the much greater focus on glycolysis and glycolytic side pathways, there are comparatively very few studies which have investigated the role of mitochondrial respiration

in endothelial function. Importantly, there are no studies which specifically investigate the role of mitochondrial respiration in diabetes-impaired angiogenesis. The disease context in which endothelial cell mitochondrial respiration is studied is critical for the interpretation of its role in cellular function.

In non-diabetic conditions, ablating or significantly decreasing mitochondrial respiration has negative effects on markers of angiogenic function. In a recent study, Govar *et al.* showed that deletion of 3-mercaptopyruvate sulfurtransferase (3-MST) decreased mitochondrial respiration and mitochondrial ATP production, and this was associated with an impairment to EC proliferation, migration, and tubule formation [56]. None of these functional assays were performed under high glucose or hypoxic conditions, and so suggest the general importance of maintaining mitochondrial respiration only under baseline conditions for EC function. An additional study by Diebold *et al.* supports this idea, and interrogated the role of mitochondrial metabolism directly by inhibiting the mitochondrial respiratory chain complex III using antimycin A [57]. This allowed them to bypass the effect of different mitochondrial fuel sources, and they demonstrated that this ablation of respiration was associated with a striking decrease in EC proliferation, though it had no effect on cell migration or tubulogenesis. In mice with an endothelial-specific loss of ubiquinol binding protein, which is a critical subunit of the mitochondrial respiratory chain complex III, they identified an impairment to retinal angiogenesis. Importantly, none of these *in vitro* functional assays were performed under hypoxic conditions, and the retinal angiogenesis *in vivo* model which was used may not specifically involve ischaemia-driven angiogenesis, meaning that these results can only be interpreted in the context of normoxic and normoglycaemic conditions.

In the alternative context of microvascular ischaemia/reperfusion injury, Zou *et al.* demonstrated that the sodium/glucose cotransporter 2 (SGLT2) inhibitor empagliflozin, which

is known to protect patients against endothelial dysfunction regardless of diabetes status, did so in part by increasing the mitochondrial capacity for respiration, and by increasing mitochondrial ATP production [58].

These results suggest that maintenance of mitochondrial respiration is important for endothelial function under normal conditions, and suggests that perturbation of the system can have negative effects on angiogenesis. However, very little is known about the importance of mitochondrial respiration in diabetic endothelial cells, and this represents a critical gap in our knowledge. A better understanding of this specific context is critical if we are to attempt to improve ischaemia-driven angiogenesis through augmentation of cellular metabolism.

1.3.4. Fatty acid oxidation

Fatty acid oxidation (FAO) represents an alternate avenue for production of acetyl CoA from long chain fatty acids, and bypasses the PDC. This is achieved by direct production of acetyl CoA from long chain fatty acids, which can then condense with oxaloacetate to form citrate and fuel the TCA cycle. In endothelial cells specifically, the main mechanism which regulates FAO involves AMP-activated protein kinase (AMPK), which is activated by hypoxia [59]. AMPK indirectly activates carnitine palmitoyl transferase 1A (CPT1A), which shuttles long-chain fatty acids into the mitochondria and represents a rate-limiting step of FAO [60].

While FAO can be used for generation of ATP through mitochondrial respiration, endothelial cells rely predominantly on glycolysis for energy production. Recent research does, however, point to FAO as an essential contributor to endothelial cell functions beyond energy production.

Kalucka *et al.* examined the metabolism of quiescent endothelial cells. They found that quiescent endothelial cells upregulated FAO three times more than proliferative endothelial cells and that this was primarily in support of NADPH regeneration for redox homeostasis.

Blocking FAO in these cells induced significant oxidative stress, but supplementing the cells with acetate rescued this. This demonstrates that FAO is essential for maintaining redox balance in quiescent endothelial cells [61].

In contrast, Schoors *et al.* investigated FAO in proliferative endothelial cells undergoing vessel sprouting, again with a focus on identifying an alternative role for the process beyond energy production. Schoors *et al.* knocked down CPT1A and found that this impaired vessel sprouting in EC spheroids due to decreased cell proliferation. CPT1A knockdown did not lower ATP levels, and only increased ROS levels by approximately 20%, a level believed to have a positive effect on endothelial cell proliferation. It was then determined that acetyl CoA from FAO was cycling through the TCA cycle and contributing to *de novo* synthesis of deoxyribonucleotides in endothelial cells, and that knockdown of CPT1A reduced this and subsequently impaired *de novo* DNA synthesis. This culminated in the impairment of endothelial cell proliferation and overall vessel sprouting [62]. This contrasts with the role of FAO in maintaining redox balance in quiescent endothelial cells, but nevertheless suggests that FAO is important for correct endothelial cell function and angiogenesis.

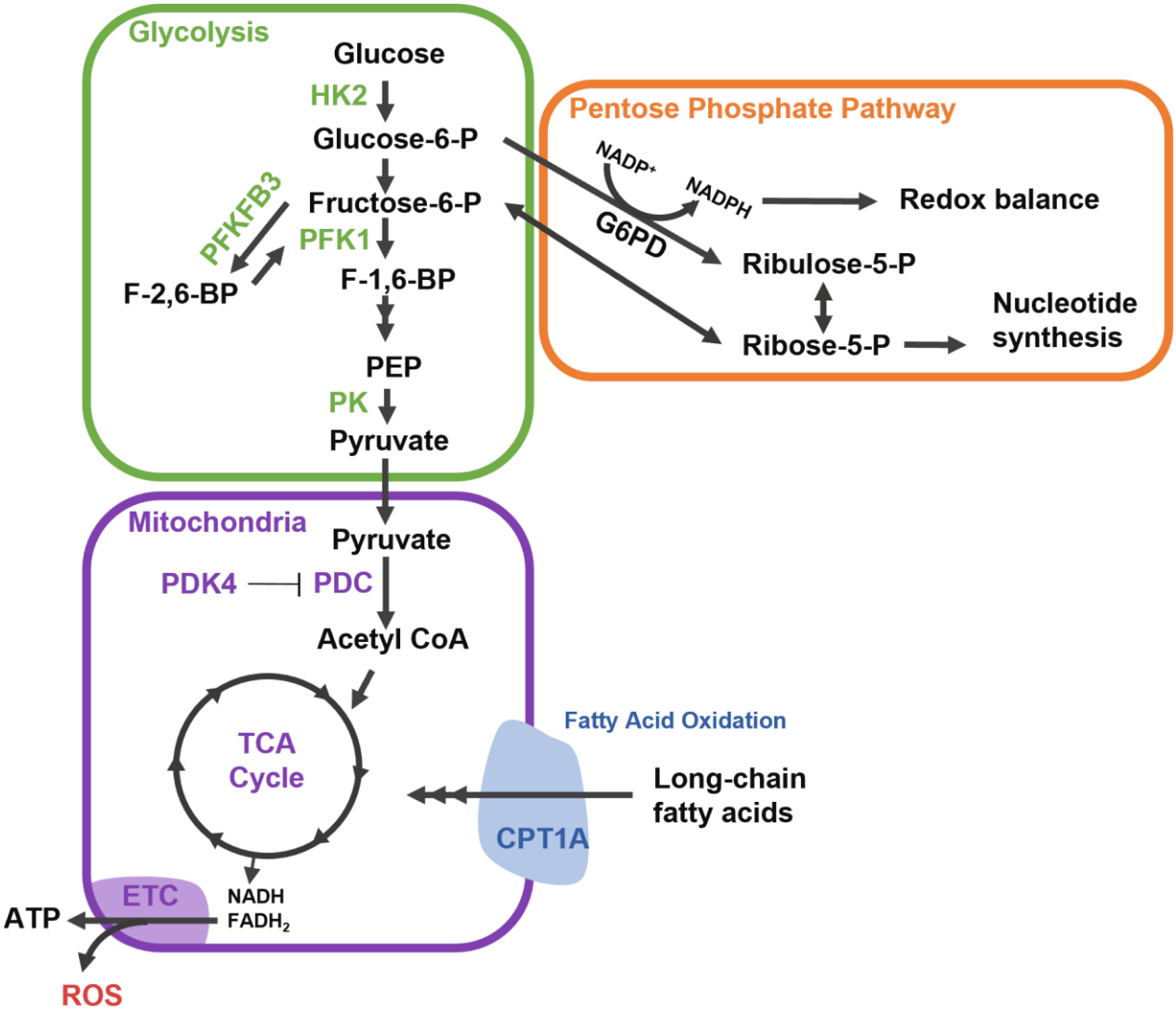

Figure 1.5. Diagram of endothelial cell metabolism. A simplified diagram of endothelial cell metabolism depicting some of the metabolic pathways known to be important for endothelial cell function and their rate-limiting enzymes. CPT1A, carnitine palmitoyltransferase 1A; ETC, electron transport chain; G6PD, glucose-6-phosphate dehydrogenase; HK2, hexokinase 2; NADPH, nicotinamide adenine dinucleotide phosphate; PDC, pyruvate dehydrogenase complex; PDK4, pyruvate dehydrogenase kinase 4; PFK1, phosphofructokinase 1; PFKFB3, phosphofructokinase-2/fructose-2,6-bisphosphatase isoform 3; PK, pyruvate kinase.

1.4. The Pyruvate Dehydrogenase Complex

The 9.5 megadalton pyruvate dehydrogenase complex (PDC) is a large complex of three different enzymatic subunits located inside the mitochondrial matrix. It catalyses the conversion of pyruvate to acetyl-CoA, which condenses with oxaloacetate to form citrate and enters the citric acid cycle. In this way, the PDC couples glycolysis to mitochondrial respiration, and it represents an extremely important point at which endothelial cell metabolism can be reprogrammed.

The E1 subunit of the PDC is called the pyruvate dehydrogenase subunit and consists of an α and β chain. It is this subunit which interacts with the thiamine diphosphate (TPP) cofactor that is directly involved with the decarboxylation of pyruvate. The E2 subunit is called dihydrolipoyl transacetylase, and the E3 subunit is called dihydrolipoyl dehydrogenase. The genes for the three enzymatic subunits are encoded in the nucleus, not the mitochondria [63].

In eukaryotes, the PDC structure is comprised of 60 E2 molecules arranged into an icosahedron. The E2 core is then complexed with 30 subunits of E1 and 12 copies of E3 [63].

Genetic mutations that cause deficiency of the PDC have been linked to several metabolic and neurological conditions. Pyruvate dehydrogenase deficiency is diagnosed when a genetic mutation occurs in one of the three components of the complex [64]. A deficiency of the PDC means that a person's cells are unable to completely oxidise, through mitochondrial respiration, the pyruvate or lactate that results from glycolysis, leading to the export of lactate from cells and lactic acidosis. Lactic acidosis is the hallmark of the metabolic form of this condition, though there is also a neurological form that presents with brain structure abnormalities and can lead to seizures and microcephaly [64].

While pyruvate dehydrogenase deficiency is associated with a number of neurological conditions, there is nothing documented about the effect of genetic PDC deficiency on the cardiovascular system or on risk of developing diabetes.

1.4.1. The pyruvate dehydrogenase complex in diabetes

While there may not be any evidence for a genetic deficiency of the PDC exacerbating diabetes, there is certainly evidence for its involvement in the pathology. Diabetes is a disease of impaired glucose utilisation, and it is therefore logical that the enzyme responsible for allowing glucose-derived pyruvate to enter the citric acid cycle and be fully oxidised might play a pivotal role.

This idea is related to the concept of metabolic inflexibility. Metabolic inflexibility refers to the inability of a cell to alter its metabolism in response to changing nutrient conditions. In diabetes, this can be related to insulin resistance, as the inability of a cell to respond to insulin constitutes a type of inflexibility. However, chronic hyperglycaemia and an excess of dietary lipids can also cause other forms of metabolic inflexibility separate from insulin resistance.

The PDC plays a role in metabolic inflexibility in key metabolic tissues through its ability to allow a switch from glycolytic to oxidative metabolism and has previously been targeted to improve glucose utilisation.

Skeletal muscle is a central tissue responsible for glucose utilisation. In diabetes, skeletal muscle exhibits both insulin resistance and lipid-induced metabolic inflexibility, which contributes to chronic hyperglycaemia. A central hypothesis for why this metabolic inflexibility occurs has existed since the 1960s, with Randle *et al.* proposing that increased fatty acid oxidation increases the cellular pool of acetyl-CoA in myocytes, which impairs PDC activity by overstimulating the enzymes that inhibit the PDC. This therefore impairs glucose

utilisation [65]. Although more recent studies have suggested that the mechanism is far more complex than this, researchers have nevertheless hypothesised that stimulating the PDC may improve metabolic inflexibility in skeletal muscle. Chien *et al.* recently demonstrated, using an *in vitro* model of palmitate-induced myotube insulin resistance, that the cells exhibited strikingly reduced rates of PDC activity, and that this was associated with an increase in pyruvate dehydrogenase kinase 4 (PDK4) [66]. A study by Park *et al.* used hyperpolarised nuclear magnetic resonance (NMR) to show that the muscle of type 2 diabetic rats exhibited much lower PDC activity than the muscle of non-diabetic rats [67].

In almost direct contrast to the metabolism of skeletal muscle and many other cell types, endothelial cells rely primarily on glycolysis for their metabolic needs, and otherwise suppress mitochondrial respiration. This reliance on glycolysis is essential for angiogenesis, and allows the cells to produce adequate ATP without requiring oxygen. As mentioned in the previous sections, there have been many studies conducted into the role of glycolysis in endothelial cell function and angiogenesis, and a very limited number that have focused on mitochondrial respiration. There is almost no published work regarding the PDC in endothelial cells, let alone in the specific context of diabetic endothelial cells and angiogenesis.

One recent study aimed to investigate the role of the PDC in endothelial cell function by treating human umbilical vein endothelial cells (HUVECs) with dichloroacetate, which pharmacologically inhibits the pyruvate dehydrogenase kinases (PDKs) and activates the PDC. The authors showed that activating the PDC and enhancing mitochondrial respiration reduced HUVEC proliferation and migration, indicating that suppression of mitochondrial respiration is required for normal endothelial cell function [68]. This study is the only published work that could be identified which addressed the PDC specifically, and was undertaken in the context of tumour angiogenesis rather than the diabetic context. However, there are other relevant

studies that focus on the expression and activity of the pyruvate dehydrogenase kinases rather than the PDC itself in endothelial cells, some in diabetes, and these will be discussed in the following section.

1.4.2. Enzymatic regulation of the PDC through kinases and phosphatases

Regulation of the PDC is achieved primarily by phosphorylation and dephosphorylation of three serine residues on the α chain of the E1 enzyme. The three sites are ser232, ser293, or ser300, and they are phosphorylated by the pyruvate dehydrogenase kinases, of which there are four isoforms (PDK1-4). These four isozymes phosphorylate the different serine residues with varying affinity. PDK1 is the only enzyme to phosphorylate all three sites, while PDK2-4 target ser232 and ser293 with different affinities reported *in vitro*. The activity of the PDKs is affected by the availability of metabolic end-products such as acetyl-CoA, NADH, and ATP [69].

There are also two PDC phosphatase enzymes (PDP1-2) which dephosphorylate the PDC. The activity of the PDPs is affected by the availability of substrates such as ADP and NAD^+. PDP1 and PDP2 can dephosphorylate the three serine sites with similar preference, however they do show small differences in their activity for each site [70, 71].

The transcription and translation of these enzymes, as well as their preference for serine site, provides additional levels of regulation of the PDC.

Importantly, each of these enzymes exhibits striking differences in their distribution across human tissues. For example, PDK2 has been reported in multiple studies to be the most widely expressed isozyme, and can be found in all studied tissues [72, 73]. However, endothelial cells have not been specifically included in these studies.

PDK1 is highly expressed in the heart but only moderately expressed in the liver, skeletal muscle and pancreas, though a recent study by Kluyeva *et al.* asserted that PDK1 can be readily detected in all studied metabolic tissues [73].

PDK3 is generally shown to have the most limited tissue distribution, with significant levels of the protein only being found in the kidney, brain, testis, and lung [73].

PDK4 is unique among the PDKs as it is believed to have a limited role in the well-fed state, yet becomes far more important in the context of starvation or hypoxia. The study by Kluyeva *et al.* found that PDK4 was expressed primarily in tissues of muscle origin, including skeletal muscle and the heart [73]. It was also expressed in brown adipose tissue. However, the authors note that they only studied PDK4 in the well-fed state, and its expression may well be altered in other tissues in response to starvation or hypoxia. PDK4 has been studied in many different cell types in the context of hypoxia alone, and it is generally agreed that it is strikingly induced in response to low oxygen levels [74, 75]. This is likely to reduce cellular oxygen consumption through inhibition of mitochondrial respiration, potentially allow for upregulation of glycolysis, and protect against oxidative stress. However, this phenomenon has not been studied in the context of diabetes or endothelial cell angiogenesis, and represents a critical gap in our knowledge.

To our knowledge, there are no published studies that specifically examine the relative expression of the PDKs and PDPs in endothelial cells. While the PDKs may not be thoroughly studied in endothelial cells, there are studies that describe the important role of the PDKs in general endothelial cell function under diabetic conditions, though these do not focus specifically on angiogenic functions.

One study investigated the role of PDK4 in high glucose-impaired insulin signalling in endothelial cells. The authors found that PDK4 activation was associated with the rescue of

endothelial cell function under high glucose conditions, and that it preserved correct insulin signalling [76]. An additional study investigating high glucose-impaired endothelial relaxation also found that PDK4 induction was associated with the restoration of cAMP-induced relaxation and attenuation of oxidative stress [77].

These studies represent the extent of the literature regarding the PDKs in diabetic endothelial cells, highlighting a significant gap in our knowledge about how the PDK/PDC axis affects endothelial cell function and how it may be targeted to improve endothelial cell angiogenesis in the diabetic context.

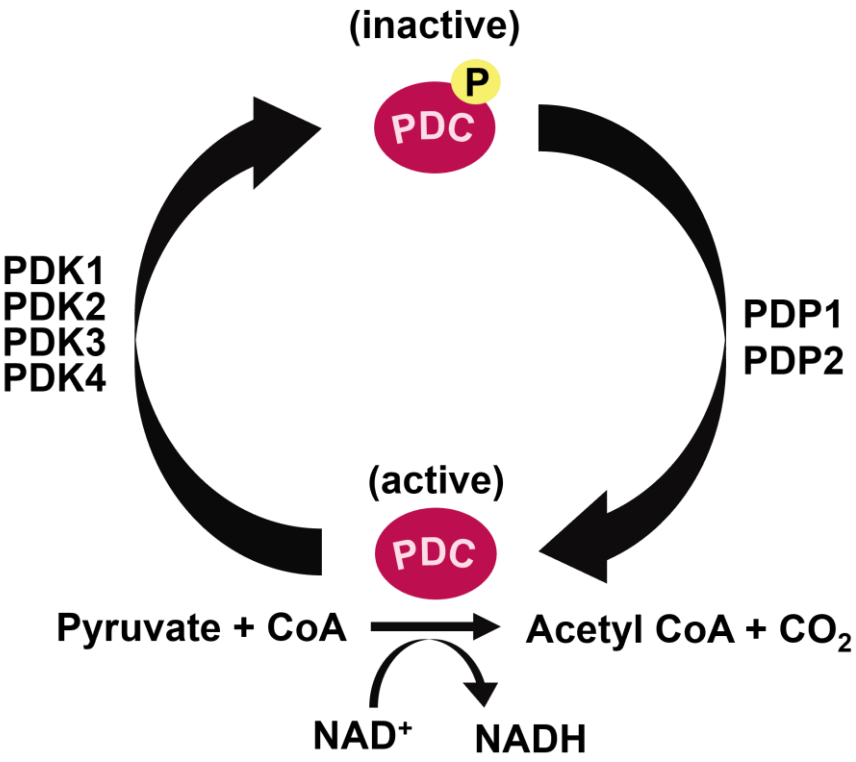

Figure 1.6. Regulation of the pyruvate dehydrogenase complex. Schematic depicting the active and inactive states of the PDC, and which enzymes are responsible for either phosphorylating (PDK1-4) or dephosphorylating (PDP1-2) the complex. PDK, pyruvate dehydrogenase kinase; PDP, pyruvate dehydrogenase phosphatase.

1.5. High-density Lipoproteins

1.5.1. Structure of high-density lipoproteins

High-density lipoproteins (HDL) are highly heterogenous particles composed of an outer layer of apolipoproteins (apo) and phospholipids, surrounding a core of esterified cholesterol. ApoA-I is the predominant protein moiety in HDL and is thought to impart the many biological properties of HDL. HDL cholesterol (HDL-C) refers to the HDL particles in the bloodstream that are specifically carrying cholesterol. This is distinct to 'HDL' which refers to the particle itself, and which can have specific effects independent of cholesterol efflux and can be modified by various disease milieu [78]. It is necessary to distinguish between these two forms of notation as this highlights the breadth of effects had by HDL. Additionally, investigating the role of HDL as a discrete particle independent of cholesterol efflux may help identify why HDL-C-raising therapies have demonstrated limited clinical benefit [78].

HDL primarily mediates reverse cholesterol transport by carrying cholesterol from peripheral tissues, including from macrophages in atherosclerotic plaques, to the liver for metabolism and excretion. This is a critical function that is a key contributor to the cardioprotective properties of HDL. HDL effluxes cholesterol by interacting with two cholesterol transporters ATP-binding cassette transporter A1 (ABCA1) and G1 (ABCG1), and the scavenger receptor BI (SR-BI) [79, 80].

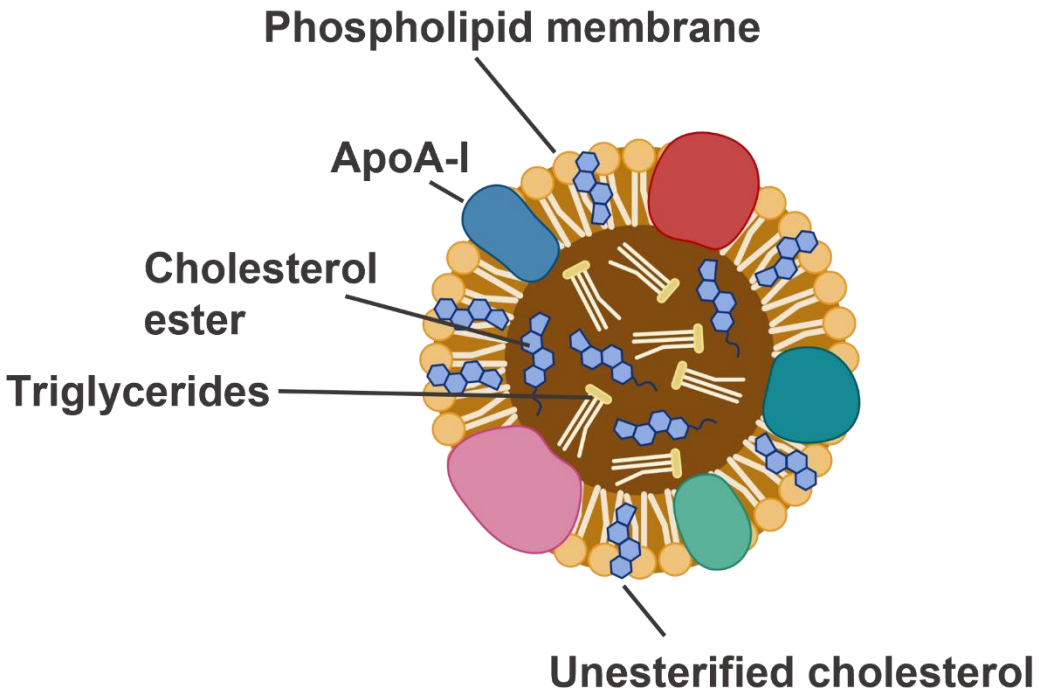

Figure 1.7. The structure of a high-density lipoprotein particle. The particle is comprised of a lipid core containing triglycerides and both esterified and unesterified forms of cholesterol. The outer phospholipid membrane is embedded with proteins – in high-density lipoproteins the must abundant apolipoprotein is apoA-I. Apo, apolipoprotein.

1.5.2. HDL receptors

ABCA1 mediates cholesterol efflux and interacts specifically with lipid-free apoA-I. Once apoA-I has acquired lipid to become a discoidal particle, it can then interact with ABCG1 and SR-BI. ABCA1 and ABCG1 contribute to the majority of the cholesterol efflux exchange conducted by lipoproteins but are also linked to a number of downstream signalling pathways, some of which are associated with angiogenesis. ABCG1, for example, mediates downstream signalling events that lead to elevated endothelial nitric oxide synthase (eNOS) activity, an important promoter of neovascularisation. This pathway is dependent on cholesterol efflux as it reduces the intracellular concentration of oxysterol 7-ketocholesterol [80].

Of the three cell-surface proteins that interact with HDL, SR-BI mediates the highest number of downstream signalling pathways, and these can be either dependent or independent of cholesterol efflux. SR-BI is distinct to the other cholesterol transporters in that cholesterol can be exchanged bidirectionally between the cell and the HDL particle. Many of the signalling pathways downstream of SR-BI overlap significantly with those that regulate angiogenesis, including the phosphoinositide 3-kinase (PI3K)/Akt and MAPK pathways [81]. For the most part, apoA-I is believed to be the key component that mediates the multiple effects of HDL. The only other reported component of HDL that stimulates significant vascular biological effects is a sphingolipid, which interacts with the S1P1 receptor and activates downstream signalling events that are very similar to those downstream of SR-BI in endothelial cells and regulates angiogenesis [81]. It should be noted, however, that sphingolipid makes up only a tiny proportion of the HDL particle, and it has been suggested that its physiological relevance within HDL is likely to be limited, making apoA-I the target of HDL-based studies.

1.5.2.1. The effect of HDL on angiogenesis

HDL regulates ischaemia-driven angiogenesis via multiple mechanisms. An early study showed that in a murine model of hindlimb ischaemia, infusions of reconstituted HDL (rHDL, apoA-I complexed with phospholipid) increased the number of endothelial progenitor cells (EPCs) which homed to the ischaemic limb, resulting in improved reperfusion [82]. Mechanistically, *in vitro* studies demonstrated that rHDL promoted the differentiation of EPCs through the PI3K/Akt pathway [82]. Furthermore, studies conducted in patients with type 2 diabetes mellitus found that infusions of rHDL improved vascular function [83], and increased the number of circulating EPCs [84].

Studies have also examined the effects of rHDL on the HIF-1α/VEGFA hypoxia signalling pathway which initiates angiogenesis. Neovascularisation and blood flow reperfusion were increased by apoA-I infusions in the murine hindlimb ischaemia model. This study also examined the effect of rHDL on endothelial cell function *in vitro* and found that rHDL enhanced hypoxia-stimulated migration, proliferation, and tubulogenesis. It was then determined that these effects were mediated by augmentation of HIF-1α, VEGFA and VEGF receptor 2 (VEGFR2) [85]. It was demonstrated by a second study that these effects were due to changes in the post-translational modulation of HIF-1α induced by rHDL. In this study Tan *et al.* found that, through an interaction with scavenger receptor B I (SR-BI) and the PI3K/Akt pathway, rHDL increased expression of the E3 ubiquitin ligases Siah1 and Siah2, which are responsible for targeting the PHD proteins for degradation. This resulted in decreased PHD protein activity, allowing HIF-1α to accumulate and promote transcription of VEGFA [86].

The exact mechanism by which HDL achieves these various salutary effects is complex and may be due to multiple factors. The effects on the HIF-1α/VEGFA signalling pathways have been shown to be dependent on an interaction between the rHDL particle and scavenger

receptor class B type 1 (SR-BI) [45]. SR-BI plays a role in reverse cholesterol transport and its presence was essential for rHDL to elicit its pro-angiogenic effects [45]. However, the role of cholesterol efflux was not directly addressed in these studies. Additionally, several studies have demonstrated positive effects on the vasculature or EPCs with only the apoA-I protein moiety of HDL. This indicates that there may be multiple mechanisms by which HDL and its apoA-I component are able to elicit positive effects on endothelial cell function, potentially including cellular metabolism.

Taken together, these studies highlight that rHDL regulates multiple aspects of pro-angiogenic signalling pathways to achieve a positive effect or 'rescue' of diabetes-impaired angiogenesis. However, given the complexity of diabetes and the associated vascular complications, it is necessary to fully understand the breadth of effects had by rHDL on angiogenesis in order to develop it as a potential therapeutic agent.

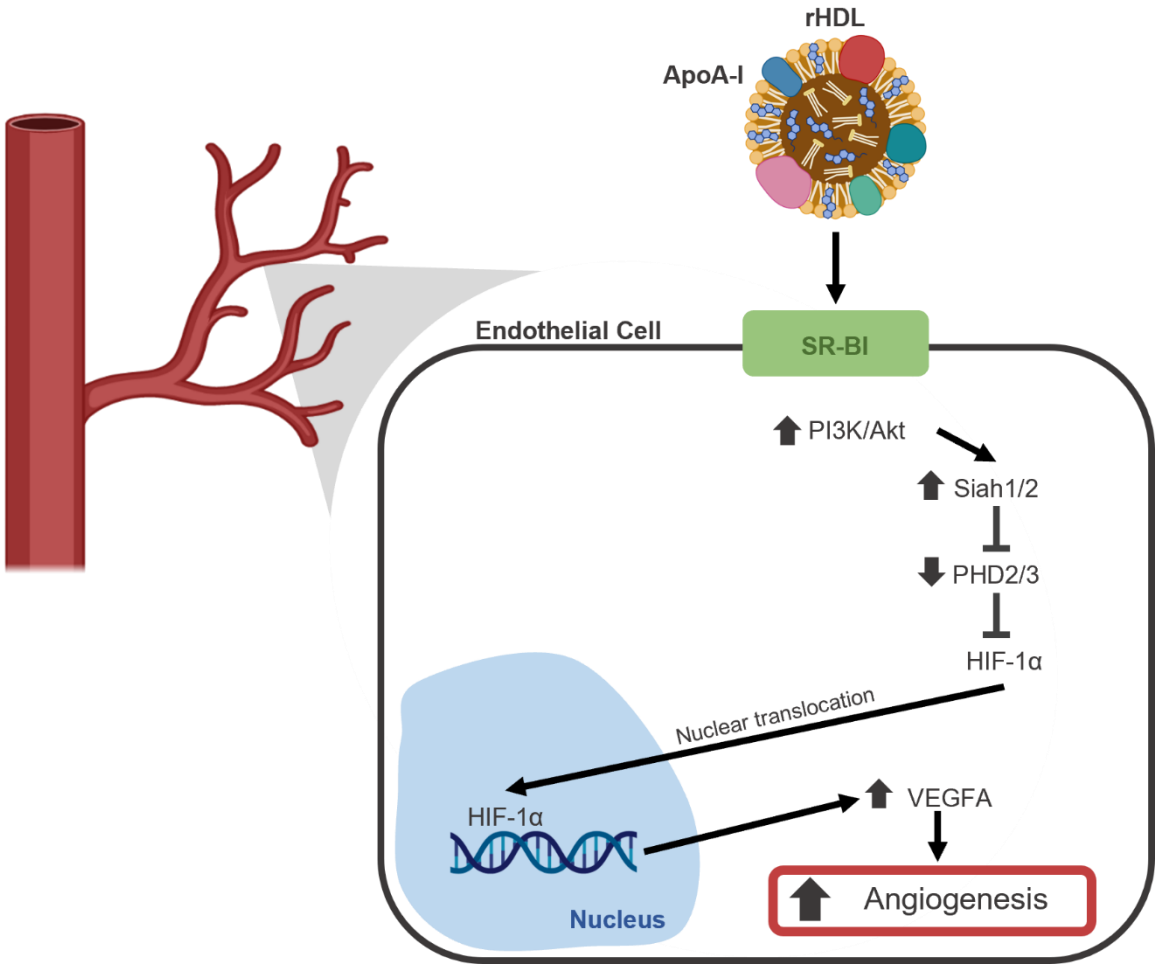

Figure 1.8. The known effects of high-density lipoproteins (HDL) on angiogenic signalling pathways in endothelial cells. In an SR-BI-dependent manner, rHDL increases PI3K/Akt signalling and increases the expression of Siah1/2. This leads to a downregulation of the PHD proteins, and enhances the stabilisation of HIF-1α, leading to increased expression of pro-angiogenic genes including VEGFA. HIF-1α, hypoxia-inducible factor 1α; PHD, prolyl hydroxylase domain; PI3K, phosphoinositide 3-kinase; SR-BI, scavenger receptor B; VEGFA, vascular endothelial growth factor A.

1.6. Lentiviral Gene Therapy

Viral vectors for delivery of genetic material to target cells were developed almost five decades ago, with the first usage occurring in the 1970s when Paul Berg and Stephen Goff used a modified SV40 virus to infect simian kidney cells *in vitro* [87]. The field has progressed significantly over the years, with some high-profile viral gene therapies recently being approved by the United States' Food & Drug Administration (FDA) for clinical use [88]. A gene therapy is defined as the delivery of a functional gene to correct a genetic or phenotypic deficit in a diseased cell or tissue. It does not inherently need to involve a viral vector, but they are commonly used because of a virus' inherent ability to deliver genetic material to target cells. In comparison to the pleotropic effects elicited by a particle like rHDL, viral gene therapies can be engineered to exhibit a high level of cell-specificity, and are usually created to target a single gene. This allows for the creation of therapies with a highly regulated mechanism of action, and potentially fewer off-target effects.

1.6.1. Types of viruses

There are several types of viruses that are commonly used as gene delivery vectors, each with slightly different characteristics and methods of gene delivery. The most common types are adenoviruses, adeno-associated viruses, and lentiviruses, which are a subclass of retrovirus [89].

Adenoviruses are medium-sized (90nm in diameter), nonenveloped viruses with an icosahedral capsid that contains their double-stranded DNA genome [90]. Their ability to infect both replicating and non-replicating cells has made them a popular choice of gene therapy vector, as does their larger size which allows them to package larger transgenes than other viruses. Adenoviruses do not incorporate their DNA into the host's genome, but rather deposit the DNA as an episome in the nucleus, which means that the transgene expression they elicit will not be

passed down through cell generations [90]. This is appealing in some cases where transient gene expression is preferred, as opposed to permanent gene expression. Adenoviruses also exhibit tropism for a very wide range of different tissue targets depending on the variant [90].

Adeno-associated viruses (AAVs) are also nonenveloped, but are much smaller than adenoviruses (26nm in diameter), and are not known to cause any human diseases [91]. Similar to adenoviruses, the forms of AAV that have been engineered for gene therapy purposes also deposit their DNA in the host cell nucleus in episomal concatemers. AAVs also elicit a smaller immune response than adenoviruses, though their use does present some disadvantages. For example, they cannot be used to package large genes due to their small physical size and limited genome capacity [91].

Lentiviruses are subclass of retrovirus, which possess an RNA genome as opposed to a DNA genome, and a reverse transcriptase gene which converts the RNA to DNA. In comparison to the previous two viruses, lentiviruses are enveloped, and are generally approximately 100nm in diameter [89]. Lentiviruses are the only retrovirus which is able to infect dividing and non-dividing cells. Rather than depositing their genetic payload in the nucleus using episomes, lentiviruses integrate their DNA into the host genome. This integration is performed in a "non-random" manner and occurs preferentially in transcriptionally active sites [92]. Genome integration allows the transgene expression to persist through cell generations, though does raise some concerns regarding the potential for disruption of normal gene expression which can lead to cancer. However, the potential for permanent transgene expression, combined with the fact that lentiviruses have a relatively large packaging capacity of up to 9 kilobases, makes them an attractive option for gene therapies which require complex, long term gene expression [92].

The type of lentivirus system most commonly used in gene therapy applications is derived from the human immunodeficiency virus (HIV-1) and has evolved significantly since its development through specific engineering to improve its safety. The field is currently employing a third-generation HIV-1-based lentiviral vector, which is produced using four distinct plasmids (Figure 1.9). Three of these plasmids encode only the essential genes required to generate the lentiviral particles, and all other accessory genes associated with replication-competence or other functions have been excluded [93]. One plasmid contains the sequence for *gag-pol*, which encompasses the genes required to produce proteins for the virion interior, and viral enzymes like polymerases. Another plasmid contains the *Rev* component, which encodes an important post-transcriptional regulator. A third plasmid contains the genes for essential viral envelope glycoproteins which allow the virion to enter a host cell. This plasmid will be named specifically for the glycoproteins it encodes, and may be referred to as *env*. The fourth plasmid acts as a transfer vector, and encodes the transgene that will be delivered to the host cell [93, 94].

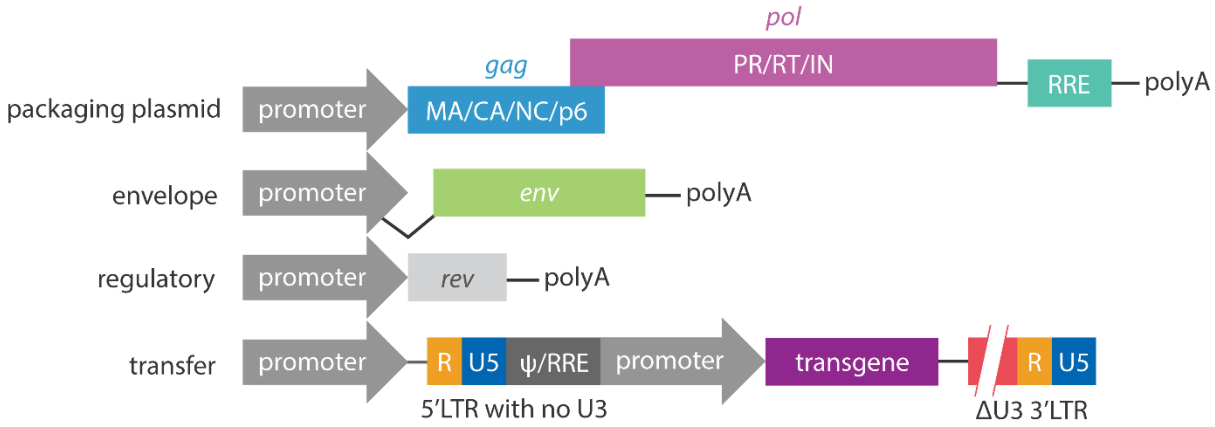

Figure 1.9. The third-generation lentiviral vector system. The vector system is split into four plasmids, a packaging construct which contains the *gag* and *pol* genes, a plasmid which expresses *env* or other glycoproteins, a plasmid expressing *rev*, and a transfer vector which contains the transgene driven by a specific promoter.

1.6.2. Engineering tissue-specificity and temporal regulation of gene expression

There are several approaches researchers can employ to maximise the tissue-specificity of lentiviral vectors, and enact temporal control of gene expression. Pseudotyping involves the production of a virus with viral envelope proteins from a different type of virus to either broaden or restrict its tropism. This is a well-established strategy and has been in use for over twenty years. An early example of this is the study by MacKenzie *et al.* wherein lentiviral vectors were pseudotyped with glycoproteins from the vesicular stomatitis virus (VSV-G), Mokola virus, or Ebola virus envelope [95]. They found that VSV-G was the most efficient in transducing hepatocytes, whereas the Mokola and Ebola glycoproteins allowed for more efficient transduction of myocytes. This has progressed to have therapeutic implications for genetic diseases like Duchenne Muscular Dystrophy. There are many ongoing studies which aim to identify new lentiviral pseudotypes that can be used for different tissue-specific applications, and some have attempted to create endothelial-specific pseudotypes using glycoproteins from the *Nipah virus* [96] or Hantavirus [97], with some success.

Another way to obtain tissue-specific transgene expression is to drive gene expression using a cell-specific promoter sequence. Marodon *et al.* demonstrated that this was possible in the early 2000s by generating a lentivirus which expressed a GFP reporter gene under the control of a promoter and proximal enhancer derived from the *CD4* gene [98]. They found that this elicited the highest level of GFP expression in $CD4^+$ T cells, and minimal expression in $CD4^-$ B cells and immature monocytes. As genetic analysis technologies have advanced over the past twenty years, it has become easier to identify highly cell-specific genes, and utilise their regulatory elements to direct transgene expression. Endothelial cell-specific promoters have been identified, beginning with *fms*-like tyrosine kinase-1 (FLT-1) in the early 2000s [99]. Vascular endothelial (VE)-cadherin was identified as a strictly endothelial-specific adhesion molecule

at a similar time, and its regulatory elements may be used to elicit endothelial cell-specific transgene expression [100, 101].

In addition to cell-specificity, temporal regulation can also be created using inducible promoters like the tetracycline (Tet)-On system, which allows transgene expression to be induced with exposure to tetracycline molecules [102]. This was again demonstrated in the early 2000s with studies such as that conducted by Vigna *et al.* wherein a chimeric transcriptional regulator protein which becomes active in the presence of tetracycline, tetracycline-controlled transactivator (tTA), was expressed, and transgene expression was driven by a promoter which contains multiple repeats of the tet operator sequence (*tetO*) [102]. The Tet-On system has been further characterised over time, with more refined chimeric transactivators and *tetO* promoter sequences [103].

1.6.3. Lentiviral vectors in clinical trials

Lentiviral vectors comprise approximately 20% of the current ongoing clinical trials involving viral vectors, with 315 trials reported at the end of 2021. They face potentially the highest level of social hesitancy given their derivation from HIV-1, but have also achieved some of the most high-profile clinical success with the advent of chimeric antigen receptor (CAR)-T cell therapy.

The use of third-generation self-inactivating lentiviral vectors has significantly mitigated the risk of insertional mutagenesis, which unfortunately occurred in some early trials which used gammaretroviral vectors. In a trial that attempted to treat X-linked severe combined immunodeficiency (SCID) using a gammaretroviral vector, four out of nine patients developed T-cell leukaemia as a result of insertional mutagenesis [104]. There are approaches involving the insertion of "buffer" or insulator sequences into the gene expression systems delivered by lentiviruses that aim to further mitigate any potential activation of neighbouring genes [105].

The unique characteristics of lentiviruses, along with the various techniques employed to enforce cell-specific and temporal regulation of transgene expression make them an attractive option for the modulation of endothelial cell metabolic gene expression. Their ability to infect both dividing and quiescent cells and the ability to achieve permanent transgene expression through multiple generations of cells is essential when targeting a process like angiogenesis, which involves extensive cell proliferation.

1.7. Assessment of Endothelial Cell Function *In Vitro* and *In Vivo*

1.7.1. Cellular metabolism in vitro

There are multiple techniques that can be used to quantify cellular metabolism *in vitro.* The longitudinal measurement of oxygen concentration in cell media is generally considered to be the gold standard for determining changes in mitochondrial respiration, since respiration is the main oxygen-consuming process in eukaryotic cells. This approach can be combined with the sequential and cumulative inhibition of different components that contribute to mitochondrial respiration, which allows a researcher to determine the relative contribution of each of those components to the overall metabolic phenotype.

The Seahorse Bioanalyser XF96 system provides researchers with a way to perform many technical replicates and inject the various inhibitors directly into the plate wells, while concurrently measuring oxygen consumption. The inhibitors that are commonly used to interrogate cellular metabolism are as follows, and are generally administered in this order.

Oligomycin A is a potent inhibitor of ATP synthase, and acts by blocking the proton channel in the F_0 subunit. Blocking the function of ATP synthase significantly reduces the flow of electrons through the electron transport chain and therefore significantly reduces oxygen consumption, which can be observed on the tracing chart. There will, however, be some

residual oxygen consumption which indicates a phenomenon called “proton leak”, which describes electron transport that is not coupled to ATP synthesis. Elevated proton leak can be indicative of mitochondrial damage, or of poor integrity of the inner mitochondrial membrane.

Carbonyl cyanide-p-trifluoromethoxyphenylhydrazone (FCCP) is an ionophore, and is commonly referred to as an uncoupling agent. It disrupts ATP synthesis by transporting hydrogen ions across the inner mitochondrial membrane, which mimics a very high level of electron transport and increased energy demands. On an oxygen consumption tracing chart, FCCP treatment will elicit a sharp increase in oxygen consumption, and this level indicates the maximum level of respiration that it is possible for a cell to achieve.

Antimycin A and rotenone are the final two inhibitors, and they are commonly administered together. Antimycin A can be used as an antibiotic, and it further inhibits electron transport by binding to the Q_i site of cytochrome c reductase, blocking the conversion of ubiquinol to ubiquinone. This blocks the creation of a proton gradient. Rotenone is an isoflavone and acts similarly, blocking the transfer of electrons from iron-sulphur centres in complex I to ubiquinone. On the oxygen consumption tracer chart, this appears as a sharp decrease, and indicates complete attenuation of oxidative phosphorylation. Any residual oxygen consumption measured by the XF analyser indicates oxygen consumption from non-mitochondrial sources.

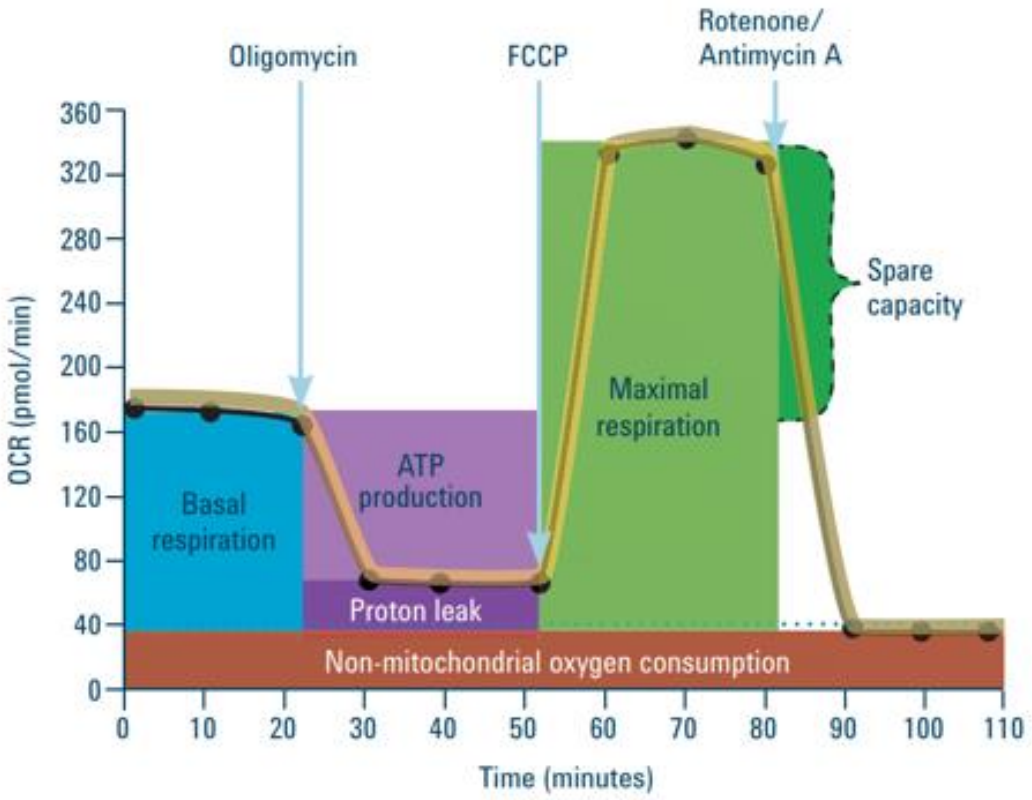

Figure 1.10. Example of an oxygen consumption tracer chart. A schematic depicting how cellular oxygen consumption responds to the inhibitors oligomycin, FCCP, and rotenone/antimycin A. The parameters such as basal or maximal respiration are highlighted in relation to the change in oxygen consumption, to show how each parameter is calculated. Figure copyright Agilent Technologies, 2020.

1.7.2. Angiogenesis in vitro

There are several assays that can be used to quantify the angiogenic functions of endothelial cells *in vitro,* each with their own benefits and challenges. It is useful to employ a number of different strategies to characterise the overall function of the cells. We are able to measure the fundamental functions that ECs must undergo to participate in angiogenesis, such as proliferation and migration, and we can also employ a more holistic assessment of angiogenesis using a tubulogenesis assay. These functional assays allow researchers to assess the effect of various treatments such as high glucose or hypoxia on EC function.

In these studies, we have assessed migration using the Boyden chamber method, which involves the seeding of treated endothelial cells on a permeable membrane within a transwell. The transwell can then be inserted into a larger well which contains media and an angiogenic stimulus such as VEGFA. The endothelial cells will migrate through the permeable membrane towards the angiogenic stimulus, and we can then quantify the number of migrated cells to determine their relative migratory capacity.

Tubulogenesis assays involve the seeding of treated cells into a gel matrix. The cells will be required to attach, migrate, and differentiate into capillary-like tubule structures, which mimics the angiogenic process which occurs *in vivo*. We can quantify the number of tubules that have formed, as well as their length and number of branching points. This allows us to characterise different aspects of cellular function required for tubule formation.

1.7.3. Angiogenesis in vivo

Many *in vivo* models have been developed to assess angiogenesis, each providing insight into a unique context. The most commonly used model of ischaemia-driven angiogenesis is the hindlimb ischaemia model, which involves unilateral ligation of the femoral artery to induce

distal ischaemia in the hindlimb, and assessment of revascularisation using laser Doppler perfusion imaging. This is a very simple model and can be useful in certain contexts. However, to characterise angiogenesis in the context of diabetic wound healing, we will use a unique model that was developed to better mimic human wound healing through re-epithelialisation [106]. This model allows for the assessment of angiogenesis within a more complex disease phenotype, and takes into account the many factors which are involved in wound healing.

The model involves injection of the mice with streptozotocin, which is toxic to pancreatic beta cells and attenuates insulin production. This causes the mice to become hyperglycaemic. Two full-thickness excisional wounds are created on the dorsal midline of the mice, and silicone splints are secured around them to reduce the contractile healing that is typical in murine skin. This means the wounds are forced to heal through re-epithelialisation mechanisms, and are therefore more accurately mimicking human wound healing. Treatments can then be applied topically, and wound characteristics tracked longitudinally. Laser doppler perfusion imaging can be used to efficiently quantify wound angiogenesis throughout the course of the study, and wound tissue can be collected at the study endpoint for histological analysis of angiogenesis and wound healing markers.

1.8. Hypothesis and Aims

Ischaemia-driven angiogenesis is a fundamentally important process for tissue recovery and repair following an ischaemic injury. Patients with diabetes experience significant impairments to angiogenesis, which is highlighted by their insufficient formation of collateral vessels and reduced wound neovascularisation. Because endothelial cell metabolic reprogramming underpins their angiogenic function, and is negatively impacted by diabetes on multiple levels, it represents an ideal target for development of new therapies that support endothelial cell function in hyperglycaemic environments. Our understanding of how mitochondrial respiration and the PDK4/PDC axis contribute to endothelial cell angiogenesis is relatively unexplored, even though this mechanism sits at a critical juncture between nutrient sensing and angiogenic functions. The way that metabolic pathways contribute to cellular function is highly context-dependent, and the role of endothelial cell metabolism in diabetes-impaired angiogenesis is currently unknown.

The hypotheses of this thesis were:

(1) The PDK4/PDC axis plays a critical role in endothelial cell angiogenesis, and
(2) The integrity of the axis is impaired in diabetes but can be rescued with rHDL treatment or by lentiviral overexpression of PDK4.
(3) Finally, restoration of the PDK4/PDC axis will improve endothelial cell angiogenesis *in vitro* in high glucose and wound angiogenesis and healing in diabetic mice.

The overarching aim of this work was to characterise the role of the PDK4/PDC axis in endothelial cell angiogenesis, the effect of diabetes upon the axis, and determine the efficacy of targeting the axis as a potential therapeutic strategy for diabetic vascular complications.

More specifically, the aims of this thesis were to:

i) Determine the role of PDK4 in endothelial cell angiogenesis through *in vitro* siRNA-mediated knockdown.

ii) Determine the effect of diabetes on the induction of the PDK4/PDC axis in response to hypoxia/ischaemia *in vitro* and *in vivo*.

iii) Investigate the effects of restoring the PDK4 through lentiviral-mediated overexpression of PDK4 and incubation with rHDL on endothelial cell metabolism and angiogenesis *in vitro.*

iv) Develop and validate an endothelial cell-specific, inducible lentiviral vector for overexpression of PDK4, and determine its effects upon endothelial cell angiogenesis *in vitro* and in a murine model of wound healing.

2. General Methods

2.1. Materials

Reagent/Material (Product Code)	**Manufacturer**
1-Bromo-3-chloropropane (B9673)	Sigma-Aldrich, MO, USA
Agarose (A9539)	Sigma-Aldrich, MO, USA
Biotium-GelRed™ 10,000X in Water (GTS41003)	Adelab Scientific, SA, Australia
Bolt™ 4-12% Bis-Tris Plus Gels, 10-wells (NW04120BOX)	Life Technologies, CA, USA
Bolt™ 4-12% Bis-Tris Plus Gels, 12-wells (NW04122BOX)	Life Technologies, CA, USA
Bolt™ 4-12% Bis-Tris Plus Gels, 17-wells (NW04127BOX)	Life Technologies, CA, USA
Bolt™ LDS Sample Buffer 4X (B0007)	Life Technologies, CA, USA
Bolt™ MES SDS Running Buffer 20X (B0002)	Life Technologies, CA, USA
Bolt™ Reducing Agent 10X (B0004)	Life Technologies, CA, USA
Bovine serum albumin (A7906)	Sigma-Aldrich, MO, USA
Chloroform (AJA152-2.5L GL)	Ajax Finechem, NSW, Australia
Clarity Western ECL Substrate (1705061)	Bio-Rad Laboratories, CA, USA
Library Efficiency™ DH5α Competent Cells (18263012)	ThermoFisher Scientific, MA, USA
DuoSet ELISA Ancillary Reagent Kit (DY008)	In Vitro Technologies, VIC, Australia
Ethanol (E7023)	Sigma-Aldrich, MO, USA
Ethanol (100%) for histopathology (FNNJJ008)	Fronine, NSW, Australia
Fluorescence Mounting Media (S302380-2)	Dako, CA, USA
Foetal bovine serum (AU-FBS/PG)	CellSera, NSW, Australia
Formalin (HT501128)	Sigma-Aldrich, MO, USA
GeneJET Gel Extraction Kit (K0691)	ThermoFisher Scientific, MA, USA
Glacial acetic acid (AJA1-2.5L PL)	Ajax Finechem, NSW, Australia
Glycine (G7126)	Sigma-Aldrich, MO, USA
Goat serum (G9023)	Sigma-Aldrich, MO, USA
Human/Mouse Total HIF-1 alpha/HIF1A DuoSet IC ELISA (DYC1935-2)	R&D Systems, MN, USA
Hydrochloric Acid, 37% (258148)	Sigma-Aldrich, MO, USA
Hydrogen peroxide solution (216763)	Sigma-Aldrich, MO, USA
iBlot™ 2 Transfer Stacks, regular size (IB23001)	Life Technologies, CA, USA
iBlot™ 2 Transfer Stacks, mini size (IB23002)	Life Technologies, CA, USA

ImmPACT® DAB Peroxidase Substrate (SK-4015)	Vector Laboratories, CA, USA
iScript cDNA Synthesis Kit (1708841)	Bio-Rad Laboratories, CA, USA
Isopropanol (I9516)	Sigma-Aldrich, MO, USA
Lillie Mayer's haematoxylin (AHLM)	Australian Biostain, VIC, Australia
Matrigel® Growth Factor Reduced Basement Membrane Matrix (356231)	Corning Life Sciences, NY, USA
MesoEndo Cell Growth Medium (212-500)	Cell Applications Inc., CA, USA
Methanol (MA004)	Chem-Supply, SA, Australia
Normal horse serum (S-2000)	Vector Laboratories, CA, USA
Nuclease-free water (P1193)	Promega, WI, USA
Opti-MEM™ I Reduced Serum Media (31985070)	Life Technologies, CA, USA
Paraformaldehyde (C004)	ProSciTech, QLD, Australia
PDK4 (Mouse) SimpleStep ELISA Kit (ab215544)	Abcam, Cambridge, UK
Phosphatase Inhibitor Cocktail 2 (P5726)	Sigma-Aldrich, MO, USA
Phosphate-buffered saline (D1408-500ML)	Sigma-Aldrich, MO, USA
Phenylmethylsulfonyl fluoride solution (93482)	Sigma-Aldrich, MO, USA
Pierce BCA Protein Assay Kit (23227)	ThermoFisher Scientific, MA, USA
Pierce™ ChIP-grade Protein A/G Magnetic Beads (26162)	ThermoFisher Scientific, MA, USA
Ponceau S solution (P7170-1L)	Sigma-Aldrich, MO, USA
Potassium Chloride(P5405)	Sigma-Aldrich, MO, USA
Potassium dihydrogen phosphate	Sigma-Aldrich, MO, USA
Precision Plus Protein Dual Color Standards (1610374S)	Bio-Rad Laboratories, CA, USA
Press-to-Seal™ Silicone Sheet, 0.5 mm thick (P18178)	Life Technologies, CA, USA
Protease Inhibitor Cocktail (P8340)	Sigma-Aldrich, MO, USA
Proteinase K (17916)	ThermoFisher Scientific, MA, USA
QIAGEN Plasmid Kit (12123)	QIAGEN, MD, USA
QIAquick PCR and Gel Cleanup Kit (28104)	QIAGEN, MD, USA
Reagent Diluent Concentrate 3 (DY004)	In Vitro Technologies, VIC, Australia
Recombinant human VEGF 165 (293-VE-010)	R&D Systems, MN, USA
Restore™ Western Blot Stripping Buffer (21059)	ThermoFisher Scientific, MA, USA
SalI-HF® Restriction Enzyme (R3138S)	New England BioLabs, MA, USA
Sample Diluent Concentrate 1 (DYC001)	In vitro Technologies, VIC, Australia
Sodium azide (SA189)	Chem-Supply, SA, Australia
Sodium chloride (71380)	Sigma-Aldrich, MO, USA

Sodium citrate tribasic dihydrate (C8532)	Sigma-Aldrich, MO, USA
di-Sodium hydrogen phosphate anhydrous	Sigma-Aldrich, MO, USA
SsoAdvanced™ Universal SYBR® Green Supermix (1725275)	Bio-Rad Laboratories, CA, USA
Streptozotocin (S0130)	Sigma-Aldrich, MO, USA
Tissue-Tek® O.C.T. compound (IA018)	ProSciTech, QLD, Australia
TRI® Reagent (T9424)	Sigma-Aldrich, MO, USA
Trichrome Stain Kit (ab150686)	Abcam, Cambridge, UK
Tris-Ethylenediaminetetraacetic acid (93283)	Sigma-Aldrich, MO, USA
Tris hydrochloride (T3253)	Sigma-Aldrich, MO, USA
Tris(hydroxymethyl)aminomethane (AJA2311)	Ajax Finechem, NSW, Australia
Triton X-100 (X100)	Sigma-Aldrich, MO, USA
Trypsin-EDTA (15400054)	ThermoFisher Scientific, MA, USA
Trypan Blue solution (T8154)	Sigma-Aldrich, MO, USA
Tween®-20 (P9416)	Sigma-Aldrich, MO, USA
Vectashield® Antifade Mounting Medium with DAPI (H-1200)	Vector Laboratories, CA, USA
Vector ImmPACT™ 3,3-Diaminobenzidine (DAB) (VESK4105)	Vector Laboratories, CA, USA
Vector® Red Alkaline Phosphatase Substrate kit (SK-5100)	Vector Laboratories, CA, USA
Xylene (FNNJJ028)	Fronine, NSW, Australia

2.2. *In Vitro* Methodology

2.2.1. Cell culture and treatments

Human coronary artery endothelial cells (HCAECs; Cell Applications Inc.) were used from passage 3-5 and maintained in MesoEndo Endothelial Media (Cell Applications Inc.) in T75 flasks.

Human aortic smooth muscle cells (HAoSMC; Lonza Bioscience) were used at passage 4 and maintained in SmGM™- 2 Smooth Muscle Cell Growth Medium (Lonza Biosciences) in T75 flasks.

Human dermal fibroblasts (HDFs) were used at passage 4 and maintained in Dulbecco's Modified Eagle Medium (DMEM; Sigma-Aldrich) with 10% foetal bovine serum in T75 flasks.

HEK293T cells were used for production of viral particles. Cells were used at passage 3-6 and were maintained in Dulbecco's Modified Eagle Medium (DMEM; Sigma-Aldrich) with 10% foetal bovine serum in T175 flasks.

To harvest the cells, two washes with pre-warmed PBS were conducted, and cells were incubated with 0.05% (w/v) trypsin-EDTA in PBS for 5 minutes at 37°C, typically using 5 mL per T75 culture flask. After visual confirmation of complete cell detachment, trypsin was inactivated by adding an equal volume of FBS-containing cell medium, and the cell suspension transferred to clean tubes before centrifuging at 2500 rpm for 5 minutes at room temperature. After removing the supernatant, the cells were re-suspended in the relevant cell media and counted using haemocytometer after mixing 1:1 with Trypan Blue to identify non-viable cells. Cells were subsequently seeded at the required density and underwent exposure to additional treatments or conditions.

For high glucose exposure, cells were treated with the relevant cell culture medium which was supplemented with D-glucose to a final concentration of 25mM for 72 hours.

To create a hypoxic environment, cells were placed in a hypoxia incubator with 1.2% O_2 and 5% CO_2 balanced with N_2. Hypoxia exposure was typically completed for 6 hours either as a terminal exposure or during the functional component of a functional assay.

2.2.2. Mechanistic studies

2.2.2.1. RNA extraction

Total RNA was isolated from treated cells by addition of 250µL TRI reagent (Sigma-Aldrich), followed by 25µL of 1-bromo-3-chloropropane (Sigma-Aldrich). Cells were then centrifuged at 14,000 RPM at 4ºC for 15 minutes. The top aqueous phase was removed and added to 125µL of isopropanol (Sigma-Aldrich), which was then left to rest at -20ºC at least overnight. The isopropanol solution was then centrifuged at 14,000 RPM at 4ºC for 15 minutes, and the resulting RNA pellet was washed with 75% ethanol before being resuspended in 20-30µL of nuclease-free water. The suspended pellet was stored at -80ºC until quantitation.

2.2.2.2. RNA quantitation and normalisation

The RNA concentration was quantified using a NanoDrop 8000 spectrophotometer (Thermo Fisher Scientific). Absorbance was measured at 260 and 280nm, and the relative purity of the isolated RNA was calculated from the absorbance ratio (A260/A280). For all samples, the ratio was within the range of 1.7 – 2.0. RNA samples were normalised to 100 ± 3ng/µL by adding the appropriate amount of nuclease-free water and stored at -80ºC until further use.

2.2.2.3. Reverse transcriptase polymerase chain reaction (RT-PCR)

300-1000ng of total RNA was reverse transcribed in triplicate using the iScript cDNA Synthesis Kit (BioRad). The PCR cycle was run on the T100 Thermal Cycler (BioRad) using the pre-set protocol for first-strand cDNA synthesis: annealing at 25°C for 5 minutes, extension at 42°C for 30 minutes, then inactivation at 95°C for 5 minutes. Triplicate samples were pooled, diluted 1:3 in nuclease-free water and stored at -20°C until ready to use for real-time PCR.

Table 1. Reaction mix for RT-PCR, per tube.

Component	**Volume (uL)**
iScript Reverse Transcriptase	2.0
Nuclease-free H_2O	5-X
Normalised RNA	X
Total	10.0

2.2.2.4. Quantitative RT-PCR (qRT-PCR)

Quantitative real-time PCR was performed to measure the mRNA expression of various genes. Changes in gene expression were normalised using the ΔΔ threshold cycle method to human β2-microglobulin (*B2M)* or murine *36b4*.

Primers for these genes were designed by our group using the Primer BLAST application (National Centre for Biotechnology Information, NCBI). Primer sets used were manufactured by Sigma-Aldrich and sequences shown in Table 2.

Table 2. qRT-PCR primer sequences

Target		**Sequence**
hPDK1	Forward	5’GGCCAGGTGGACTTCTACG3’
	Reverse	3’TGAACGGATGGTGTCCTGAG5’
hPDK2	Forward	5’AACACATCGGCAGCATCGAC3’
	Reverse	3’CCATGTGAATCGGCTGTTTGG5’
hPDK3	Forward	5’GCCATTACAAGACCACGCCT3’
	Reverse	3’GTCTTGATCTTGTCTTGTTTTGCTT5’
hPDK4/mPdk4	Forward	5′-CACGTACTCCACTGCTCCAA-3′
	Reverse	5′-AGCGTCTGTCCCATAACCTG-3
hPDP1	Forward	5’ACCACCGATTAAGGCCACAG3’
	Reverse	3’GCATCTGTCCCAGAGTCACC5’
hPDP2	Forward	5’TACCTGACTGCTGAGCCTGA3’
	Reverse	3’TGTCTTGTGCCAATCTGCCT5’
hB2M	Forward	5’-CATCCAGCGTACTCCAAAGA-3
	Reverse	5’-GACAAGTCTGAATGCTCCAC-3
m36b4	Forward	5-CAACGGCAGCATTTATAACCC-3
	Reverse	5'-CCCATTGATGATGGAGTGTGG-3

Table 3. Reaction mix for qRT-PCR analysis

Component	**Volume (uL)**
iQ SYBR Green Supermix	7.5
Forward primer, 10µM	0.6
Reverse primer, 10µM	0.6
Nuclease-free H_2O	3.3
cDNA	3.0
Total	15.0

The PCR reactions were performed in duplicate. Primers were used at 10µM in combination with the iQ SYBR green Supermix (Bio-Rad) in a Bio-Rad thermocycler, in the reaction mix described in Table 3. The protocol conditions included: initial denaturation and enzyme activation at 95°C for 3 minutes; 40 cycles of denaturation at 95°C for 30 seconds, annealing at 60°C for 30 seconds, followed by extension at 72°C for 30 seconds. A non-template control

(NTC) was included for each gene to detect contamination and primer-dimer formation that could produce a false positive result.

2.2.2.5. Protein extraction

To collect treated cells, media was removed and cells washed once in cold PBS. 100µL radioimmunoprecipitation assay (RIPA) lysis buffer (20 mM Tris-HCl, 1 mM EDTA, and 0.2% Triton X-100; pH 7.4), which also contained protease inhibitor cocktail (1:100, Sigma-Aldrich), and phenylmethanesulfonyl fluoride (PMSF) solution (1:100, Sigma-Aldrich), was added and cells were scraped and transferred to Eppendorf tubes. For ELISA analyses, cells were processed in the relevant cell extraction buffer. Each sample was sonicated for 3 seconds to further lyse the cells. Samples were centrifuged for 10 minutes at 14,000 rpm at 4ºC then stored at -80ºC.

2.2.2.6. Protein concentration estimation

The protein concentration for each sample was determined using the Bicinchoninic (BCA) Protein Assay (Thermo Fisher Scientific). A standard curve using bovine serum albumin (BSA, Sigma-Aldrich) concentrations of 0, 0.25, 0.5, 0.75, 1.0, 1.25, 1.5, 2.0 mg/mL was constructed from 2 mg/mL BSA stock.

The assay was conducted in a 96-well plate. Each well contained 5µL of standard or sample in duplicate, and 195µL of reagent mix consisting of 50 parts reagent A (Thermo Fisher Scientific) and 1 part reagent B (copper (II) sulphate) (Thermo Fisher Scientific). The assay was incubated at 37ºC for 30 minutes and absorbance of each well measured at 595nm using a microplate reader (Glomax) for data acquisition and analysis. The protein concentration of unknown samples was interpolated from the standard curve.

2.2.2.7. Western blot

Whole cell protein lysates were used to determine changes in the expression of various proteins. 10-20μg of protein was loaded into each gel. Protein samples were prepared by adding sample buffer (BioRad) and reducing agent (BioRad) in the quantities shown in Table 4, and made up to a variable total volume using distilled water. Samples were denatured by boiling at 95ºC for 5 minutes, then rested on ice for 5 minutes. Samples and the Precision Plus Protein™ Dual Color Standard (Bio-Rad) were added to a 10- or 12-well Bolt® 4% Bis-tris plus gel (Life Technologies) and run at 100 V for 90 minutes in Bolt® MES SDS Running Buffer (Life Technologies) diluted in distilled water. Proteins from the gel were then transferred onto nitrocellulose membranes (Life Technologies) using the iBlot Gel Transfer system (Life Technologies) run at 20 V for 7 minutes. Membranes were blocked in 5% (w/v) BSA in TBST (20 mM Tris, 136 mM NaCl, and 0.1% [w/v] tween 20, pH 7.4) for 1 hour at room temperature on a rocking platform. Following this, membranes were washed 3 times in TBST for 5 minutes at room temperature before probing with the relevant primary antibody overnight (Table 4). The membranes were washed again before incubation with goat anti-rabbit or anti-mouse secondary antibody conjugated with horseradish peroxidase (HRP) (1:1000, Company) in 1% BSA in TBST for 2 hours at room temperature. To assess even protein loading, membranes were ultimately probed for α-tubulin.

Table 4. Antibodies used for western blotting.

Target	Dilution	Product Code	Manufacturer
PDC (Ser^{293})	1:1000	ab92696	Abcam
PDC (Total)	1:1000	ab110334	Abcam
PHD1	1:1000	RDSAF6394SP	R&D Systems
PHD2	1:1000	NOVNB1002219	Novus Biologicals
PHD3	1:1000	NOVNB100303	Novus Biologicals
FOXO1 (Ser^{256})	1:1000	9461S	Cell Signalling Technologies
FOXO1 (Total)	1:1000	2880S	Cell Signalling Technologies
SR-BI	1:1000	ab52629	Abcam
α-tubulin	1:500	3873S	Cell Signalling Technologies

Table 5. Western blot sample dilution ratios

Total volume (µL)	1X Reducing agent (µL)	4X Sample buffer (µL)
20.0	2.0	5.3
25.0	2.5	6.7
30.0	3.0	8.0
40.0	4.0	10.7
50.0	5.0	13.3

Membranes were developed by chemiluminescence on the Chemidoc MP Imaging System (BioRad) with ECL reagents in a 1:1 ratio of Clarity Western Peroxide Reagent and Clarity Western Luminol/Enhancer Reagent (Biorad). Images were recorded and analysed using Image Lab Software (BioRad).

2.2.2.8. Enzyme-linked immunosorbent assay (ELISA)

Protein lysates as extracted in section 2.2.2.5 were analysed by ELISA to determine expression of human or murine PDK4 and HIF-1α.

For human or murine PDK4, ELISA kits from Abcam were used. 50-100µg of total protein in 150µL of Cell Extraction Buffer was added to a 96-well plate and combined with the Antibody Cocktail, then incubated for 1 h at room temperature on a plate shaker set to 400rpm. 100µL of the final substrate required for enzymatic colour production (TMB Substrate) was added to each well, followed by a 10 minute incubation, protected from light. 100µL of Stop Solution was added to each well, and absorbance recorded at 450nm.

For human HIF-1α, an ELISA kit from R&D Systems was used. For preparation of the ELISA plate, the capture antibody was diluted to a working concentration of 4µg/mL in PBS. A 96-well microplate was coated with 100µL per well of the diluted capture antibody, then sealed and incubated overnight at room temperature. Each well was aspirated and washed three times with Wash Buffer. Plate was blocked by adding 300µL of Reagent Diluent to each well and incubated at room temperature for 1 hour. After washing, 100µL of sample or standard in Reagent Diluent was added to each well, then incubated at room temperature for 2 hours. After washing, 100µL of the diluted detection antibody was added and again incubated for 2 hours at room temperature. 100µL of the diluted Streptavidin-HRP was added and incubated for 20 minutes, then washed, and 100µL of Substrate Solution was added, followed by 50µL of Stop Solution. The absorbance was recorded at 450 nm.

2.2.3. Functional studies

Three functional assays were used to assess the effect of various conditions and treatments on HCAEC angiogenic function. All experiments were performed in triplicate and repeated at least three times under normoxic, or hypoxic conditions stimulated by 1.2% O_2/5% CO_2 and N_2 balance in a hypoxic incubator. The Seahorse Bioanalyzer system was used to assess changes in cellular metabolic phenotype.

2.2.3.1. Matrigel tubulogenesis assay

Thawed growth factor-reduced Matrigel (BD Bioscience) was carefully plated at 40µL/well into a 96-well plate, ensuring no bubbles were present, and left to polymerise at 37ºC for 30 minutes. Treated HCAECs were trypsinised using 500µL of trypsin, counted, and seeded at 1 x 10^5 cells/mL in 50µL on polymerised growth factor-reduced Matrigel (In Vitro Technologies), then incubated at 37ºC in normoxia or hypoxia (1.2% O2 balanced with N2) for 6 hours. Endothelial cell tubules were imaged at 2.5X magnification under light microscopy. The total number of tubules and branch points formed was determined using ImageJ (National Institutes of Health).

2.2.3.2. Boyden chamber migration assay

A 24-well plate was prepared by adding 600µL of Opti-MEM containing 3% foetal bovine serum (FBS) and 10ng/mL of recombinant VEGF to each well. A transwell insert containing a membrane with 6.0µm diameter pores was carefully placed into each well. Treated HCAECs were trypsinised using 500µL of trypsin, and a diluted cell suspension of 2 x 10^5 cells/mL was prepared using Opti-MEM containing 3% FBS. 100µL of cell suspension was added to each well and the plate was incubated overnight at 37ºC. Media was aspirated from each transwell, which was then rinsed in PBS before being fixed in 4% paraformaldehyde in PBS for 10 minutes. A scalpel was used to cut out each membrane, which were then placed on a Superfrost slide and stained with 20µL of DAPI. Slides were imaged using an epifluorescence microscope. Five images were taken at 5X magnification from the same location on each membrane. The number of migrated cells was determined by counting the number of DAPI-stained nuclei using ImageJ (National Institutes of Health).

2.2.3.3. Seahorse XF Cell Energy Phenotype Test and Mito Stress Test

The Cell Energy Phenotype and Mito Stress Tests were used to determine the oxygen consumption rate (OCR) of treated HCAECs. The provided sensor cartridge was hydrated by adding 200µL distilled water to each well and placing the cartridge in a non-CO_2 37°C incubator overnight.

Treated HCAECs were gently trypsinised using 500µL of trypsin and counted. Cell suspension was diluted to 2.5 x 10^5 cells/mL using the provided assay media, and 80µL was added to each well of a 96-well microplate. The microplate was left to rest in the tissue culture hood for 1 hour to promote even cell distribution. Following this, the microplate was placed in a non-CO_2 37°C incubator for 45 minutes.

For the Cell Energy Phenotype Test, the injection ports of the sensor cartridge were then loaded with 20µL of the stressor mix, which was comprised of 500µL oligomycin and 250µL FCCP in 4250µL assay media when prepared as per manufacturer's instructions.

For the Mito Stress Test, the injection ports of the sensor cartridge were loaded with the following compounds, which were purchased independently from other suppliers.

Table 6. Seahorse XF Mito Stress Test inhibitors

Inhibitor	**Final Well Concentration (µM)**	**Final Well Volume (µL)**
Oligomycin	1.5	20.0
FCCP	0.25	22.0
Rotenone	0.5	25.0
Antimycin A	0.5	25.0

The sensor cartridge was then placed into the XF instrument and calibrated. Once the calibration was complete, the cell microplate was placed inside the machine and the assay was completed.

For normalisation of the data by assessing cell number/well, the CyQuant Direct Cell Proliferation kit (Thermo Fisher) was used. The direct nucleic acid stain (component A) and the direct background suppressor I (component B) reagents were combined in PBS and 50µL was added to each well. The microplate was incubated at 37°C for 30 minutes, and the fluorescent signal was then read using the GloMax® Discover Microplate Reader (Promega).

2.3. *In Vivo* Methodology

2.3.1. Animal studies

All experimental procedures were conducted with ethical approval from the SAHMRI Animal Ethics Committee. Mice were housed in a temperature/humidity-controlled environment under a 12-hour light/dark cycle with access to water and standard mouse chow ad libitum. For all studies male or female C57BL/6J mice were used at 6 – 8 weeks old. Mice were housed for up to one week in quarantine prior to experimentation. To assess the effects of various conditions and treatments, a surgical wound healing model was used.

2.3.2. Murine diabetic wound healing model

To conduct the surgical wound healing model, mice were anaesthetised by 2% isoflurane inhalation, with pedal reflex tested to ensure adequate analgesia. Two full-thickness excisions 4-6mm in diameter were made either side of the dorsal midline. A 10mm diameter splint was cut from a 0.5mm thick silicone sheet and secured around the wound using adhesive (superglue) and 6-8 interrupted sutures. Wound diameter measurements were taken on the x-axis, y-axis, and z-axis of the wounds using micro callipers before topical application or

injection of the relevant treatment was completed. A clear, occlusive dressing (OPSITE FLEXIFIX Transparent Film) was cut into 10mm diameter circles and placed over each wound. Following surgery, mice were injected subcutaneously with 0.1mL buprenorphine and monitored closely for signs of discomfort. Buprenorphine was administered daily following surgery.

Wound tissue was collected from cohorts of mice at day 1, day 3, and day 10 of the wound healing study. Collection at day 1 and day 3 allowed for examination of early-stage wound healing mechanisms, while collection at day 10 allowed for examination of late-stage wound healing mechanisms and histological analysis.

This model allows for examination of angiogenesis as it occurs post-induction of the ischaemic wound environment in the early and later stages of healing.

2.3.2.1. rHDL treatment in the murine diabetic wound healing model

To assess the effect of rHDL on wound angiogenesis and healing, rHDL or a PBS vehicle control was topically applied to each wound daily throughout the study. 50µg of rHDL was added to each wound, as quantified by apoA-I protein concentration.

2.3.2.2. Lentiviral treatment in the murine diabetic wound healing model

To assess the effect of PDK4 overexpression by lentiviral gene transfer on wound angiogenesis and healing, a PDK4-expressing or GFP-expressing control virus was injected into the wound tissue at a single site at the time of surgery. 25µL of lentivirus particles were injected into each wound at a concentration of 2×10^8 TU/mL

2.3.2.3. Doxycycline administration

Doxycycline hyclate was administered in the drinking water of the mice at a concentration of 1mg/mL, in light-protected water bottles. Water was changed every 48 hours.

2.3.3. Streptozotocin injection

Mice were rendered diabetic 2 – 3 weeks prior to surgery by a bolus intraperitoneal injection of streptozotocin (165mg/g). One week post-injection, diabetic hyperglycaemia was confirmed by testing blood glucose levels via the tail vein using an Accu-CHEK Performa Blood Glucometer, with a blood glucose level of 15.0mmol/L or above considered diabetic. Mouse weights and blood glucose levels were monitored closely following streptozotocin injection.

2.3.4. Sacrifice

Mice were sacrificed by overdose of isoflurane anaesthetic, followed by right ventricular cardiac puncture. Murine wound tissue and blood samples were collected for histology, mRNA expression, and protein expression analyses.

2.3.5. Blood collection

At the time of sacrifice, blood was collected using the right ventricular cardiac puncture method. Blood was collected into BD Vacutainer® EDTA tubes and kept on ice until centrifugation at 5000 rpm for 5 minutes. The plasma layer was retained and stored in 50µL aliquots at -80°C.

2.3.6. Laser Doppler imaging

The Laser Doppler imaging system (moorLDI2-IR, Moor instruments, Devon, UK) was used to assess blood flow perfusion at a site of injury. Mice were anaesthetised by inhalation of

isoflurane. Mice were placed flat in the prone position to image the dorsum. Images were taken at variable time-points post-surgery, with three scans taken per mouse at each time point. After imaging mice were allowed to recover in a separate cage before returning to housing.

2.3.7. RNA extraction

Tissue from the wound area was immediately frozen on dry ice following excision then stored in an Eppendorf tube at -80ºC. To extract RNA, tissues were homogenised at 6000 x g for 30 seconds in 500µL of TRI reagent using a Precellys homogeniser. Total RNA was then isolated using the method outlined in section 2.2.2.1.

2.3.8. Protein extraction

Tissue from the wound area was immediately frozen on dry ice following excision then stored in an Eppendorf tube at -80ºC. To extract total protein from the tissue, wound sections were homogenised in 150µL of RIPA lysis buffer, and total protein concentration was determined using the Pierce BCA Protein Assay Kit (Life Technologies) as outlined in section 2.2.2.5.

2.3.9. Histology

2.3.9.1. Sample preparation

For histological analysis of wound tissue, the whole wound area was excised at day 10 of the study and cut in half through the centre of the wound. The wound half was placed in 30% sucrose for 24 hours, followed by 4% paraformaldehyde for 24 hours, then in 70% ethanol at 4°C.

In a Shandon Excelsior ES® Tissue Processor (ThermoFisher Scientific), wound sections were gradually infused with paraffin using graded ethanol concentrations, xylene and then paraffin

in an 11-hour run. The wounds were then paraffin-embedded using a HistoStar^{TM} Embedding Workstation (ThermoFisher Scientific) and stored at room temperature.

Once the tissue had been processed and embedded in paraffin wax, 5µm sections were cut using a Seico Microtome, then mounted on SuperFrost+ slides. Sections were air dried and then placed at 60ºC overnight. Prior to staining, slides were deparaffinised using 2 x 5 minute incubations of xylene, then rehydrated in decreasing ethanol concentrations.

2.3.9.2. CD31 immunohistochemistry

For CD31 staining, slides were boiled for 20 minutes in sodium citrate buffer (10 mM sodium citrate, 0.05% Tween 20, pH 6.0) to achieve antigen retrieval. Slides were washed in PBST and incubated in 0.3% H_2O_2 – methanol solution for quenching endogenous peroxidase activity, then blocked for at least 4 hours with 10% goat serum. Slides were then incubated with mouse CD31 1º antibody (ab28364) at a 1:25 dilution in PBST overnight at 4ºC. After washing, slides were incubated with HRP-conjugated anti-rabbit 2º antibody at a 1:200 dilution in PBST for 2 hours at room temperature, then signal was detected for 12 minutes using a DAB Peroxidase Substrate Kit (Vector Labs). Slides were counterstained very quickly with haematoxylin, then dehydrated in ethanol and mounted with DPX Mounting Medium.

2.3.9.3. Image capture and processing

Histology samples were imaged using a Zeiss microscope attached to a digital camera. Images were recorded digitally using the Zen software. On the first image the megapixel count, aperture, shutter speed, white balance and ISO were set and used for all subsequent images.

Images of stained wound sections were taken at 10X magnification using the tile function to stitch multiple fields of view.

2.3.9.4. Image quantification

All images were analysed digitally using Image-Pro Premier software for all analyses.

For images taken under bright field, neovessels, arterioles, and collagen were quantified by setting the colour threshold of CD31, α-actin, and collagen (blue) staining and optimised visually on the first image respectively. The same parameters were used for all subsequent images.

2.4. Statistical Analysis

Data sets were analysed on GraphPad Prism software. Data were expressed as mean±SEM. Differences between treatment groups were calculated using a one-way ANOVA (Bonferroni comparison test post hoc) or Student t test. A two-way ANOVA (Bonferroni comparison test post hoc) was performed when comparing data at multiple time points. Significance was set at a two-sided $P<0.05$.

3. Characterising the role of the PDK4/PDC axis in endothelial cell angiogenic function *in vitro*

3.1. Introduction

Patients with diabetes exhibit impaired angiogenic responses to ischaemia, which underpin many of the vascular complications associated with diabetes. Ischaemia-driven angiogenesis is initiated by endothelial cells, which respond to molecular signals caused by hypoxia to become more active and undergo functions such as migration to form new blood vessels. Diabetes and high levels of glucose impair endothelial cells' ability to respond adequately to these pro-angiogenic signals through a diverse range of mechanisms, including through destabilisation of key transcription factors like HIF-1α [45], and through overstimulation of pathways which normally respond to nutrient levels and inflammation. [107, 108].

Endothelial cell metabolism, especially those pathways involving the breakdown of glucose, have been established as key drivers of the angiogenic capacity of endothelial cells. In particular, the ability for endothelial cells to upregulate glycolysis in response to hypoxia has been shown to be an essential function for the initiation of angiogenesis. Key glycolysis genes are consistently upregulated in hypoxia [41], and pharmacological inhibitors that suppress glycolysis demonstrate anti-angiogenic effects [109].

While the importance of glycolysis is clear, very few studies have been conducted to understand the role of mitochondrial respiration suppression in endothelial cell angiogenesis, particularly under hypoxic conditions. Suppression of mitochondrial respiration allows a cell to dampen its reliance on oxygen-consuming methods of ATP production, and is known to be an important mechanism for cell survival in hypoxia. The PDK/PDC axis is a key mediator of this suppression, as the PDKs phosphorylate the PDC to inhibit the conversion of glucose-derived pyruvate to acetyl-CoA. However, there are no studies which have examined the relative expression of the PDKs in endothelial cells, nor how they contribute to mitochondrial respiration under various conditions. PDK4 in particular is believed to play a central role in

nutrient and oxygen sensing, yet its role in inhibiting the PDC has not been previously studied in endothelial cells, nor have the implications this may have in diabetes-impaired angiogenesis. Since suppression of oxygen-consuming pathways is essential for endothelial cell function in the context of ischaemia-driven angiogenesis, the PDK4/PDC axis represents a previously unexplored mechanism to explain endothelial dysfunction in diabetes as well as a potential therapeutic target to stimulate angiogenesis.

The specific aims of this chapter were to (i) characterise the role of PDK4 in human endothelial cell angiogenic functions *in vitro*, including under high glucose conditions, and (ii) determine how modulation of the PDK4/PDC axis through lentiviral-mediated overexpression of PDK4 affects human endothelial cell function, including mitochondrial respiration and angiogenic functions under high glucose conditions. Based on previous findings which highlight the importance of suppression of mitochondrial respiration in endothelial cell function, it was hypothesised that disrupting the PDK4/PDC axis through siRNA-mediated knockdown of PDK4 would disturb regulation of mitochondrial respiration and impair endothelial cell angiogenic functions. Additionally, it was hypothesised that overexpression of PDK4 would enhance suppression of mitochondrial respiration, protecting the endothelial cells from metabolic overstimulation and impaired function by excess glucose.

3.2. Methods

3.2.1. Cell culture and treatments

Human coronary artery endothelial cells (HCAECs) were cultured as per section 2.2.1.

For high glucose exposure, cells were treated with MesoEndo which was supplemented with D-glucose to a final concentration of 25mM for 72 hours.

To create a hypoxic environment, cells were placed in a hypoxia incubator with 1.2% O_2 and 5% CO_2 balanced with N_2. Hypoxia exposure was completed for 2 or 6 hours.

3.2.2. Modulation of the PDK4/PDC axis

3.2.2.1. siRNA-mediated knockdown of PDK4

For small interfering RNA (siRNA) knockdown of pyruvate dehydrogenase kinase 4 (PDK4), HCAECs were seeded in 6-well tissue culture plates at 1.5 x 10^5 cells/well and cultured in MesoEndo endothelial cell media for 24 hours at 37ºC in 5% CO2. Media was then replaced with 500µL of Opti-MEM (Life Technologies), and 50nM siRNA for PDK4 or a scrambled control (Millennium Science Australia) was added in 300µL Opti-MEM containing 2.5% Lipofectamine 3000 (Thermo Fisher Scientific). Cells were incubated for 6 hours before media was replaced with fresh MesoEndo. 48 hours after siRNA treatment cells were harvested for gene expression or protein analysis.

3.2.2.2. Lentiviral-mediated overexpression of PDK4

For overexpression of PDK4 using lentiviral delivery of the human *PDK4* open reading frame (ORF), HCAECs were seeded in 6-well tissue culture plates at 5 x 10^4 cells/well. Cells were cultured in MesoEndo for 24 hours at 37ºC in 5% CO2. Media was then replaced with 800µL

of MesoEndo containing 8µg/mL polybrene. The PDK4 or GFP control lentivirus was added to each well at a concentration of 1 x 10^8 VP/mL or 1 x 10^6 TU/mL. After 24 hours, media was replaced with 3mL MesoEndo, and after a further 72 hours cells either underwent exposure to additional conditions or were processed for gene expression or protein analysis.

3.2.3. RNA extraction and analysis

RNA extraction and qRT-PCR analysis of cell mRNA expression was conducted as described in section 2.2.2.1 onward.

3.2.4. Protein extraction and analysis

Protein extraction and western blotting or ELISA analysis of cell protein expression was conducted as described in section 2.2.2.5 onward.

3.2.5. Functional studies

All functional studies, including Matrigel tubulogenesis assays, Boyden chamber migration assays, and Seahorse Bioanalyser assays were completed as described in section 2.2.3.

3.3. Results

3.3.1. Relative expression of PDK1-4 and PDP1-2 in endothelial cells

To understand how different isoforms of the PDKs and PDPs are expressed in comparison with one another, we first characterised the expression levels of the *PDK1-4* and *PDP1-2* genes in endothelial cells. In HCAECs cultured at baseline conditions, all *PDK* and *PDP* genes were detected by qPCR (Figure 3.1.). There were no differences between the mRNA levels of *PDK1, PDK2* and *PDK4*. *PDK3* mRNA levels were significantly lower compared to *PDK1* (44.1 ± 11.6 %, $P<0.01$). *PDP1* mRNA expression was significantly increased compared to *PDK1* (2987.0 ± 524.7 %, $P<0.0001$). *PDP2* mRNA expression was also significantly increased compared to *PDK1* (234.8 ± 41.8 %, $P<0.001$). In summary, the *PDK* genes are expressed at similar levels with the exception of *PDK3*, the expression level of which is significantly lower. The *PDPs* are generally expressed at a higher level than the *PDKs*.

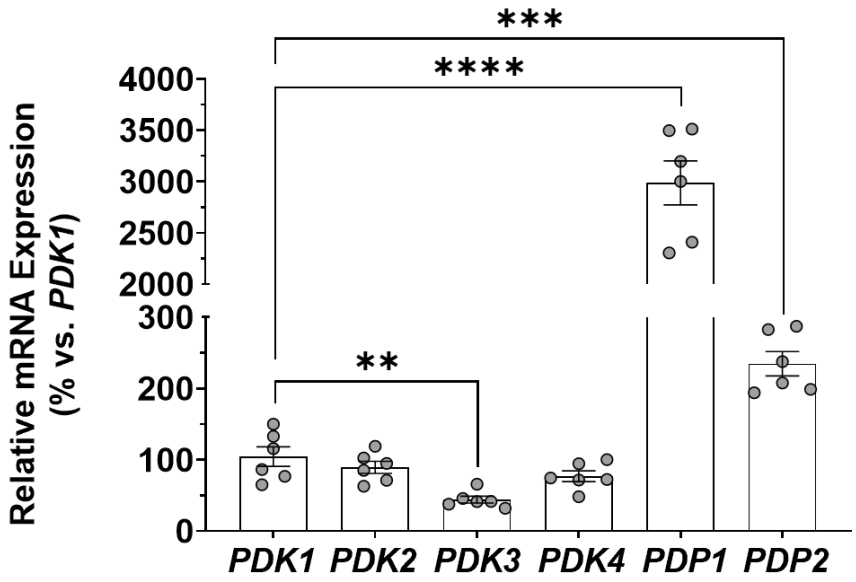

Figure 3.1. *PDK1-4, PDP1-2* mRNA levels in HCAECs under baseline conditions

HCAECs were cultured at 37°C for 24 hours. Relative mRNA levels of *PDK1, PDK2, PDK3, PDK4, PDP1, and PDP2* were measured by qPCR. mRNA expression was normalised to *18S* expression using the $^{\Delta\Delta}$Ct method, and presented relative to *PDK1* expression. Data are presented as mean ± SEM. ***P*<0.05, ****P*<0.001, *****P*<0.0001 by Two-way ANOVA with Bonferroni's *post hoc* analysis. *N* = 6, data are representative of 6 technical replicates across 2 independent experiments.

3.3.2. The effect of PDK4 knockdown on PDC phosphorylation

This experiment aimed to understand how knockdown of PDK4 affected PDC phosphorylation. In HCAECs transfected with siRNA targeting PDK4 (siPDK4), knockdown of *PDK4* was firstly confirmed using qPCR. *PDK4* mRNA levels were significantly lower in the siPDK4-treated cells, compared to the scrambled control (siScrbl)-treated cells (14.8 ± 6.8 % vs. 100.0 ± 52.3 %, $P<0.01$; Figure 3.2A). PDC phosphorylation was measured using western blotting. This revealed that siPDK4-treated cells exhibited significantly increased PDC phosphorylation compared to the siScrbl control (138.2 ± 23.5 % vs. 100.0 ± 5.8 %, $P<0.01$; Figure 3.2B). siRNA knockdown of PDK4 caused no changes in total PDC protein levels (Figure 3.2C). In summary, knockdown of *PDK4* was associated with an increase in PDC phosphorylation.

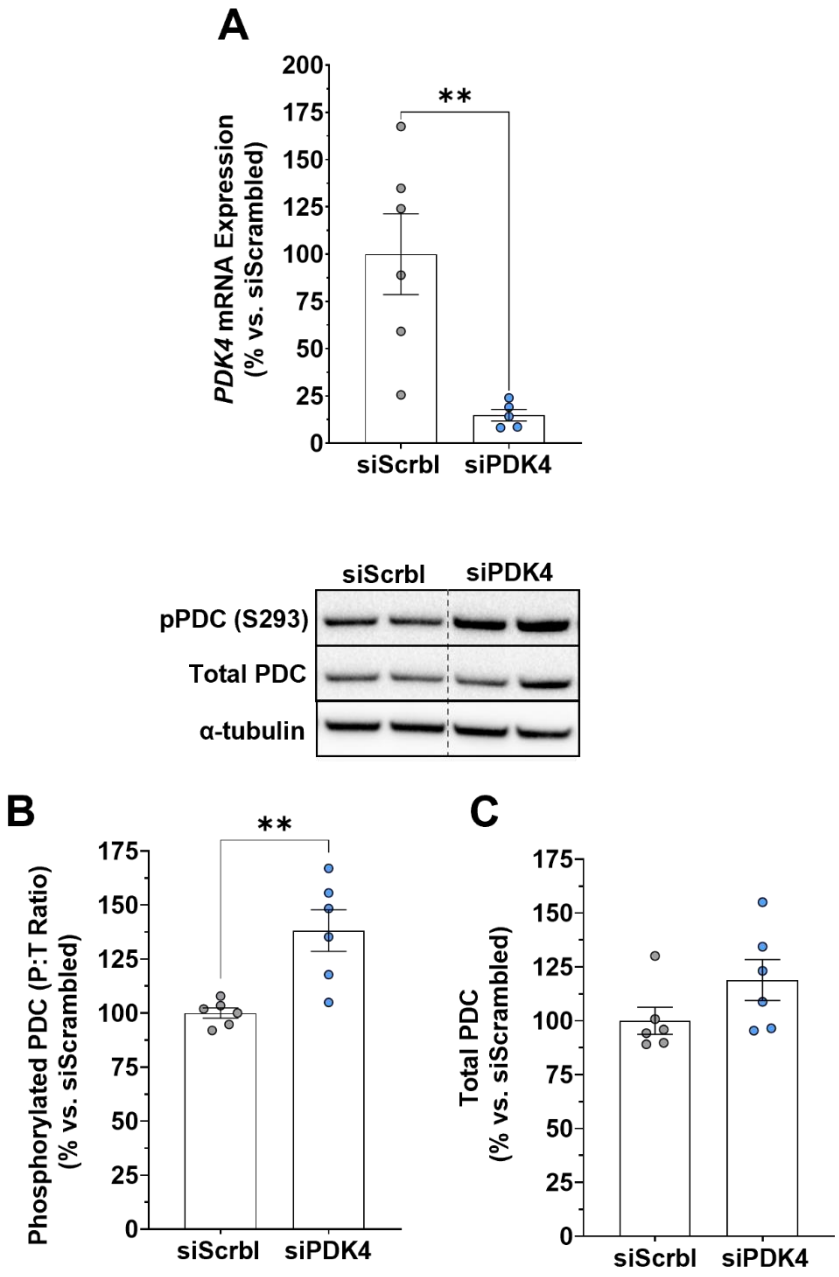

Figure 3.2. *PDK4* mRNA expression and PDC phosphorylation following PDK4 knockdown by siRNA.

HCAECs were treated with scrambled control siRNA (siScrbl) or siRNA-targeting PDK4 (siPDK4) for 48 h. Relative mRNA levels of *PDK4* were measured by qRT-PCR. PDC phosphorylation was assessed using western blotting, with representative images displayed in the upper panels. Data are presented as mean ± SEM. $^{**}P<0.01$ by unpaired student's t test. N = 5-6, data are representative of 5-6 technical replicates across 2 independent experiments.

To determine whether PDK4 knockdown elicited any compensatory effects on other PDC regulatory enzymes, we next determined changes in the *PDK1-3* and *PDP1-2* gene expression following siRNA knockdown of PDK4. This identified that PDK4 knockdown caused no significant changes in the mRNA levels of these related genes, suggesting no compensatory feedback mechanisms were operating at the mRNA level (Figure 3.3A-E).

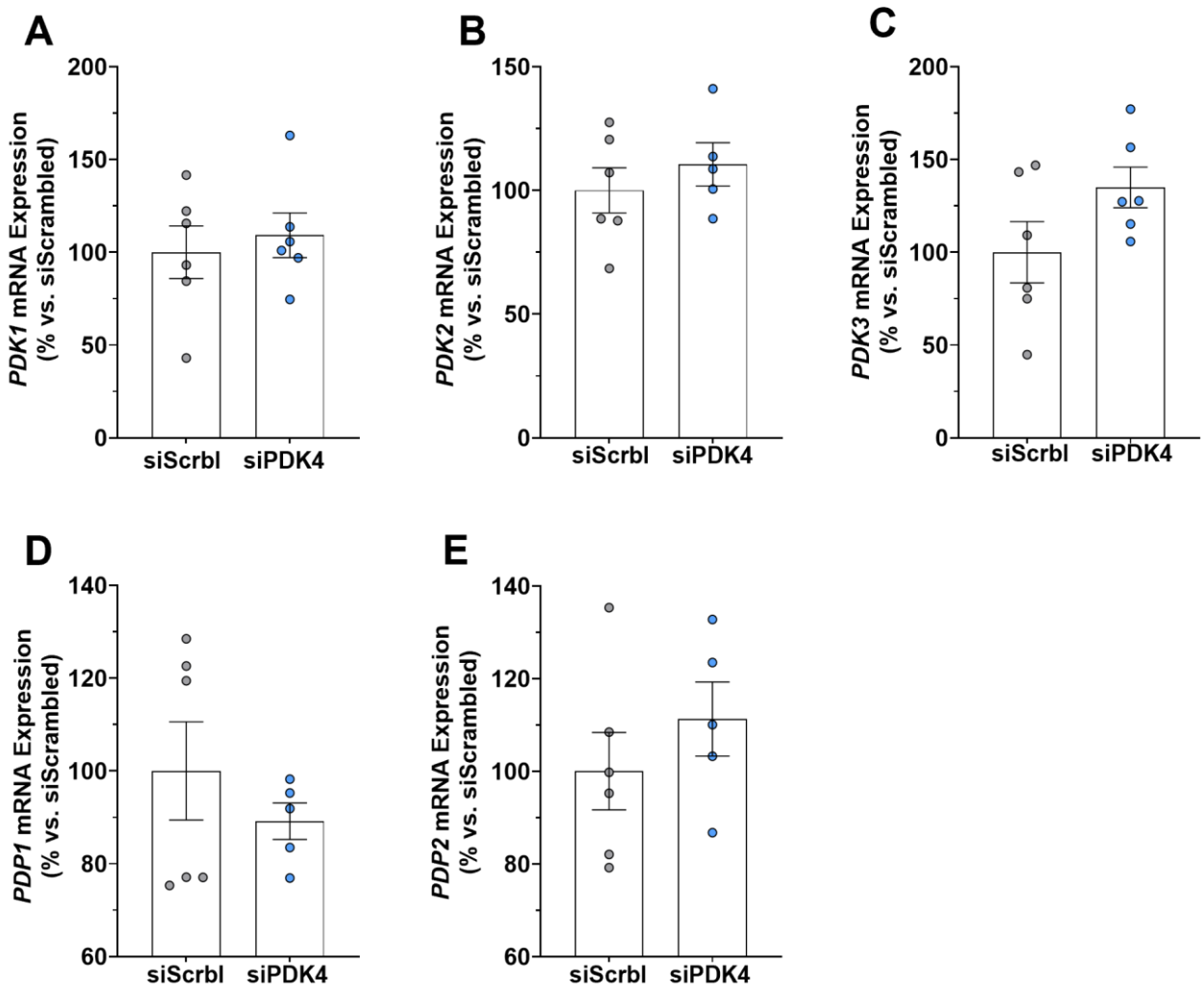

Figure 3.3. *PDK1-3* and *PDP1-2* mRNA expression following PDK4 knockdown by siRNA.

HCAECs were treated with scrambled control siRNA (siScrbl) or siRNA-targeting PDK4 (siPDK4) for 48 h. Relative mRNA levels of *PDK1*, *PDK2*, *PDK3*, *PDP1* and *PDP2* were measured by qRT-PCR. Data are presented as mean ± SEM. *N* = 6, data are representative of 6 technical replicates across 2 independent experiments.

3.3.3. siRNA knockdown of PDK4 suppresses mitochondrial respiration in vitro

This experiment aimed to determine how PDK4 knockdown affected endothelial cell mitochondrial respiration. An oxygen consumption tracing graph was generated to demonstrate the change in oxygen consumption over time (Figure 3.4A). HCAECs subjected to siPDK4 transfection exhibited a significant reduction in basal mitochondrial respiration compared to the siScrbl-treated cells (8.9 ± 1.5 vs. 10.7 ± 1.7 pmol/min, $P<0.001$; Figure 3.4B). Maximal respiration was also reduced in the siPDK4-treated cells compared to the siScrbl-treated cells (11.0 ± 1.7 vs. 14.0 ± 2.6 pmol/min, $P<0.0001$; Figure 3.4C), as was ATP production (6.6 ± 1.0 vs. 7.8 ± 1.0 pmol/min, $P<0.001$; Figure 3.4F). There was no change in non-mitochondrial oxygen consumption (Figure 3.4D) or proton leak (Figure 3.4E). In summary, PDK4 knockdown suppressed mitochondrial respiration.

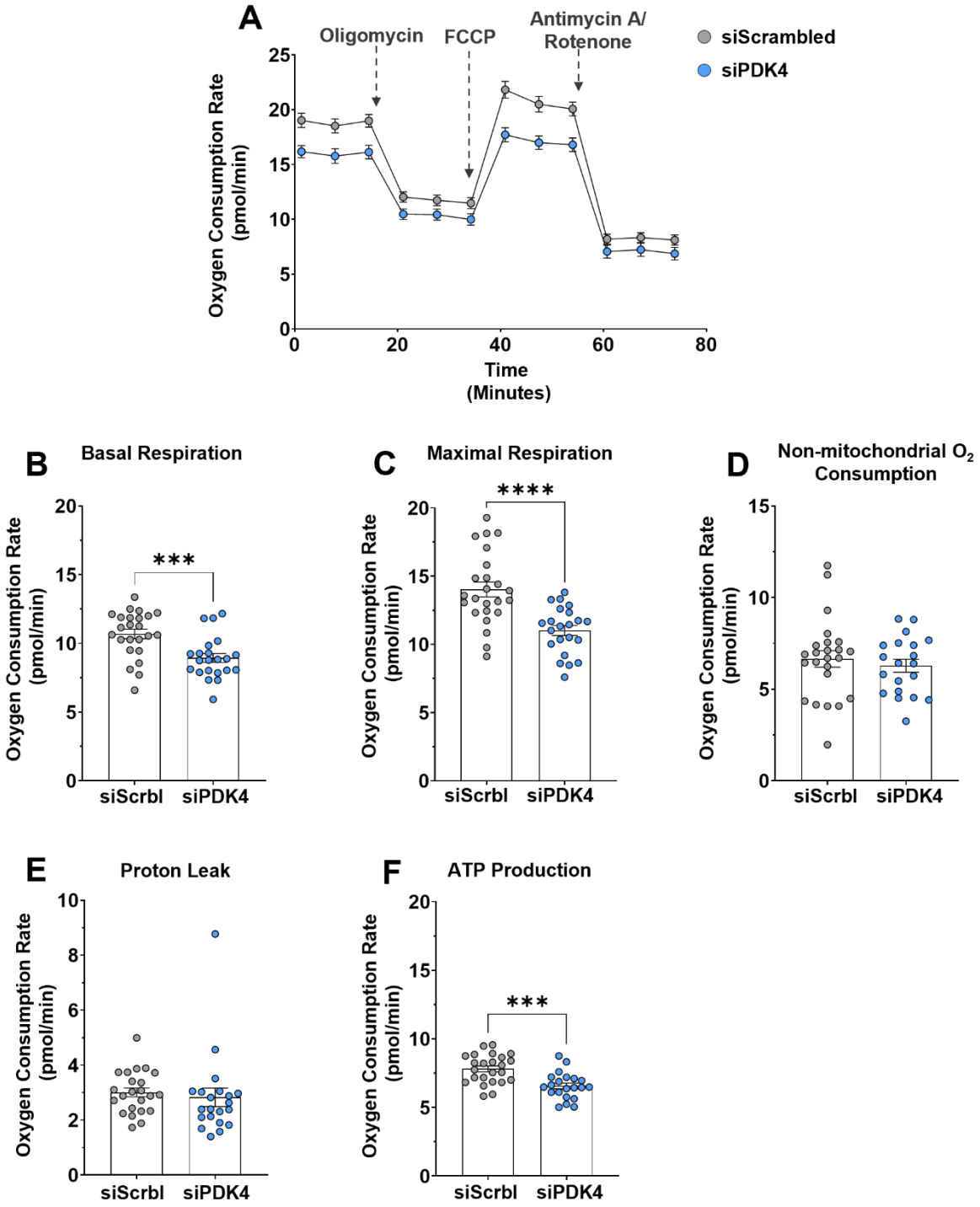

Figure 3.4. Endothelial cell mitochondrial respiration following PDK4 knockdown by siRNA

HCAECs were treated with scrambled control siRNA (siScrbl) or siRNA-targeting PDK4 (siPDK4) for 48 h. The Seahorse Bioanalyser system was used to measure cellular oxygen consumption and the effects of oligomycin, FCCP, antimycin A, and rotenone. OCR measurements were normalised to total cell number post-assay. Data are presented as mean ± SEM. ***P<0.001, ****P<0.0001 by unpaired student's t test. N = 22-24, data are representative of 22-24 technical replicates across 3 independent experiments.

3.3.4. siRNA knockdown of PDK4 impairs endothelial cell tubulogenesis in vitro

This experiment aimed to determine how PDK4 knockdown affected endothelial cell tubulogenesis. In a Matrigel tubulogenesis assay, knockdown of PDK4 significantly reduced tubule number compared to the siScrbl control in both normoxia (36.8 ± 3.1 vs. 100.0 ± 3.8 %, $P<0.0001$; Figure 3.5A) and hypoxia (28.7 ± 9.5 vs. 93.9 ± 17.1 %, $P<0.0001$), indicating that knockdown of PDK4 impairs endothelial cell angiogenic functions *in vitro.*

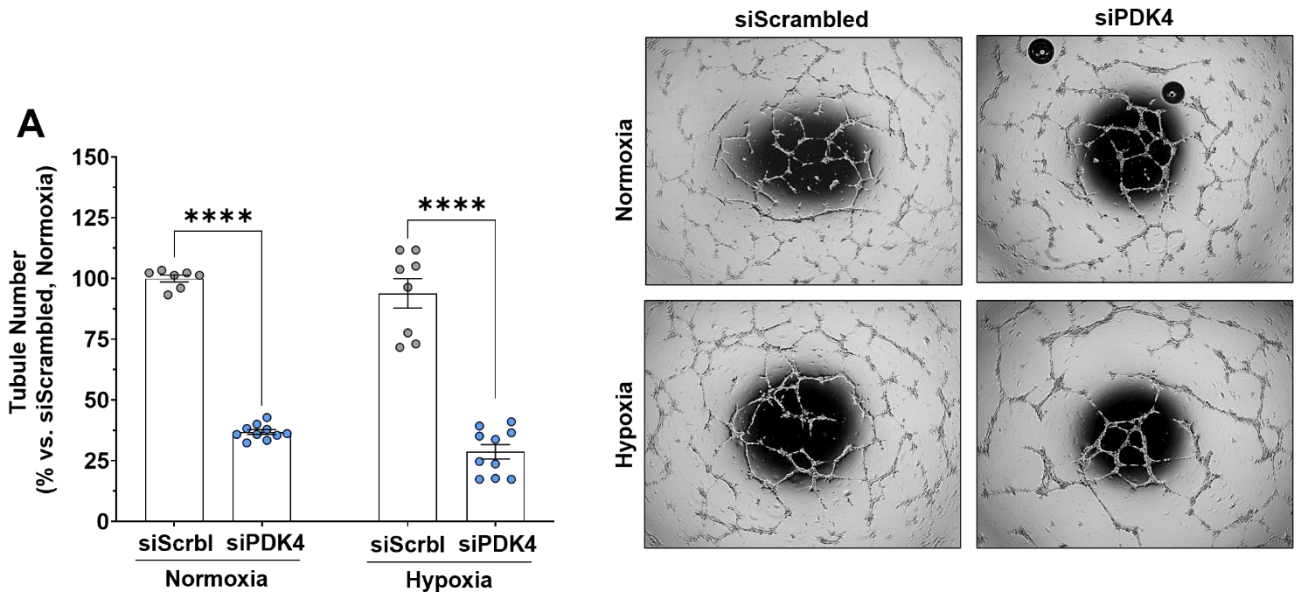

Figure 3.5. Endothelial cell tubule formation following PDK4 knockdown by siRNA

HCAECs were treated with scrambled control siRNA (siScrbl) or siRNA-targeting PDK4 (siPDK4) for 48 h. Cells were harvested and plated on growth factor-reduced Matrigel to assess tubule formation. Tubules were imaged at 5X magnification and quantified using ImageJ. Data are presented as mean ± SEM. ****P<0.0001 by unpaired student's t test. N = 7-10, data are representative of 7-10 technical replicates across 2 independent experiments.

3.3.5. The effect of siRNA knockdown of PDK4 on PDC phosphorylation under high glucose conditions

This experiment aimed to determine how PDK4 knockdown affected PDC phosphorylation with the addition of high glucose and hypoxia exposure. In hypoxia, siPDK4-treated HCAECs exhibited reduced *PDK4* mRNA expression in normal (9.5 ± 9.5 vs. 234.0 ± 34.0 %, $P<0.01$; Figure 3.6A) and high glucose (63.5 ± 51.3 vs. 251.5 ± 97.8 %, $P<0.05$; Figure 3.6A). When PDC phosphorylation was examined after 2 hours of hypoxia exposure, there was no detectable change in phosphorylation of the PDC across treatment conditions (Figure 3.6B). In hypoxia, and following exposure to high glucose, siPDK4 knockdown elicited a significant reduction in total PDC expression (74.0 ± 2.2 vs. 93.9 ± 6.9 %, $P<0.05$; Figure 3.6C). In HCAECs exposed to 6 hours of hypoxia, siRNA knockdown of PDK4 caused no detectable changes in phosphorylated or total protein levels of the PDC (Figure 3.6D-E).

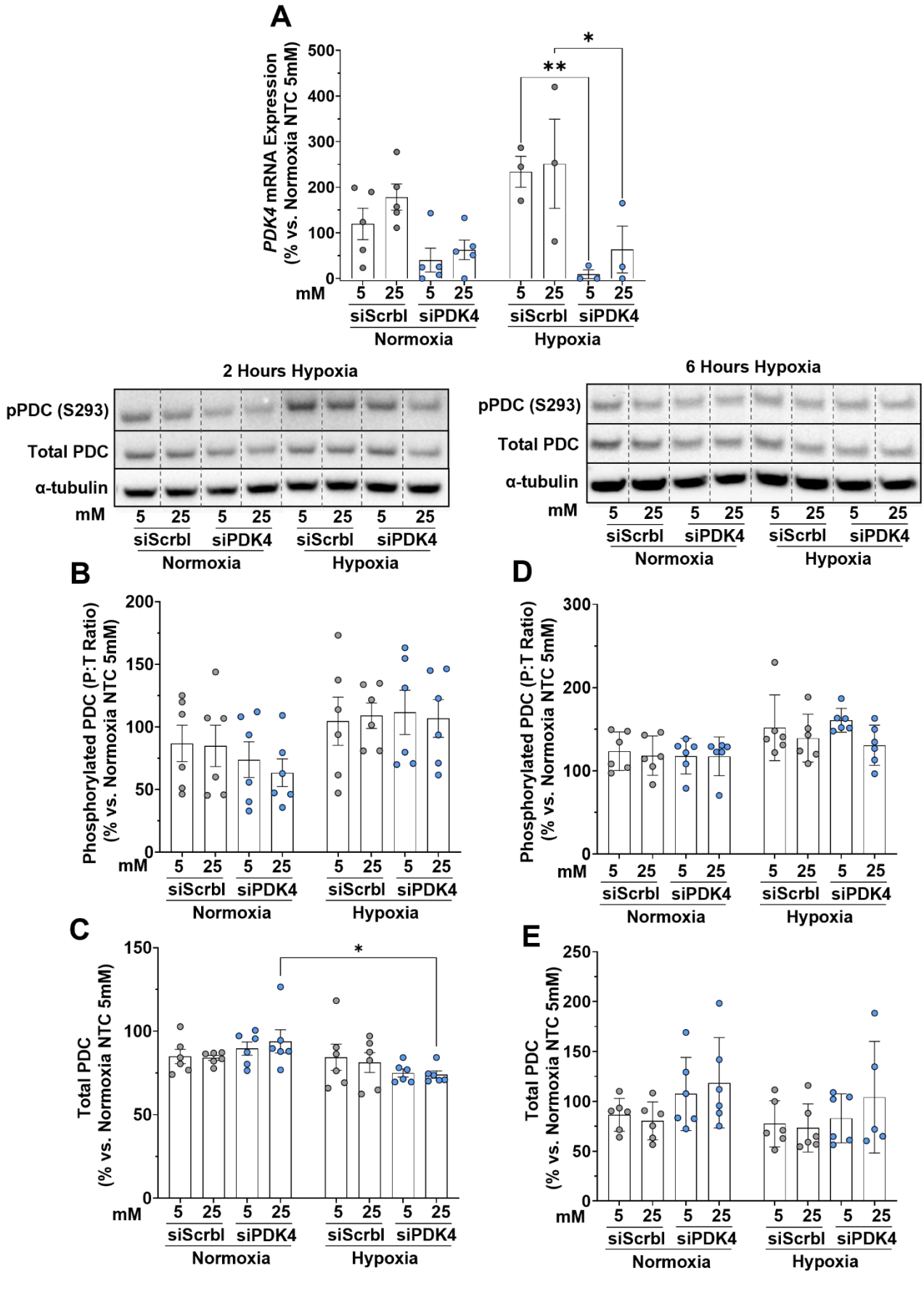
A
PDK4 mRNA Expression (% vs. Normoxia NTC 5mM)
500
400
300
200
100
0
*
**
mM
5 25 5 25 5 25 5 25
siScrbl siPDK4 siScrbl siPDK4
Normoxia
Hypoxia
2 Hours Hypoxia
pPDC (S293)
Total PDC
α-tubulin
mM
5 25 5 25 5 25 5 25
siScrbl siPDK4 siScrbl siPDK4
Normoxia
Hypoxia
6 Hours Hypoxia
pPDC (S293)
Total PDC
α-tubulin
mM
5 25 5 25 5 25 5 25
siScrbl siPDK4 siScrbl siPDK4
Normoxia
Hypoxia
B
Phosphorylated PDC (P:T Ratio) (% vs. Normoxia NTC 5mM)
200
150
100
50
0
mM
5 25 5 25 5 25 5 25
siScrbl siPDK4 siScrbl siPDK4
Normoxia
Hypoxia
D
Phosphorylated PDC (P:T Ratio) (% vs. Normoxia NTC 5mM)
300
200
100
0
mM
5 25 5 25 5 25 5 25
siScrbl siPDK4 siScrbl siPDK4
Normoxia
Hypoxia
C
Total PDC (% vs. Normoxia NTC 5mM)
150
100
50
0
*
mM
5 25 5 25 5 25 5 25
siScrbl siPDK4 siScrbl siPDK4
Normoxia
Hypoxia
E
Total PDC (% vs. Normoxia NTC 5mM)
250
200
150
100
50
0
mM
5 25 5 25 5 25 5 25
siScrbl siPDK4 siScrbl siPDK4
Normoxia
Hypoxia

Figure 3.6. *PDK4* mRNA expression and PDC phosphorylation following PDK4 knockdown by siRNA.

HCAECs were treated with scrambled control siRNA (siScrbl) or siRNA-targeting PDK4 (siRNA) for 48 h, then exposed to normal (5mM) or high (25mM) glucose for 72 h. Hypoxia exposure was completed for 2 or 6 h. Relative mRNA levels of *PDK4* were measured by qPCR. PDC phosphorylation was assessed using western blotting, with representative images displayed in the upper panels. Data are presented as mean ± SEM. ***P*<0.01 by Two-way ANOVA with Bonferroni's *post hoc* analysis. *N* = 5-6, data are representative of 5-6 technical replicates across 2 independent experiments. NTC; non-transfected control.

3.3.6. The effect of siRNA knockdown of PDK4 on endothelial cell tubulogenesis under high glucose conditions

This experiment aimed to understand how PDK4 knockdown affected endothelial cell tubulogenesis under high glucose conditions. High glucose exposure significantly reduced HCAEC tubule formation compared to normal glucose conditions in normoxia (47.3 ± 23.7 vs. 100.0 ± 20.4 %, $P<0.001$; Figure 3.7A) and hypoxia (58.8 ± 25.9 vs. 120.8 ± 16.6 %, $P<0.0001$). siPDK4 knockdown significantly further reduced tubule formation compared to the siScrbl control under normal glucose conditions in normoxia (54.2 ± 8.0 vs. 100.0 ± 20.4 %, $P<0.01$) and hypoxia (62.2 ± 15.5 vs. 120.8 ± 16.6 %, $P<0.0001$). In summary, PDK4 knockdown reduced endothelial cell tubule formation under normal glucose conditions, but did not elicit a stepwise reduction under high glucose conditions.

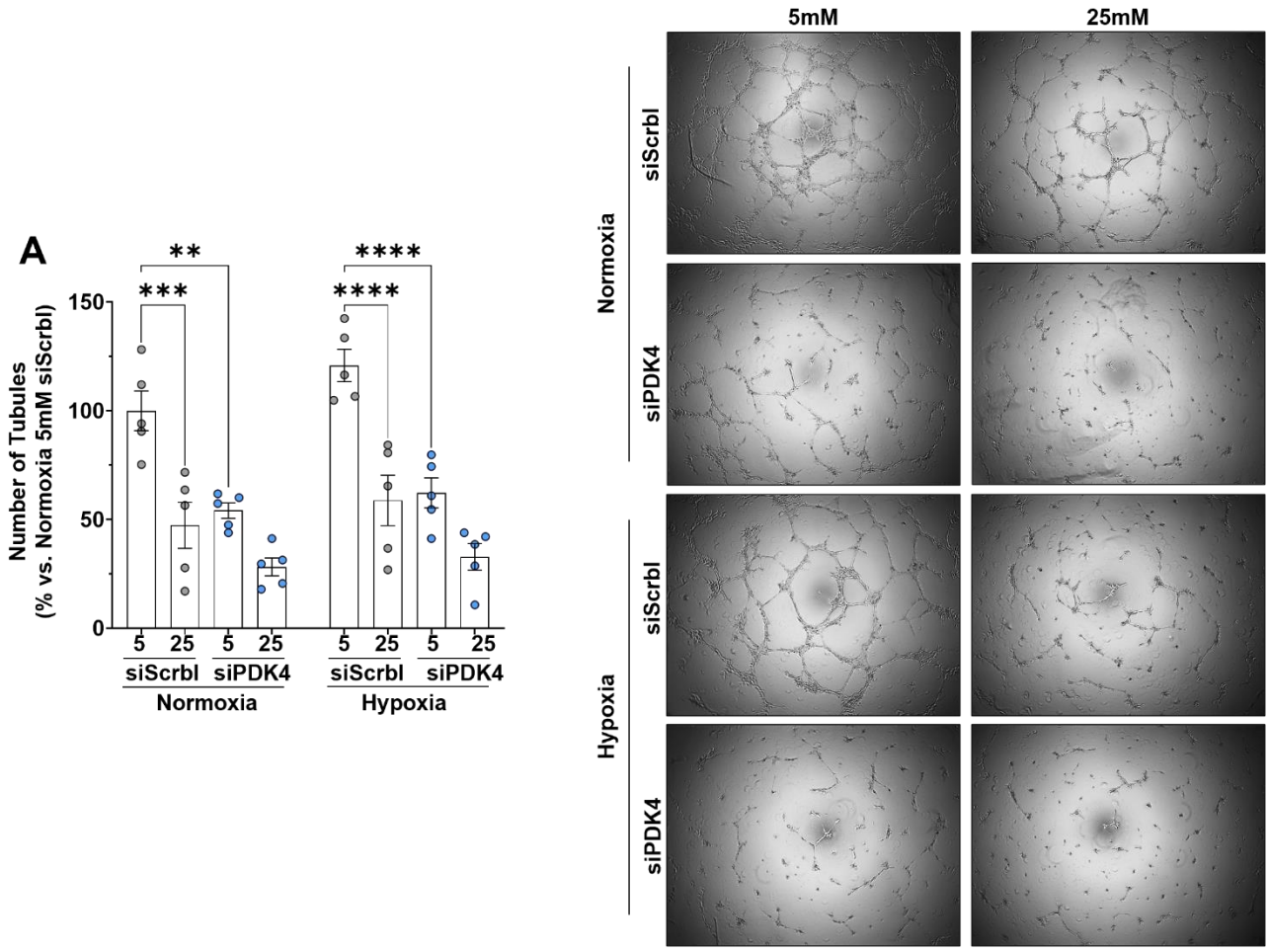

Figure 3.7. Endothelial cell tubule formation under high glucose conditions following PDK4 knockdown by siRNA

HCAECs were treated with scrambled control siRNA (siScrbl) or siRNA-targeting PDK4 (siRNA) for 48 h, then exposed to normal (5mM) or high (25mM) glucose for 72 h. Hypoxia exposure was completed for 6 h. Cells were harvested and plated on growth factor-reduced Matrigel to assess tubule formation. Tubules were imaged at 5X magnification and quantified using ImageJ. Data are presented as mean ± SEM. ***P*<0.01, ****P*<0.001, *****P*<0.0001 by two-way ANOVA with Bonferroni's *post hoc* analysis. *N* = 5-6, data are representative of 5-6 technical replicates across 2 independent experiments.

3.3.7. The effect of lentiviral PDK4 overexpression on PDC phosphorylation under high glucose conditions

This experiment aimed to determine how overexpression of PDK4 using a lentiviral vector affected PDC phosphorylation under high glucose and hypoxic conditions.

Under high glucose conditions in normoxia, treatment with a lentivirus overexpressing PDK4 (lentiPDK4) elevated *PDK4* mRNA expression (350.0 ± 97.0 vs. 87.9 ± 14.4 %, $P<0.05$; Figure 3.8A) compared to the GFP-expressing lentiviral control vector (lentiGFP). Under normal glucose conditions in hypoxia, the lentiPDK4-treated cells exhibited non-significantly elevated *PDK4* mRNA levels compared to the lentiGFP control (284.7 ± 96.7 vs. 104.5 ± 20.0 %). Under high glucose conditions in hypoxia, *PDK4* mRNA levels were again non-significantly elevated in the lentiPDK4-treated cells compared to the lentiGFP-treated cells (420.1 ± 166.6 vs. 107.6 ± 7.6 %).

We next examined PDC phosphorylation in response to hypoxia and high glucose. Hypoxia exposure significantly increased phosphorylation across all conditions ($P<0.0001$ for all comparisons; Figure 3.8B). High glucose exposure in hypoxia reduced PDC phosphorylation compared to the normal glucose control in the lentiGFP-treated cells (166.3 ± 12.9 vs. 220.8 ± 21.0 %, $P<0.01$; Figure 3.8B). In the lentiPDK4-treated cells, there was no reduction in PDC phosphorylation with high glucose exposure. In summary, PDK4 overexpression prevented a high glucose-induced reduction in PDC phosphorylation.

There were no changes in the total PDC protein levels across any conditions (Figure 3.8C).

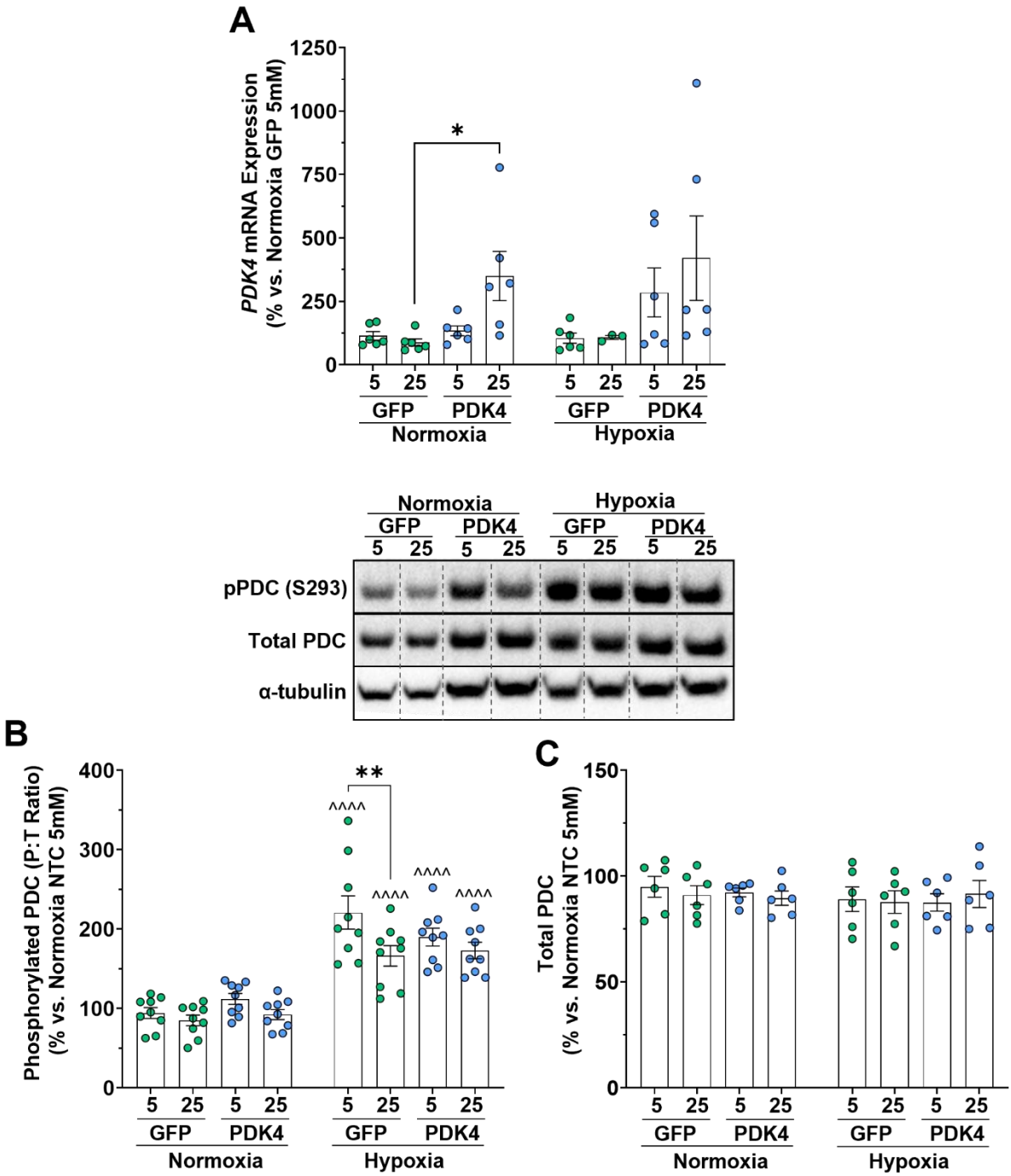

Figure 3.8. The effect of lentiviral PDK4 overexpression on PDC phosphorylation under high glucose conditions

HCAECs were transduced with a lentivirus encoding GFP or PDK4 (1 x 10^8 VP/mL), then exposed to normal (5mM) or high (25mM) glucose for 72 h. Hypoxia exposure was completed for 6 h. Relative mRNA levels of *PDK4* were measured by qRT-PCR. PDC phosphorylation was assessed using western blotting, with representative images displayed in the upper panels. Data are presented as mean ± SEM. **P*<0.05, ***P*<0.01 vs. the annotated controls. ^^^^*P*<0.0001 vs. normoxia controls by two-way ANOVA with Bonferroni's *post hoc* analysis. *N* = 6-9, data are representative of 6-9 technical replicates across 3 independent experiments.

3.3.8. Lentiviral PDK4 overexpression suppresses mitochondrial respiration in vitro

This experiment aimed to determine how PDK4 overexpression affected endothelial cell mitochondrial respiration. Hypoxia exposure reduced basal respiration compared to the normoxia control in the lentiGFP- (4.2 ± 0.6 vs. 8.2 ± 0.3 pmol/min, $P<0.0001$; Figure 3.9B) and lentiPDK4-treated HCAECs (2.0 ± 0.2 vs. 8.3 ± 0.9 pmol/min, $P<0.0001$). Under hypoxic conditions, overexpression of PDK4 using lentiPDK4 elicited a further reduction in basal respiration compared to the lentiGFP-treated cells (2.0 ± 0.2 vs. 4.2 ± 0.6 pmol/min, $P<0.05$; Figure 3.9B).

Hypoxia exposure also reduced maximal respiration compared to the normoxia control in the lentiGFP- (3.3 ± 0.8 vs. 17.7 ± 0.7 pmol/min, $P<0.0001$; Figure 3.9C) and lentiPDK4-treated HCAECs (1.4 ± 0.1 vs. 13.7 ± 0.6 pmol/min, $P<0.0001$). Under normoxic and hypoxic conditions, overexpression of PDK4 in lentiPDK4-treated HCAECs exhibited reduced maximal respiration compared to the lentiGFP-treated cells (normoxia: 13.7 ± 0.6 vs. 17.7 ± 0.7 pmol/min, $P<0.05$), (hypoxia: 1.4 ± 0.1 vs. 3.3 ± 0.8 pmol/min, $P<0.05$; Figure 3.9C).

Under hypoxic conditions, the lentiPDK4-treated HCAECs exhibited a reduction in non-mitochondrial O_2 consumption compared to the normoxic control (2.3 ± 0.3 vs. 3.8 ± 0.4 pmol/min, $P<0.05$; Figure 3.9D).

Under hypoxic conditions, the overexpression of PDK4 caused a reduction in proton leak compared to the normoxic control (1.2 ± 0.1 vs. 2.8 ± 0.2 pmol/min, $P<0.05$; Figure 3.9E).

Finally, hypoxia exposure reduced ATP production compared to the normoxia control in the lentiGFP- (2.8 ± 0.4 vs. 5.8 ± 0.2 pmol/min, $P<0.0001$; Figure 3.9F) and lentiPDK4-treated cells (0.8 ± 0.1 vs. 5.6 ± 0.5 pmol/min, $P<0.0001$). Under hypoxic conditions, the lentiPDK4-treated cells displayed reduced ATP production compared to the lentiGFP-treated cells (0.8 ±

0.1 vs. 2.8 ± 0.4 pmol/min, $P<0.05$). In summary, PDK4 overexpression suppresses endothelial cell mitochondrial respiration.

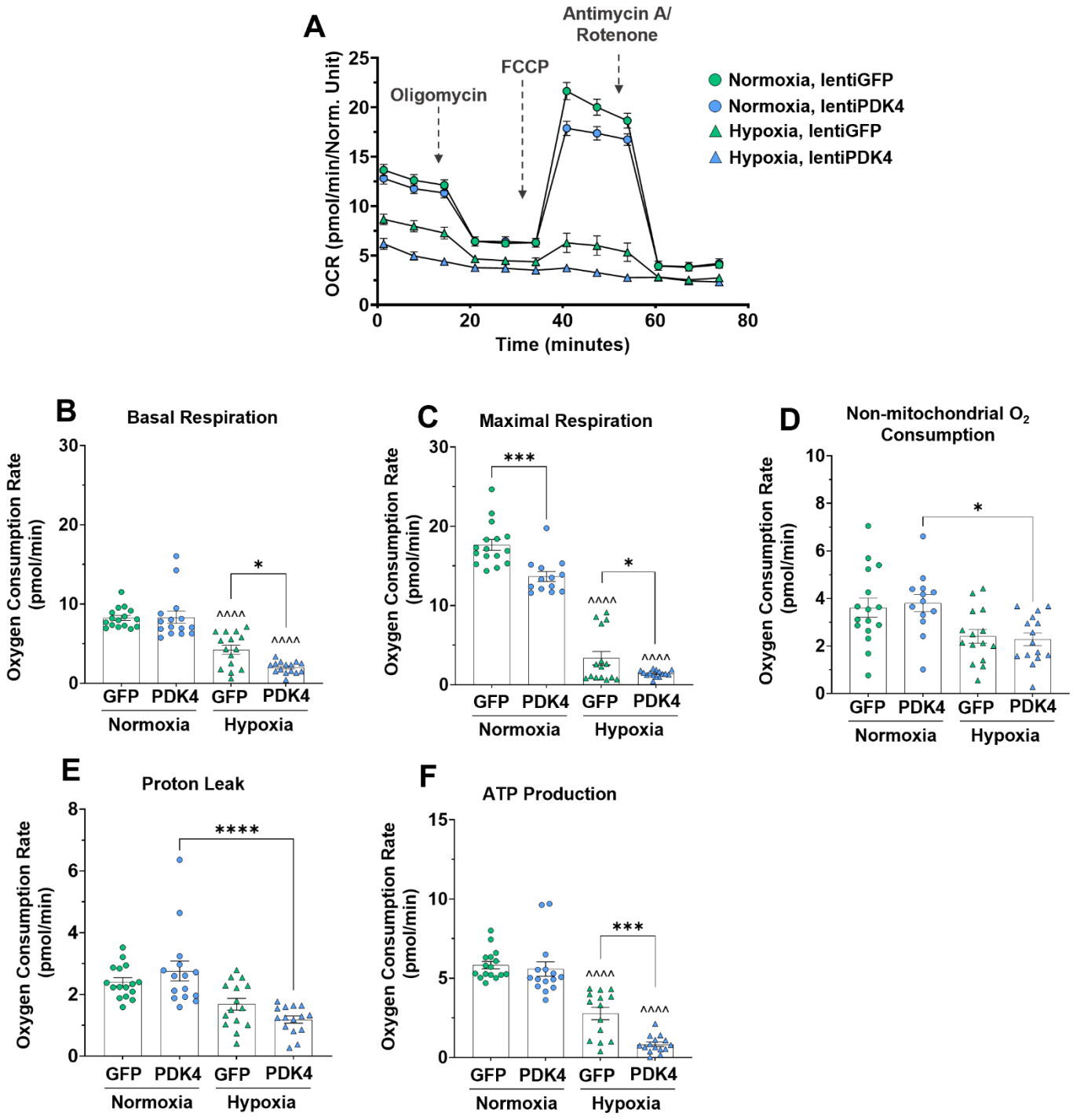

Figure 3.9. Lentiviral PDK4 overexpression suppresses mitochondrial respiration *in vitro*

HCAECs were transduced with a lentivirus encoding GFP or PDK4 (1 x 10^8 VP/mL), then exposed to hypoxic conditions for 6 h. The Seahorse Bioanalyser system was used to measure cellular oxygen consumption and the effects of oligomycin, FCCP, antimycin A, and rotenone. OCR measurements were normalised to total cell number post-assay. Data are presented as mean ± SEM. *P<0.05, ***P<0.001, ****P<0.0001 vs. the annotated controls. ^^^^P<0.0001 vs. the relevant normoxia control by two-way ANOVA with Bonferroni's *post hoc* analysis. N = 15-16, data are representative of 15-16 technical replicates across 3 independent experiments.

3.3.9. Lentiviral PDK4 overexpression rescues high glucose-impaired endothelial cell tubulogenesis in vitro

This experiment aimed to determine how PDK4 expression affects endothelial cell tubulogenesis under high glucose and hypoxic conditions. In normoxia, high glucose exposure reduced tubule number compared to the normal glucose control in the lentiGFP- (144.7 ± 9.0 vs. 265.3 ± 8.2 tubules, $P<0.0001$; Figure 3.10A) and in the lentiPDK4-treated HCAECs (174.7 ± 13.8 vs. 232.0 ± 12.3 tubules, $P<0.01$). Interestingly, the extent of tubule impairment was less in HCAECs overexpressing PDK4 compared to the lentiGFP control cells.

In hypoxia, high glucose exposure reduced tubule number in the lentiGFP-treated cells compared to the normal glucose control (164.8 ± 9.3 vs. 283.4 ± 11.8 tubules, $P<0.0001$). Under the same conditions, the lentiPDK4-treated cells exhibited a significantly increased number of tubules compared to the lentiGFP-treated cells (306.3 ± 17.8 vs. 164.8 ± 9.3 tubules, $P<0.0001$), completely abrogating the impairment of tubule formation in high glucose and hypoxia.

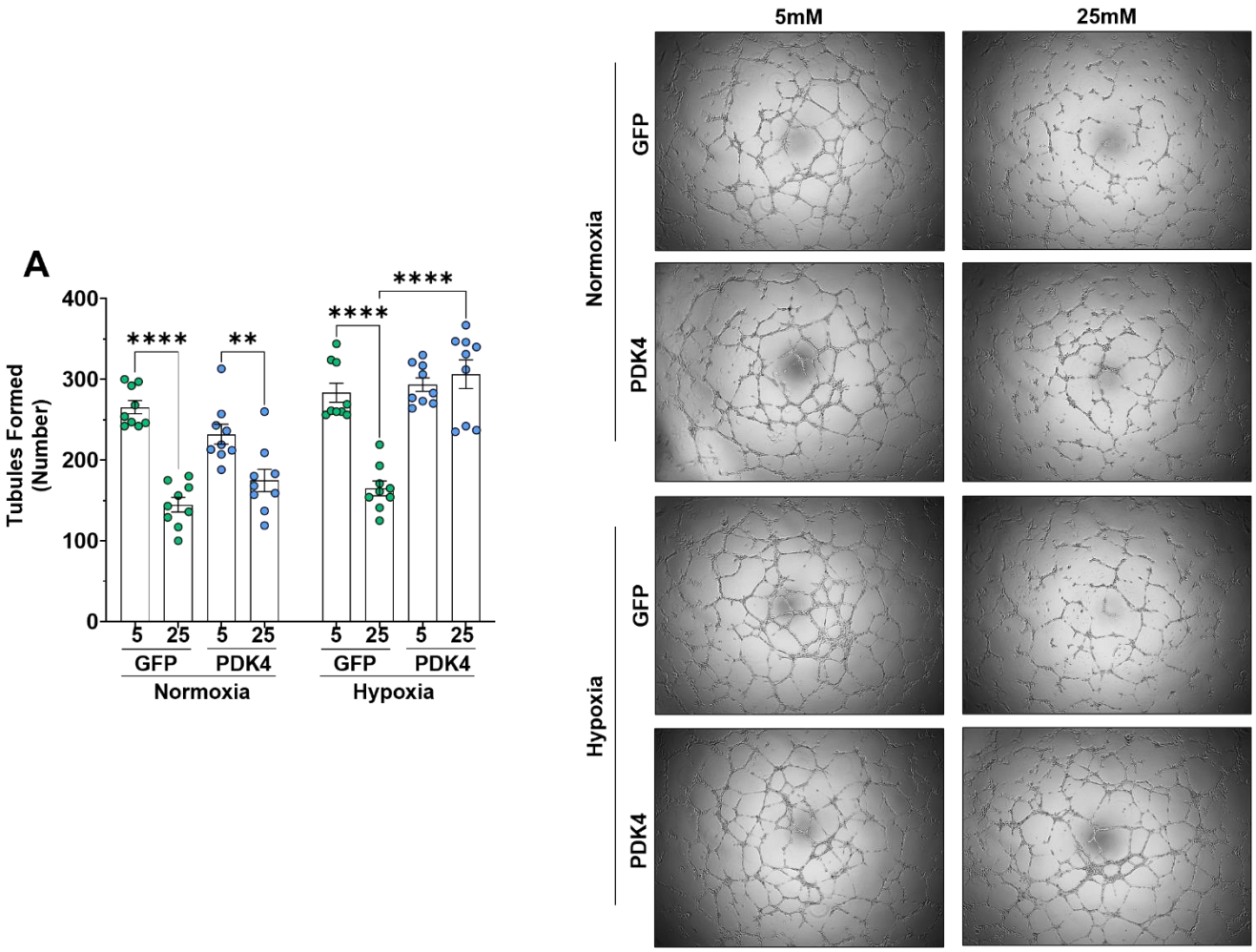

Figure 3.10. Lentiviral PDK4 overexpression rescues high glucose-impaired endothelial cell tubulogenesis *in vitro*

HCAECs were transduced with a lentivirus encoding GFP or PDK4 (1 x 10^8 VP/mL), then exposed to normal (5mM) or high (25mM) glucose for 72 h. Hypoxia exposure was completed for 6 h. Cells were harvested and plated on growth factor-reduced Matrigel to assess tubule formation. Tubules were imaged at 5X magnification and quantified using ImageJ. Data are presented as mean ± SEM. ***P*<0.01, *****P*<0.0001 by two-way ANOVA with Bonferroni's *post hoc* analysis. *N* = 9, data are representative of 9 technical replicates across 3 independent experiments.

3.3.10. Lentiviral PDK4 overexpression improves endothelial cell migration in high glucose and hypoxia in vitro

This experiment aimed to determine how PDK4 overexpression affected endothelial cell migration under high glucose and hypoxic conditions. In normoxia, high glucose exposure reduced the migration of the lentiGFP-treated HCAECs (631.6 ± 78.8 vs. 1022.9 ± 124.6 migrated cells, $P<0.05$; Figure 3.11A). High glucose exposure did not significantly reduce migration in the lentiPDK4-treated HCAECs in normoxia.

In hypoxia, high glucose exposure again reduced the migration of the lentiGFP-treated HCAECs compared to the normal glucose controls (405.3 ± 63.4 vs. 820.5 ± 79.3 migrated cells, $P<0.05$). High glucose exposure also reduced migration in the lentiPDK4-treated HCAECs in hypoxia, compared to the normal glucose control (676.9 ± 72.7 vs. 1123.3 ± 165.7, $P<0.05$). However, under high glucose conditions overexpression of PDK4 using lentiPDK4 transduction elicited more HCAEC migration than lentiGFP transduction (676.9 ± 72.7 vs. 405.3 ± 63.4; $P<0.05$).

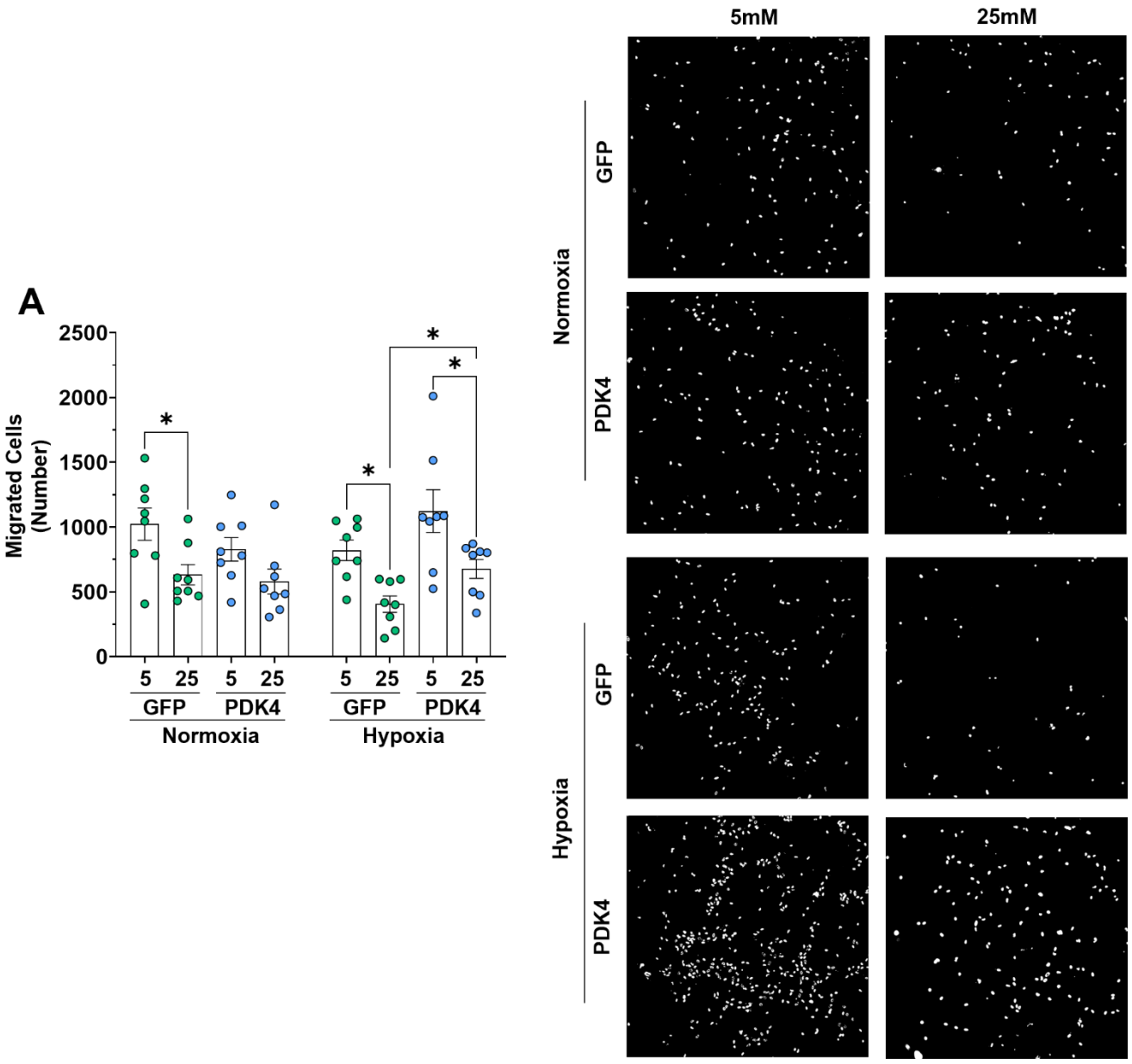

Figure 3.11. Lentiviral PDK4 overexpression rescues high glucose-impaired endothelial cell migration *in vitro*

HCAECs were transduced with a lentivirus encoding GFP or PDK4, then exposed to normal (5mM) or high (25mM) glucose for 72 h. Hypoxia exposure was completed for 6 h. Cells were harvested and seeded in Boyden chamber transwells to assess cellular migration. Migrated cells were imaged at 5X magnification and quantified using ImageJ. Data are presented as mean ± SEM. **P*<0.05 by two-way ANOVA with Bonferroni's *post hoc* analysis. *N* = 8, data are representative of 8 technical replicates across 3 independent experiments.

3.4. Discussion

These studies firstly tested the hypothesis that knocking down PDK4 would disrupt suppression of mitochondrial respiration in human endothelial cells, and impair their angiogenic function. Secondly, PDK4 overexpression was achieved using a lentivirus in order to test the hypothesis that PDK4 overexpression would enhance suppression of mitochondrial respiration and improve endothelial cell angiogenic functions under high glucose conditions.

As mentioned in this chapter's introduction, no previous studies had examined the relative expression of the PDKs and PDPs in endothelial cells. Previous studies in other cell types have noted that PDK3 exhibits the most limited expression pattern, and has not been reported to be expressed in tissues other than the kidney, brain, testis, and lung. In line with this, we observed that *PDK3* was detectable above non-template control levels in HCAECs, but in significantly lower levels than the other PDKs (Figure 3.1). *PDK1, PDK2* and *PDK4* were expressed in very similar levels in our HCAECs under baseline conditions. Interestingly, previous studies have shown that PDK4 may normally be expressed in very low levels to the point where it cannot be detected, then be upregulated by a nutrient-related stimulus. PDK4 was expressed at a similar level to the other PDKs in HCAECs, perhaps suggesting a higher level of importance in endothelial cells than other cell types.

It is important to note that our studies were completed in HCAECs, which are a specific type of endothelial cell, and therefore it may be possible that the PDKs are differentially expressed in endothelial cells of different tissue origin such as microvascular endothelial cells (HMECs) or umbilical vein endothelial cells (HUVECs). It may be of interest to study these expression patterns in HMECs in the future given their role in physiological angiogenesis. However, our research group has previously conducted parallel studies comparing HCAECs and HMECs in terms of their *in vitro* angiogenic capacity and found that they exhibited comparable

characteristics. Additionally, it is our experience that HMECs are supplied by fewer donors, and are more difficult to maintain in culture, meaning that HCAECs are the most physiologically and logistically appropriate model for our *in vitro* studies.

Also of interest is the fact that the mRNA expression of the PDPs was significantly higher than that of the PDKs in HCAECs under baseline conditions. Since the PDPs dephosphorylate the PDC, allowing it to remain in its active state, such a result may indicate that endothelial cells preferentially maintain the PDC in its active state. This would be at odds with the idea that endothelial cells are highly glycolytic, since suppression of mitochondrial respiration is closely tied to a cell's ability to upregulate glycolysis. However, we only measured *PDP1-2* mRNA expression under baseline conditions, and so to understand the significance of these contrasting expression patterns, the protein expression of each enzyme should be examined, along with their relative contribution to PDC phosphorylation under various conditions.

This study characterised these effects specifically with a focus on PDK4. Interestingly, we found that knocking down PDK4 when assessing its role in endothelial cell angiogenesis did not elicit the anticipated downstream mechanistic changes in the PDC.

siRNA-mediated knockdown of PDK4 was very effective when examined at the mRNA level, with siPDK4 treatment reducing *PDK4* mRNA by more than 80% (Figure 3.2A). We expected to observe a subsequent decrease in PDC phosphorylation, which would allow the PDC to become more active and increase cellular oxygen consumption. Interestingly, we observed the exact opposite, with PDC phosphorylation being significantly increased (Figure 3.2B). In support of this, oxygen consumption was also reduced (Figure 3.4). This suggests that when PDK4 was knocked down, one of the other PDKs or the PDPs was upregulated in a compensatory response. We did not, however, observe any change in the mRNA levels of these factors when PDK4 was knocked down (Figure 3.3). Due to technical limitations, we were

unfortunately unable to measure the protein expression of the PDKs in human cells. Antibodies targeting the human PDKs are widely reported to be non-specific and unreliable, and this is something we also experienced when using western blotting to measure these factors. Nevertheless, we were able to reliably measure PDC phosphorylation by western blotting, and the data show that knockdown of PDK4 increased PDC phosphorylation through a compensatory response, yet the pathway for this is remains unclear.

Despite the unexpected regulatory response of the PDC to PDK4 knockdown, deletion of PDK4 inhibited endothelial cell tubule formation (Figure 3.5). This suggests that, in some contexts, a decrease in mitochondrial respiration in endothelial cells can impair their functional capabilities, including their angiogenic capacity. This aligns with studies completed by Govar *et al.* and Diebold *et al.*, who both showed that under baseline conditions, a decrease in mitochondrial respiration was associated with impaired endothelial cell function [56, 57]. Given that our initial knockdown studies were conducted under baseline conditions, this points to a context-specific role for mitochondrial respiration in EC angiogenic functions. It is also possible that the disruption of the regulation of the PDC by PDK4 knockdown is the underlying cause for the suppression of angiogenesis, via a yet unknown pathway. Interestingly, PDK4 knockdown in high glucose conditions caused no significant changes in PDC phosphorylation in HCAECs (Figure 3.6). Regardless, HCAEC tubulogenesis was impaired under these conditions (Figure 3.7).

The unexpected changes, or lack of change, in PDC phosphorylation may be attributed to the use of western blotting as the method of detection, which has inherent limitations. Phosphorylation of protein targets is a post-translational modification that commonly occurs extremely quickly. The timing of each condition is critical, and it may be that western blotting is simply not sensitive enough to detect transient changes in the phosphorylation state of the

PDC under complex conditions. It may of interest for future studies to assess PDC phosphorylation using proteomic methods, and support assessments of the phosphorylation state with assays that indicate the activity of the PDC, such as the PDH Activity Assay (Sigma-Aldrich).

We next utilised lentiviral gene transfer to overexpress PDK4 in HCAECs. While *PDK4* mRNA expression was consistently increased in both normal and high glucose conditions with lentiPDK4 transduction, an anticipated increase in PDC phosphorylation did not follow (Figure 3.8). Hypoxia exposure significantly induced PDC phosphorylation, confirming the importance of reducing mitochondrial respiration in endothelial cells in low oxygen environments. In the lentiGFP-treated HCAECs, high glucose exposure reduced PDC phosphorylation, which points to a diabetes-induced impairment in the regulation of the PDC. LentiPDK4 treatment did not elicit an increase in PDC phosphorylation under normal glucose conditions even though PDK4 mRNA levels were elevated, but did prevent a high glucose-induced decrease. It would be of interest to determine what the maximum achievable level of PDC phosphorylation is in HCAECs. It is possible that the hypoxia exposure caused PDC phosphorylation to reach its peak in these cells, meaning that even with elevated PDK4 expression, further increases in PDC phosphorylation would be too small to detect. When high glucose exposure was introduced, the higher levels of PDK4 may compensate for any potential decrease and maintain PDC phosphorylation at the necessary level. It may be possible, again, that measuring PDC phosphorylation by western blot is not a sensitive-enough method, especially given that we did observe significant changes in cellular oxygen consumption, which is a more direct method of observing the cellular phenotype.

Importantly, we found that hypoxia exposure induced significant reductions in cellular oxygen consumption, highlighting the importance of oxygen conservation in these conditions (Figure

3.9). In hypoxia, cells treated with the lentiGFP control exhibited a significantly blunted response in the Seahorse assay to all the relevant inhibitors, which delineate different aspects of mitochondrial respiration, when compared to the normoxia control. This blunted response to the inhibitors indicates a generally lower level of mitochondrial energetic function. In addition, these cells exhibited significantly lower levels of basal and maximal respiration, as well as ATP production. The treatment with lentiPDK4 under hypoxic conditions elicited a further blunting of all of these effects, with a further reduction in basal and maximal respiration, and ATP production compared to the lentiGFP-treated cells in hypoxia. In particular, the response of the lentiPDK4-treated cells to FCCP, which uncouples the proton gradient to induce a sharp increase in oxygen consumption and assess maximal respiration, was practically non-existent in hypoxia. We have interpreted this to mean that the mitochondria may be in an enforced state of inactivity due to the additional PDK4 present. and FCCP was therefore unable to elicit any change in oxygen consumption.

We found that suppression of mitochondrial oxygen consumption was associated with an angiogenic functional benefit in hypoxia. Similar to the predominantly hypoxia-specific effects observed on mitochondrial respiration, the positive effect on *in vitro* angiogenesis was most apparent under hypoxic conditions. Overexpression of PDK4 rescued both high glucose-impaired tubule formation and migration only in response to hypoxia, indicating that suppression of mitochondrial respiration protects the cells from the negative effects of high glucose (Figure 3.10, 3.11).

There was little-to-no effect of PDK4 overexpression on endothelial cell function under normoxic conditions. Perhaps the much higher levels of *PDP1* and *PDP2* that we observed earlier, also under normoxic conditions, make it more difficult for increased PDK4 expression to gain a foothold in the system, as PDP1 and PDP2 could dephosphorylate the PDC quickly.

Those very high levels of *PDP1* and *PDP2* may not persist with hypoxia exposure, allowing increased PDK4 to have more of an effect, and this should be investigated further. In addition, the mechanism behind exactly how PDK4 overexpression and reduction of mitochondrial respiration is protective under high glucose conditions should be investigated. Whether this is due to a reduction in oxidative stress, altered regulation of fatty acid oxidation or production of key nutrient building blocks like amino acids, or affects flux of upstream pathways like glycolysis and its side-pathways is something for further investigation.

In conclusion, this study has, for the first time, demonstrated the importance of the integrity of the PDK4/PDC axis in endothelial cell angiogenic function, and shown that knocking down PDK4 at the mRNA level elicits functional changes in endothelial cells. Furthermore, we have highlighted that high glucose can impair the induction of PDC phosphorylation in response to hypoxia, and that overexpression of PDK4 can protect endothelial cells from the negative effects of high glucose, suppressing mitochondrial respiration and improving their function.

The following chapters will focus on the modulation of PDK4 using two different approaches in the context of diabetes-impaired angiogenesis.

4. The effect of reconstituted high-density lipoproteins on the PDK4/PDC axis in diabetes-impaired angiogenesis

4.1. Introduction

We have demonstrated that the PDK4/PDC axis plays a novel, important role in endothelial cell angiogenesis *in vitro*. We showed that high glucose disrupted the PDK4/PDC axis response to hypoxia and, in parallel, impaired angiogenesis. Furthermore, augmenting PDK4 expression using lentiviral gene transfer prevented the impairment to endothelial cell angiogenesis in high glucose (Chapter 3).

Next, we aimed to characterise the effects of the known pro-angiogenic agent reconstituted high-density lipoprotein (rHDL) on the PDK4/PDC axis, and determine whether the PDK4/PDC plays a critical role in these effects.

HDL is an endogenous lipoprotein particle that exhibits a myriad of biological effects on lipid metabolism and the vasculature. HDL interacts with three cell-surface proteins including the cholesterol transporters ABCAI and ABCGI, and the scavenger receptor SR-BI [81, 110]. Reconstituted HDL is produced in a laboratory setting by complexing human plasma-derived apoA-I with phospholipid to form discoidal particles, and allows researchers to examine the specific effects of the rHDL particle without interference from other biological factors such as specific cholesterol or triglyceride species.

Previous studies by our laboratory have shown that rHDL rescues diabetes-impaired angiogenesis, both in endothelial cells *in vitro* and in the diabetic murine model of wound healing *in vivo*. Topical rHDL treatment in the wound healing model not only enhances wound angiogenesis, but also rescues diabetes-impaired wound healing [45]. Our group has shown that rHDL stabilises the central hypoxia transcription factor HIF-1α under high glucose conditions, which contributes to enhanced VEGFA production and other pro-angiogenic signalling in hyperglycaemic endothelial cells and the rescue of diabetes-impaired angiogenesis [45, 85].

Factors through which rHDL achieves positive effects on endothelial cell function include the PI3K/Akt signalling pathway, wherein rHDL enhances Akt phosphorylation and promotes EPC differentiation [82], increases expression of angiopoietin-like-4 (ANGPTL4) [111], and supports general endothelial angiogenic functions [45, 85].

However, questions remain about the full mechanism through which rHDL enacts these pro-angiogenic effects on endothelial cells. For example, it is unknown which pathways downstream of HIF-1α are central to these effects, and if there are other nutrient-sensing transcription factors involved. A deep understanding of these mechanistic pathways is essential for the translation of rHDL as a novel therapy for diabetic vascular complications. The underlying biology of the pro-angiogenic effects of rHDL must be characterised in order for the therapy to be delivered and regulated in such a way as to mitigate off-target or unwanted side-effects.

PDK4 is a downstream target of HIF-1α, as demonstrated by Lee *et al.* who showed that HIF-1α was essential for the upregulation of PDK4 in response to hypoxia [74]. This relationship is consistent with the notion that PDK4 is the most nutrient-sensitive of the PDKs, and is upregulated in response to low-oxygen or starvation conditions [112-114]. In addition, the upregulation of PDK4 leads to suppression of mitochondrial respiration, which we hypothesise is critical for oxygen conservation and endothelial cell survival in hypoxic conditions.

Given that rHDL supports endothelial cell function through pathways central to hypoxia tolerance, and that PDK4 plays a significant role in metabolic functions that are critical for endothelial cell survival in hypoxia, it may be that the PDK4/PDC axis plays a central role in the pro-angiogenic effects of rHDL. Importantly, the effect of rHDL on endothelial cell metabolism and the PDK4/PDC axis has never been studied before in the context of diabetes-impaired angiogenesis.

Accordingly, the main aims of the present study were to determine whether rHDL corrects impairment to the PDK4/PDC axis in hypoxia and high glucose, and to determine whether PDK4 plays an essential role in the pro-angiogenic effects of rHDL. We hypothesised that rHDL treatment would rescue a high glucose-induced impairment to the PDK4/PDC axis, and that this would be a critical part of its positive effects on endothelial cell function, angiogenesis and wound healing.

4.2. Methods

4.2.1. Preparation of discoidal reconstituted high-density lipoproteins

Purified apolipoprotein A-I (apoA-I) was reconstituted in reconstitution buffer (100 mM Tris, 3 M Guanidine HCL, pH 8.2), at a concentration of 1mL reconstitution buffer to 10mg of apoA-I, then dialysed against Tris-buffered saline (TBS; 10mM Tris, 150mM NaCl, 4.6mM NaN3 and 0.17mM EDTA). Reconstituted apoA-I was complexed with 1-palmitoyl-2-linoleoyl-phosphatidylcholine (PLPC) via incubation with TBS and sodium cholate for 2 hours to form reconstituted discoidal HDL (rHDL). The rHDL was then dialysed against TBS, followed by dialysis against endotoxin-free phosphate-buffered saline (PBS; Sigma-Aldrich). rHDL was filter sterilised with a 0.22μM low protein-binding low-retention filter (Merck Millipore, Ltd.), and the final concentration of apoA-I was determined using a Pierce BCA Protein Assay Kit (Life Technologies). rHDL was stored under N_2 gas for up to two weeks at 4ºC.

4.2.2. Cell culture and treatments

Human coronary artery endothelial cells (HCAECs) were cultured as per section 2.2.1.

For rHDL treatment, HCAECs were treated with rHDL at a concentration of 0.6·g/mL (final apoA-I protein concentration) for 18 hours.

For high glucose exposure, cells were treated with the MesoEndo which was supplemented with D-glucose to a final concentration of 25mM for 72 hours.

To create a hypoxic environment, cells were placed in a hypoxia incubator with 1.2% O_2 and 5% CO_2 balanced with N_2. Hypoxia exposure was typically completed for 6 hours.

4.2.3. RNA extraction and analysis

RNA extraction and qRT-PCR analysis of cell and wound tissue mRNA expression was conducted as described in section 2.2.2.1 onward.

4.2.4. Protein extraction and analysis

Protein extraction and western blotting or ELISA analysis of cell and wound tissue protein expression was conducted as described in section 2.2.2.5 onward.

4.2.5. Functional studies

All functional studies, including Matrigel tubulogenesis assays, Boyden chamber migration assays, and Seahorse Bioanalyser assays were completed as described in section 2.2.3.

4.2.6. Chromatin immunoprecipitation assay

Following cell treatments, proteins and DNA were crosslinked by addition of 37% formaldehyde (final concentration of 1%). After 10 minutes, 1M ice-cold glycine was added. Cells were washed and scraped in ChIP lysis buffer. DNA was sonicated to 300bp fragments. Chromatin samples were pre-cleared by incubation with ChIP-grade protein G magnetic beads for 2h at 4°C. Samples were incubated with an antibody for FOXO1 or an IgG Normal Rabbit control overnight at 4°C. Protein was immunoprecipitated using the protein G magnetic beads, washed 3x with low salt buffer and 1x with high salt buffer before elution of DNA. Crosslinks were reversed with 5M NaCl, and Proteinase K. DNA was purified using a QIAquick PCR clean-up kit (Qiagen), and qPCR performed to amplify a region of the PDK4 promoter region.

4.2.7. Murine diabetic wound healing model

All *in vivo* studies and the diabetic murine wound healing model was conducted as described in section 2.3. Briefly, mice were rendered diabetic by a bolus intraperitoneal injection of streptozotocin (165mg/g). At least two weeks post-injection, mice were anaesthetised and two full-thickness excisional wounds were created either side of the dorsal midline. A silicone splint was secured, and to assess the effect of rHDL on wound angiogenesis and healing, rHDL or a PBS vehicle control was topically applied to each wound daily throughout the study. 50µg of rHDL was added to each wound, as quantified by apoA-I protein concentration. Wound closure was measured daily, and laser Doppler perfusion imaging assessed wound blood flow perfusion. Histological analysis of the wound was also conducted as described in section 2.3.9.

4.3. Results

4.3.1. Diabetes impairs metabolic reprogramming responses to wound ischemia which is rescued by rHDL in diabetic mice

This experiment aimed to determine how hyperglycaemia affected the PDK4/PDC axis in the context of diabetic wound healing *in vivo*, and how rHDL treatment impacted these effects. Mice receiving STZ injections had significantly higher blood glucose levels than non-diabetic control mice (Non-diabetic: 10.1 ±1.3 versus Diabetic: 25.7 ±6.4 mmol/L, $P<0.0001$) and lower body weights (Non-diabetic: 24.5 ±1.8 versus Diabetic: 22.9 ±2.1 g, $P<0.05$) at the time of wound surgery (Table 4.1). At day 1 post-wounding in non-diabetic mice there was an induction of PDK4 protein levels (3.0 ±1.2 to 9.3 ±2.0 ng/mL, 207% increase, $P<0.05$; Figure 4.1A). This induction did not occur in diabetic mice. However, topical rHDL restored the induction of PDK4 protein expression at day 1 post-wounding in diabetic wounds (4.4 ±1.0 to 7.4 ±1.6 ng/mL, 68% increase, $P<0.05$). Consistent with this, at day 3 post-wounding rHDL-treated wounds exhibit enhanced pPDC in diabetic mice (63 ±8 to 167 ±39 %, 165% increase, $P<0.01$; Figure 4.1B-C). In non-diabetic mice, wound *Pdk4* mRNA levels were also significantly increased at day 1 post-wounding (100 ±43 to 288 ±75 %, 188% increase, $P<0.05$, Figure 4.1D). Diabetes impaired this induction, with *Pdk4* mRNA expression significantly reduced in Day 1 diabetic wounds (288 ±75 to 127 ± 29 %, 56% decrease, $P<0.01$). In diabetic mice, topical application of rHDL enhanced *Pdk4* mRNA levels at day 3 post-wounding (22 ±5 to 40 ±9 %, 82% increase, $P<0.05$, Figure 4.1D and inset). In summary, hyperglycaemia impaired the induction of the PDK4/PDC axis in response to hypoxia, and rHDL treatment restored this induction.

	Non-diabetic	Diabetic (+STZ)	P value
Blood glucose (mmol/L)	10.1 ± 1.3	25.7 ± 6.4	<0.0001
Body Weight (g)	24.5 ± 1.8	22.9 ± 2.1	0.0043

Table 4.1. Mouse blood glucose levels and weights at time of surgery

In the murine diabetic wound healing model, blood glucose levels were measured weekly throughout the study using an Accu-CHEK Glucometer. Mouse weights were also recorded daily over the course of the study. Data are expressed as mean±SEM.

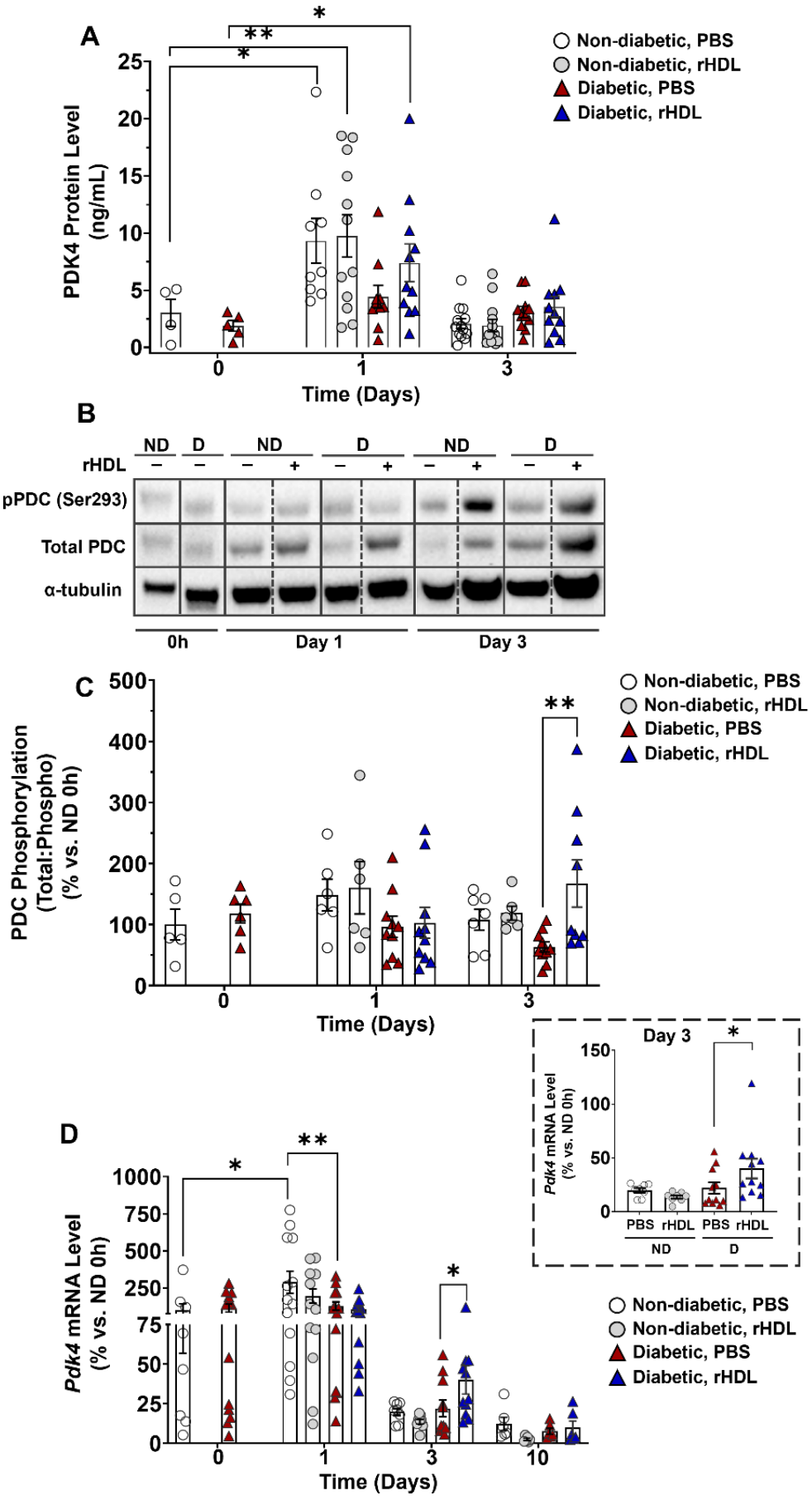
A
PDK4 Protein Level (ng/mL)
Time (Days)
Non-diabetic, PBS
Non-diabetic, rHDL
Diabetic, PBS
Diabetic, rHDL
B
ND
D
rHDL
pPDC (Ser293)
Total PDC
α-tubulin
0h
Day 1
Day 3
C
PDC Phosphorylation (Total:Phospho) (% vs. ND 0h)
Time (Days)
D
Pdk4 mRNA Level (% vs. ND 0h)
Time (Days)
Day 3
PBS
rHDL

Figure 4.1. Diabetes impairs metabolic reprogramming responses to wound ischemia and rHDL rescues this impairment in diabetic mice

In the murine diabetic wound healing model, (A) PDK4 protein expression at days 0, 1 and 3 post-wounding was measured by ELISA (N=4-13) **P*<0.05, ***P*<0.01 vs controls by two-way ANOVA. (B-C) Phosphorylation of the PDC at days 0, 1, and 3 post-wounding was measured by western blotting (N=5-10) ***P*<0.01 vs. PBS control by two-way ANOVA. (D) *Pdk4* mRNA expression was measured using qRT-PCR. Gene expression was normalized using the $^{\Delta\Delta}$Ct method to murine *36B4.* (N=6-13, data are representative of 6-13 individual wounds), **P*<0.05, ***P*<0.01 vs. control by two-way ANOVA. **P*<0.05 by paired t-test. Data are expressed as mean±SEM.

4.3.2. rHDL increases neovascularization and rescues diabetes-impaired wound healing in vivo

This experiment aimed to determine how rHDL treatment affected wound neovascularisation and healing *in vivo*. Blood flow perfusion of the wound was determined as a ratio of rHDL:PBS using laser Doppler imaging. In diabetic mice rHDL significantly increased wound blood flow perfusion 3 days post-wounding (99 ±11 to 140 ±35 %, 41% increase, $P<0.05$, Figure 4.2A-B). The PBS-treated wounds of diabetic mice contained fewer CD31+ neovessels compared to the PBS-treated wounds of non-diabetic mice (36 ±4 to 21 ±3 neovessels, 42% decrease, $P<0.05$, Figure 4.2C-D). rHDL treatment rescued this impairment in diabetic mice (21 ±3 to 34 ±4 neovessels, 62% increase, $P<0.05$). The PBS-treated wounds of diabetic mice exhibited reduced rates of wound closure, reaching significance at Day 8 (60 ±2 to 48 ±4 % wound closure, 20% decrease, $P<0.05$, Figure 4.2E-F), compared to non-diabetic mice with PBS-treated wounds. Topically applied rHDL significantly increased the rate of wound closure in diabetic mice across all timepoints (increases ranging from 31.9-154.9%, $P<0.01$, $P<0.0001$), compared to diabetic PBS-treated wounds. In summary, rHDL increased wound neovascularisation and rescued diabetes-impaired wound healing.

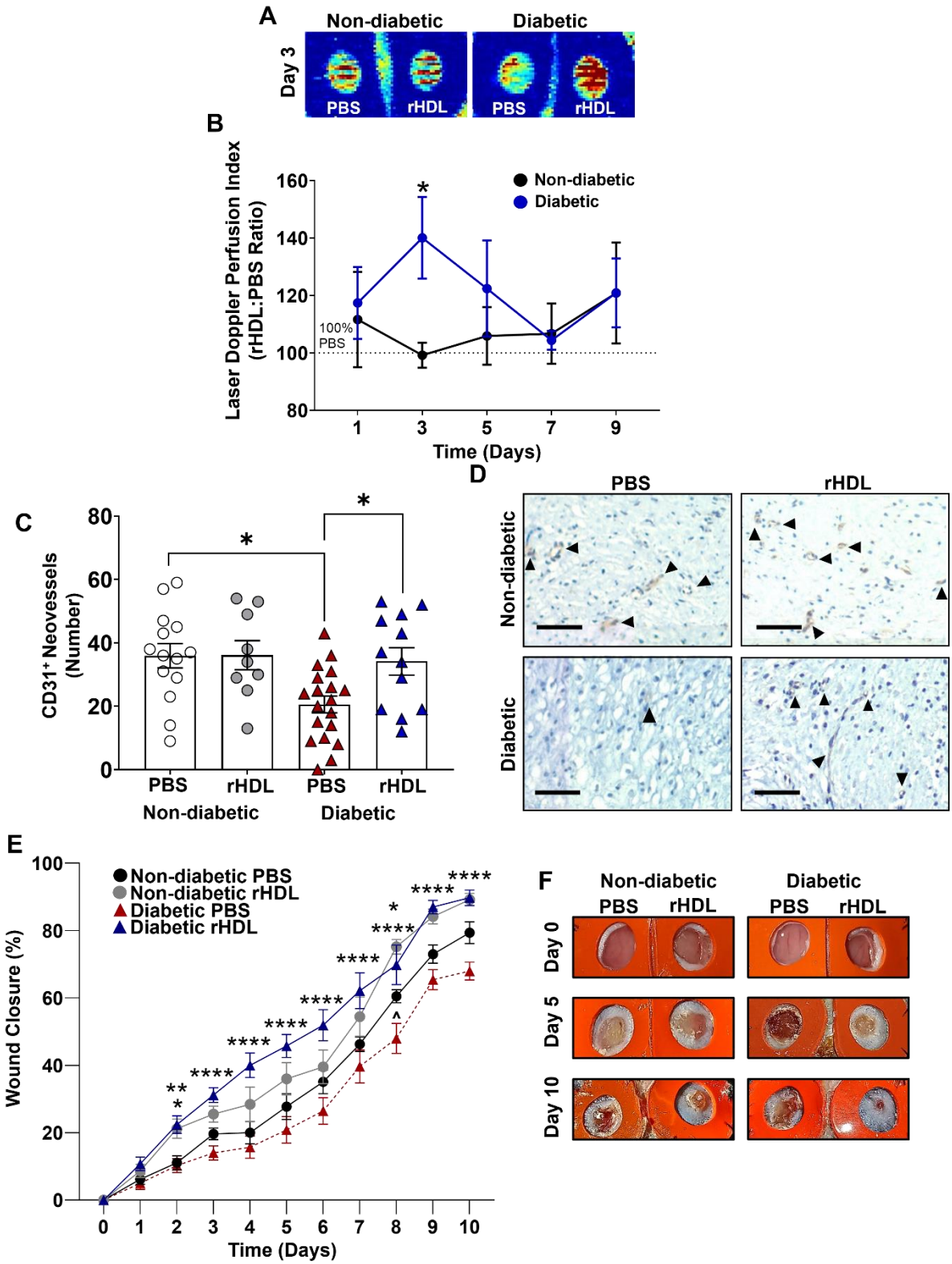
A
Non-diabetic
Diabetic
Day 3
PBS
rHDL
PBS
rHDL
B
Laser Doppler Perfusion Index (rHDL:PBS Ratio)
160
140
120
100
80
100% PBS
*
Non-diabetic
Diabetic
1
3
5
7
9
Time (Days)
C
CD31+ Neovessels (Number)
80
60
40
20
0
*
*
PBS
rHDL
PBS
rHDL
Non-diabetic
Diabetic
D
PBS
rHDL
Non-diabetic
Diabetic
E
Wound Closure (%)
100
80
60
40
20
0
Non-diabetic PBS
Non-diabetic rHDL
Diabetic PBS
Diabetic rHDL
**
*
****
****
****
****
****
*
****
****
^
0
1
2
3
4
5
6
7
8
9
10
Time (Days)
F
Non-diabetic
Diabetic
PBS
rHDL
PBS
rHDL
Day 0
Day 5
Day 10

Figure 4.2. rHDL increases neovascularization and rescues diabetes-impaired wound healing in vivo.

In the murine diabetic wound healing model, (A-B) rHDL:PBS wound blood flow perfusion ratio was determined using laser Doppler perfusion imaging; images represent high (red) to low (blue) blood flow from day 1-9 in non-diabetic and diabetic mice. **P*<0.05 vs. PBS control by paired t-test. (C-D) Capillaries were identified in wound sections using immunohistochemistry for CD31. Photomicrographs represent wounds that were harvested at day 10 and stained for CD31 (stained brown, denoted by arrows). Scale bars, 200μm. **P*<0.05 vs. PBS control by one-way ANOVA (N=9-19) (E-F) Wound closure is expressed as a percentage of initial wound area at day 0. **P*<0.05, ***P*<0.01, ****P*<0.001, ******P*<0.0001 vs. relevant controls by two-way ANOVA. ^*P*<0.05 vs. non-diabetic PBS-treated wound by two-way ANOVA. (N=9-11, data are representative of 9-11 individual wounds). Data are expressed as mean±SEM.

4.3.3. High glucose impairs metabolic reprogramming responses to hypoxia and rHDL rescues this impairment in vitro

We next studied how the PDK4/PDC axis was affected in high glucose and hypoxia *in vitro*, and its regulation by rHDL. Under normal glucose conditions at 5mM, hypoxia exposure increased EC PDK4 mRNA expression (100 ±5 to 165 ±16 %, 65% increase, $P<0.05$, Figure 4.3A). However, exposure to high glucose at 25mM impaired a further stepwise induction of PDK4 in response to hypoxia. An additional stepwise induction is essential to adequately reduce the activity of the PDC to protect against both the effects of hypoxia and high glucose. However, preincubation with rHDL in high glucose restored this response to hypoxia, inducing PDK4 mRNA (176 ±15 to 240 ±17 %, 37% increase, $P<0.05$) and PDK4 protein (7.4 ±0.6 to 10.8 ±0.8 ng/mL, 44% increase, $P<0.05$, Figure 4.3B), compared to the PBS high glucose control. Consistent with these findings, in normal glucose conditions, PDC phosphorylation (pPDC) increased in response hypoxia (130 ±11 to 213 ±25 %, 64% increase, $P<0.01$, Figure 4.3C). Exposure to high glucose in hypoxia did not induce a further elevation in pPDC levels, however, rHDL corrected this, and promoted higher pPDC levels (100 ±6 to 170 ±22 %, 70% increase, $P<0.01$). There was no change in the total protein expression of the PDC (Figure 4.3E). In summary, high glucose exposure impaired the induction of the PDK4/PDC axis in response to hypoxia, and rHDL treatment restored this induction.

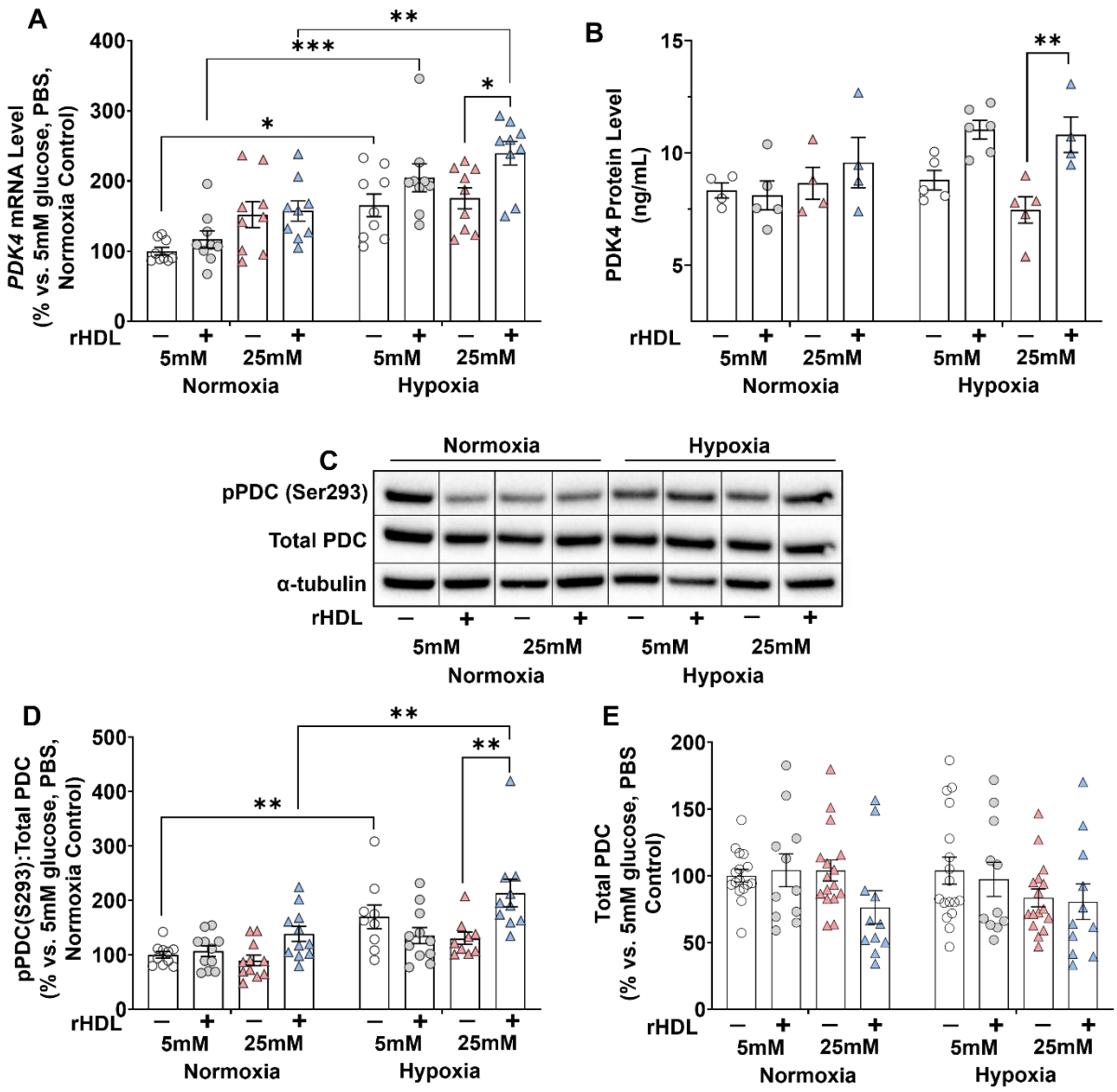

Figure 4.3. High glucose impairs induction of the PDK4/PDC axis in ECs and rHDL restores this impairment *in vitro*

HCAECs were incubated with rHDL (20 µM) or PBS (vehicle control) for 18 h, then exposed to normal (5 mmol/L,) or high (25 mmol/L) glucose conditions for 72 h. Cells were exposed to normoxia or hypoxia (1.2% O^2) for 6 h. (A) *PDK4* mRNA expression was measured using qRT-PCR and normalized using the $^{\Delta\Delta}$Ct method to human *B2M*, (N=9). (B) PDK4 protein expression was measured using an ELISA, (N=4-6). (C-E) Phosphorylation of the PDC at serine 293 was measured using western blotting densitometry, with data expressed as the ratio of pPDC(S293):Total PDC, and normalized to α-tubulin, (N=9-11, data are representative of 9-11 technical replicates across 4 independent experiments). *P<0.05, **P<0.01, ***P<0.001 by two-way ANOVA. Data are expressed as mean±SEM.

4.3.4. The effect of rHDL on endothelial cell metabolism

We next aimed to determine whether this change in regulation of the PDK4/PDC axis was associated with changes in cellular oxygen consumption rate (OCR), a measure of mitochondrial respiration [17]. In normoxia, high glucose exposure increased OCR (100 ±3 to 119 ±3 %, 19% increase, $P<0.01$, Figure 4.4E), compared to normal glucose. However, rHDL prevented this and kept OCR at baseline levels. Overall, hypoxia lowered the OCR across all treatments when compared to normoxia groups. However, high glucose exposure in hypoxia increased OCR (72 ±4 to 86 ±3 %, 19% increase, $P<0.05$), compared to the normal glucose control. rHDL prevented this high glucose-induced elevation of the OCR in hypoxia, significantly lowering the OCR (86 ±3 to 72 ±3 %, 16% decrease, $P<0.05$), compared to PBS control cells in high glucose and hypoxia. rHDL treatment significantly decreased extracellular lactate under high glucose conditions (96 ±3 to 78 ±4 %, 19% decrease, $P<0.01$, Figure 4.4F), compared to the PBS control. In summary, rHDL treatment prevented an aberrant high glucose-induced increase in mitochondrial respiration.

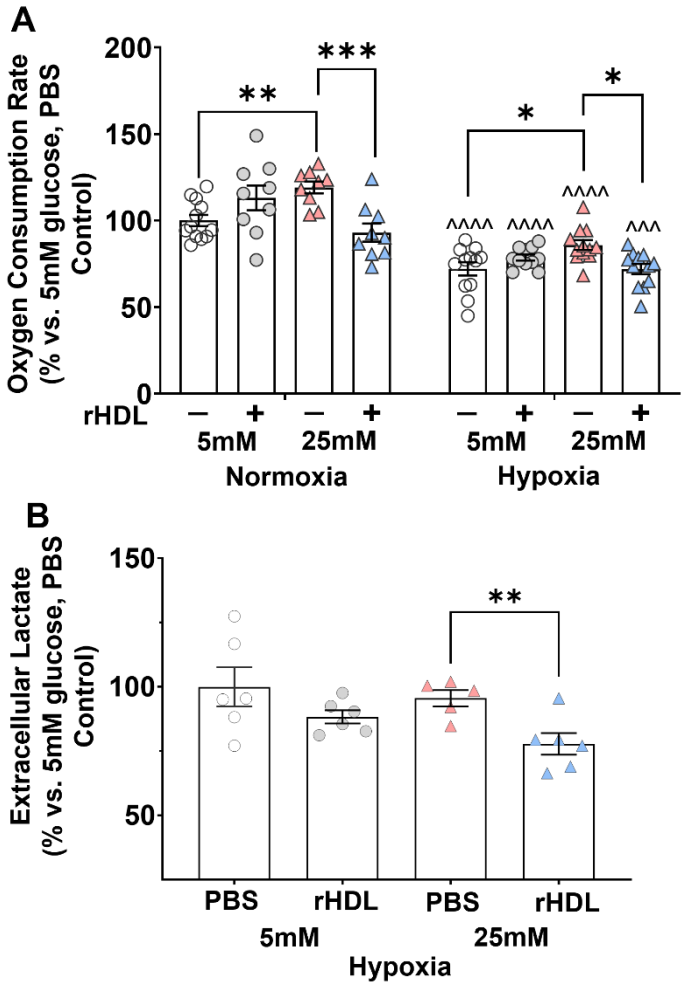

Figure 4.4. High glucose impairs suppression of oxygen consumption in ECs and rHDL restores this impairment *in vitro*

HCAECs were incubated with rHDL (20 µM) or PBS (vehicle control) for 18 h, then exposed to normal (5 mmol/L,) or high (25 mmol/L) glucose conditions for 72 h. Following this, cells were exposed to normoxia or hypoxia (1.2% O^2) for 6 h. (A) Oxygen consumption of treated cells was measured using the Seahorse Bioanalyser system, with data from each well normalized to cell number post-assay (N=9-12, data are representative of 9-12 technical replicates across 4 independent experiments). *P<0.05, **P<0.01, ***P<0.001 by two-way ANOVA. ^^^P<0.001, ^^^^P<0.0001 vs. normoxia control by two-way ANOVA. (B) Lactate in the media of hypoxia-exposed and treated cells was measured using a colorimetric assay, (N=5-6, data are representative of 5-6 technical replicates across 2 independent experiments). **P<0.01 by unpaired t-test. Data are expressed as mean±SEM.

4.3.5. rHDL rescues high glucose-impaired EC function in vitro

This experiment aimed to determine the effect of rHDL treatment on endothelial cell angiogenic function under high glucose and hypoxic conditions. In hypoxia, high glucose exposure impaired tubule (117 ±4 to 85 ±9 %, 28% decrease, Figure 4.5A-B) and branch point formation (128 ±2 to 95 ±7 %, 26% decrease, Figure 4.5C) ($P<0.05$ for both), compared to cells in normal glucose and hypoxia. rHDL rescued this impairment, increasing tubule (85 ±7 to 136 ±10 %, 60% increase, $P<0.001$) and branch points (95 ±7 to 169 ±4 %, 78% increase, $P<0.0001$). High glucose impaired migration in normoxia (100 ±6 to 60 ±7, 40% decrease, $P<0.01$, Figure 4.6A-B) and hypoxia (107 ±7 to 65 ±10, 39% decrease, $P<0.01$), compared to the respective controls. In hypoxia, rHDL rescued migration, elevating the number of migrated cells (65 ±10 to 100 ±6 %, 55% increase, $P<0.05$), compared to the PBS control. In summary, rHDL treatment restored high glucose-impaired endothelial cell tubulogenesis and migration.

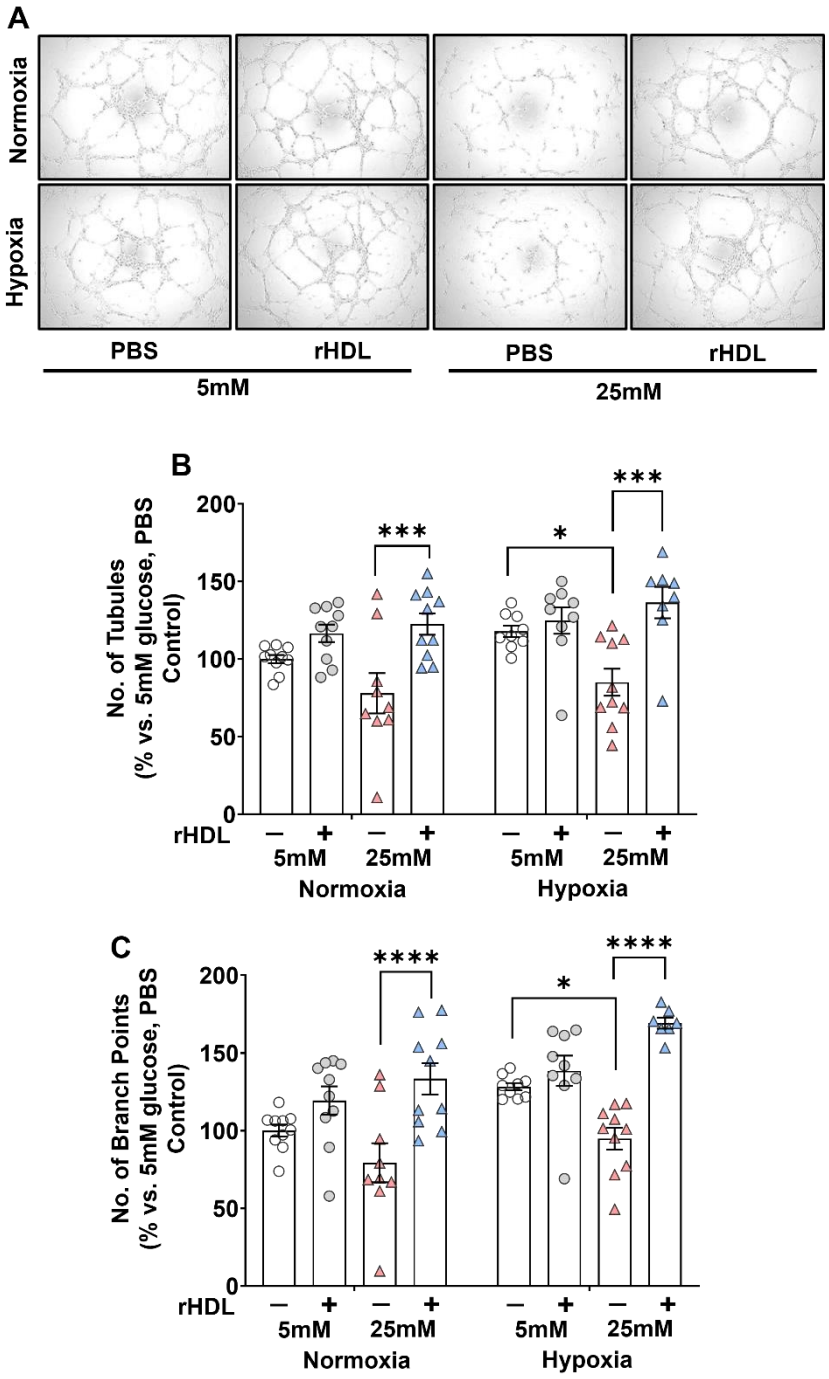

Figure 4.5. rHDL rescues high glucose-impaired EC tubulogenesis *in vitro*.

HCAECs were incubated with rHDL (20 µM) or PBS (vehicle control) for 18 h, then exposed to normal (5 mmol/L,) or high (25 mmol/L) glucose conditions for 72 h. (A) Treated cells were then seeded on Matrigel and exposed to normoxia or hypoxia (1.2% O^2) for 6 h. Matrigel tubules (B) and branch points (C) were imaged using light microscopy and quantified using ImageJ software (N=8-10, data are representative of 8-10 technical replicates across 3 independent experiments). **P*<0.05, ***P*<0.01, ****P*<0.001, *****P*<0.0001 by two-way ANOVA. Data are expressed as mean±SEM.

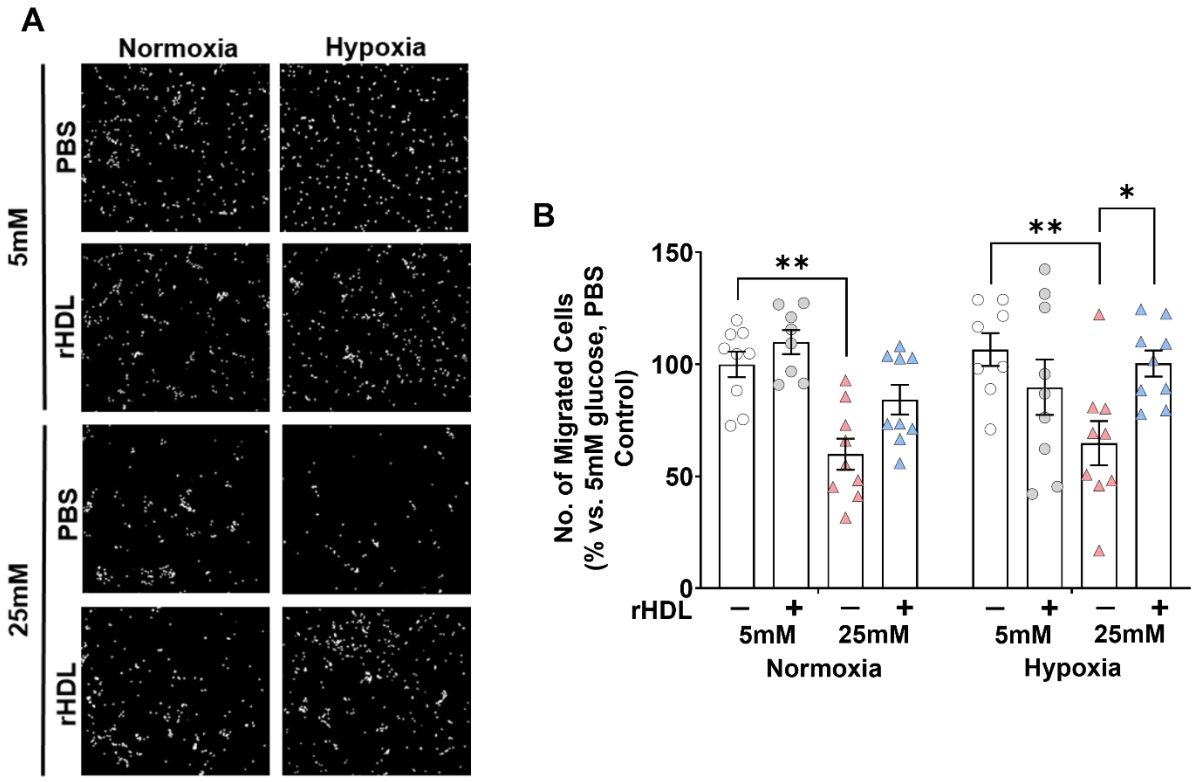

Figure 4.6 rHDL rescues high glucose-impaired EC migration *in vitro*.

HCAECs were incubated with rHDL (20 µM) or PBS (vehicle control) for 18 h, then exposed to normal (5 mmol/L,) or high (25 mmol/L) glucose conditions for 72 h. Treated cells were seeded in transwells containing a permeable membrane to measure cell migration. Membranes were imaged using fluorescence microscopy and quantified (E) using ImageJ software (N=8-9, data are representative of 8-9 technical replicates across 3 independent experiments).*P<0.05, **P<0.01, ***P<0.001, ****P<0.0001 by two-way ANOVA. Data are expressed as mean±SEM.

4.3.6. PDK4 knockdown attenuates the pro-angiogenic effects of rHDL

This experiment aimed to determine whether PDK4 was essential for the pro-angiogenic effects of rHDL by knocking down PDK4 using siRNA and assessing the effect of rHDL on tubulogenesis under high glucose and hypoxic conditions. High glucose exposure impaired tubule formation in the non-transfected (100 ±3 to 81 ±6 %, 19% decrease, $P<0.05$, Figure 4.7B), scrambled siRNA control (97 ±3 to 71 ±4 %, 27% decrease, $P<0.01$) and PDK4 siRNA ECs (72 ±7 to 63 ±6 %, 12% decrease, $P<0.05$,), when compared to their respective normal glucose controls. PDK4 knockdown impaired tubule formation in normal glucose PBS cells, compared to both the non-transfected (100 ±3 to 72 ±7 %, 28% decrease, $P<0.001$) and scrambled siRNA controls (97 ±3 to 72 ±7 %, 26% decrease, $P<0.01$). rHDL treatment rescued high glucose-impaired tubulogenesis in both non-transfected (81 ±6 to 121 ±3 %, 50% increase, $P<0.0001$) and scrambled siRNA controls (71 ±4 to 108 ±6 %, 52% increase, $P<0.0001$), but not in the cells deficient in PDK4. In summary, PDK4 appears to be essential for the ability of rHDL to rescue high glucose-impaired tubulogenesis.

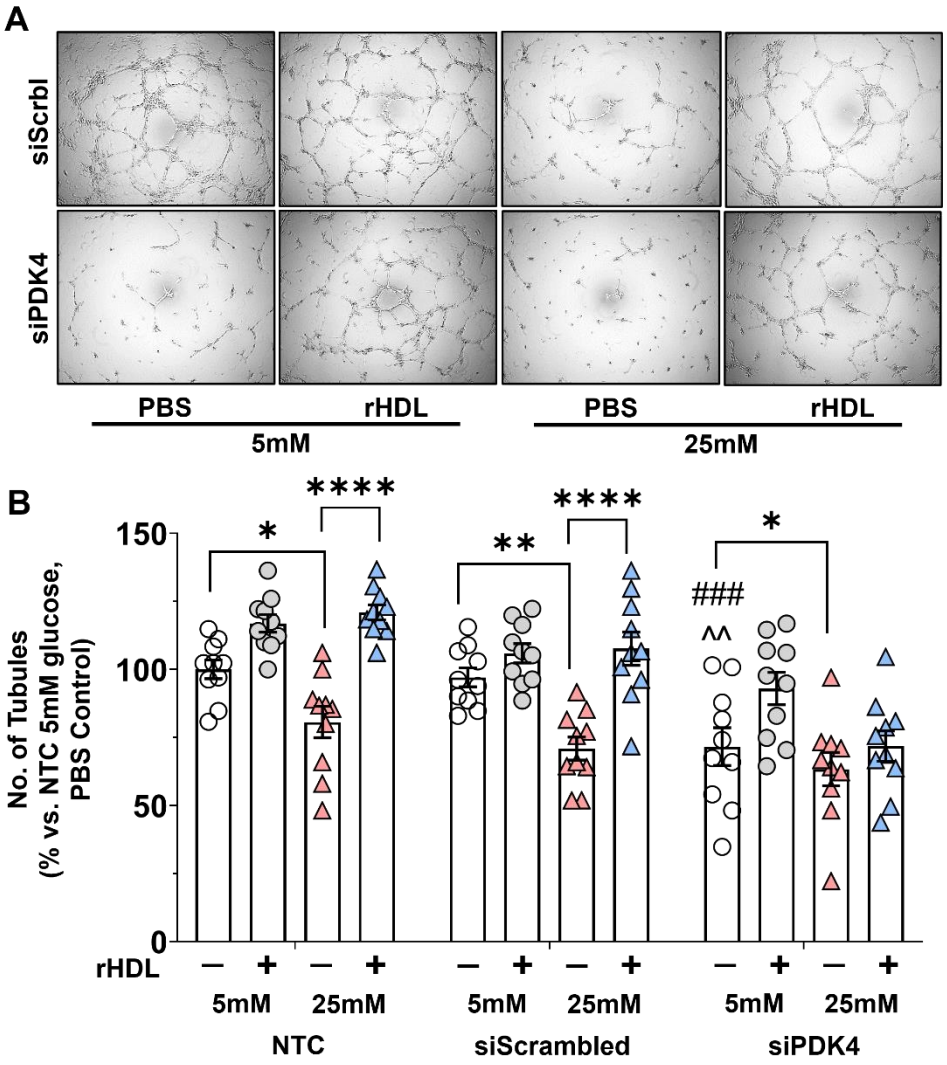

Figure 4.7. PDK4 knockdown attenuates the pro-angiogenic effects of rHDL

HCAECs were transfected with PDK4-specific siRNA (50 nM) or a scrambled control, then incubated with rHDL (20 µM) or PBS (vehicle control) for 18 h, and exposed to normal (5 mmol/L) or high (25 mmol/L) glucose conditions for 72 h. Treated cells were then seeded on Matrigel and imaged after 6 h. (A) Representative light microscopy images of tubules from the siScrambled and siPDK4 conditions. (B) Matrigel tubules were imaged and quantified using ImageJ software (N=10, data are representative of 10 technical replicates across 3 independent experiments). *P<0.05, **P<0.01, ****P<0.0001 vs. controls by two-way ANOVA. $^{###}P$<0.001 vs. non-transfected control by two-way ANOVA. $^{\wedge\wedge}P$<0.01 vs. siScrambled control by two-way ANOVA. Data are expressed as mean±SEM. NTC; non-transfected control.

4.3.7. High glucose suppresses the induction of HIF-1α in response to hypoxia, rHDL has no effect on HIF-1α, but reduces expression of PHD1, PHD2, and PHD3

HIF-1α has been demonstrated to play a role in regulation of PDK4 transcription [12], and this experiment aimed to determine how rHDL affected HIF-1 α expression. Expression of HIF-1α was significantly increased with hypoxia exposure across all conditions ($P<0.0001$, Figure 4.8A). High glucose exposure impaired expression of HIF-1α under hypoxic conditions (83 ±6 to 62 ±6 pg/mL, 29% decrease, $P<0.01$), compared to normal glucose in hypoxia. rHDL treatment had no effect on HIF-1α expression in either normal or high glucose. The role of the PHD proteins (1, 2 and 3) is primarily to target HIF-1α for degradation in normoxia, with their expression downregulated in hypoxia to allow accumulation of HIF-1α [18]. The PHD proteins also play roles in other transcription pathways [10, 19, 20]. We aimed to determine whether rHDL treatment had any impact on expression of the PHD proteins. Despite a lack of change in HIF-1α, rHDL decreased expression of PHD1 in normoxia and high glucose conditions (112 ±12 to 83 ±6 %, 26% decrease, $P<0.05$, Figure 4.8B) but this suppression was not seen in hypoxia (Figure 4.8C). Whilst there were no changes in PHD2 in normoxia (Figure 4.8D), rHDL decreased PHD2 protein levels under high glucose conditions and in hypoxia, compared to PBS high glucose controls (99 ±10 to 73 ±6 %, 26% decrease, $P<0.05$, Figure 4.8E). In normoxia, PHD3 expression was decreased with high glucose (100 ±4 to 80 ±7 %, 20% decrease, $P<0.05$, Figure 4.8F). rHDL treatment further reduced PHD3 expression in high glucose in both normoxia (80 ±7 to 54 ±5 %, 32% decrease, $P<0.01$, Figure 4.8G) and hypoxia (65 ±6 to 46 ±5 %, 29% decrease, $P<0.05$), compared to PBS high glucose-treated cells. In summary, rHDL treatment has no effect on HIF-1α expression but decreases expression of the PHDs.

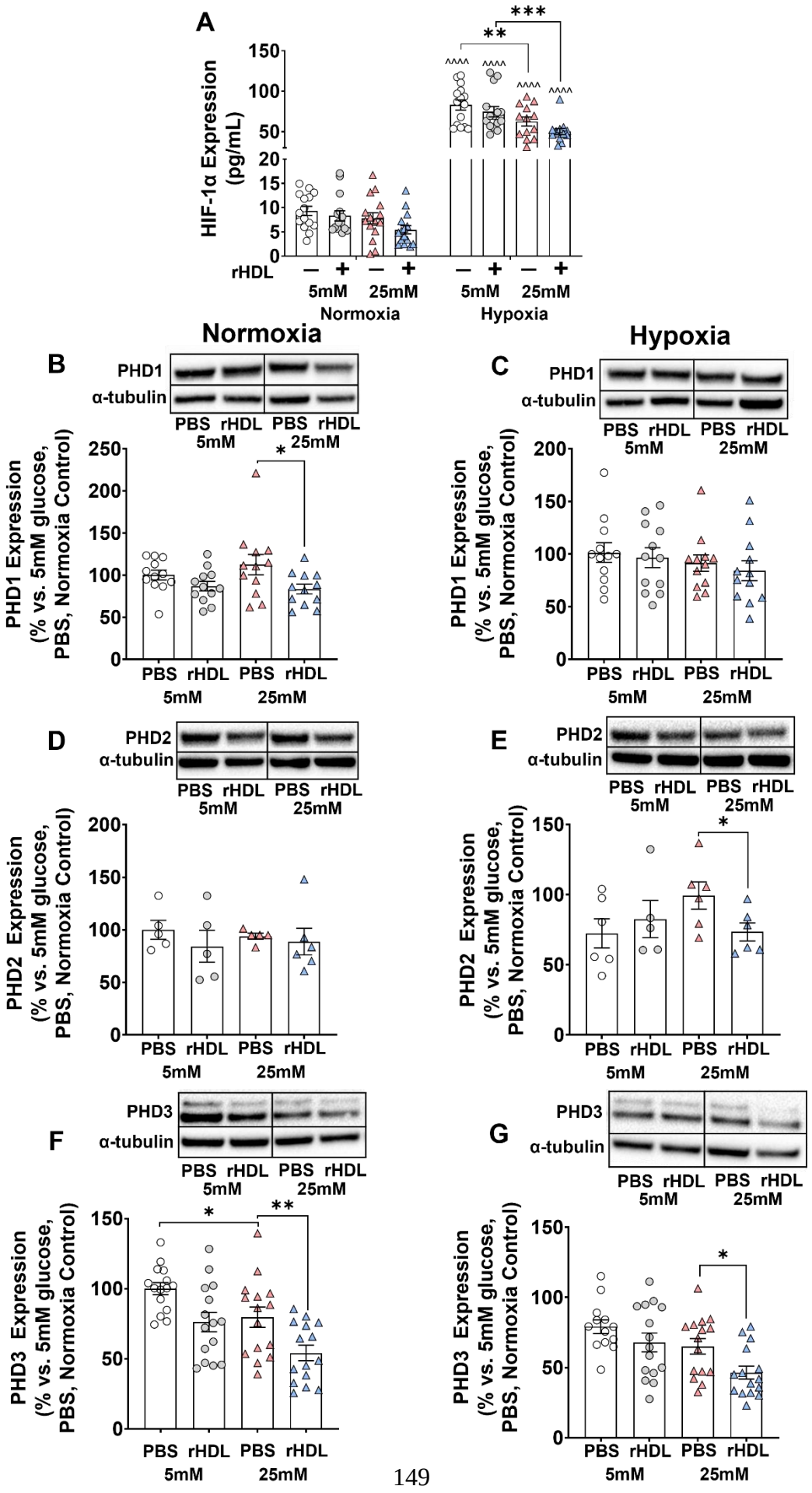
A
HIF-1α Expression (pg/mL)
rHDL
5mM
25mM
Normoxia
Hypoxia
Normoxia
Hypoxia
B
PHD1
α-tubulin
PHD1 Expression (% vs. 5mM glucose, PBS, Normoxia Control)
C
D
PHD2
PHD2 Expression (% vs. 5mM glucose, PBS, Normoxia Control)
E
F
PHD3
PHD3 Expression (% vs. 5mM glucose, PBS, Normoxia Control)
G
PBS
rHDL

Figure 4.8. High glucose suppresses the induction of HIF-1α in response to hypoxia, rHDL has no effect on HIF-1α, but reduces expression of PHD1, PHD2, and PHD3

HCAECs were incubated with rHDL (20 μM) or PBS (vehicle control) for 18 h, then exposed to normal (5 mmol/L) or high (25 mmol/L) glucose conditions for 72 h. Cells were exposed to normoxia or hypoxia (1.2% O^2) for 6 h. (A) Whole-cell HIF-1α protein expression was measured using an ELISA (N=13-15, data are representative of 13-15 technical replicates across 5 independent experiments). ***P*<0.01, ****P*<0.001 vs. controls. ^^^^*P*<0.0001 vs. normoxia controls by two-way ANOVA. Whole-cell protein expression of (B-C) PHD1 (N=12, data are representative of 12 technical replicates across 4 independent experiments), (D-E) PHD2 (N=5-6, data are representative of 5-6 technical replicates across 2 independent experiments), and (F-G) PHD3 (N=13-15, data are representative of 13-15 technical replicates across 5 independent experiments) was measured using western blotting densitometry, with data normalized to α-tubulin. **P*<0.05, ***P*<0.01 by unpaired t-test. Data are expressed as mean±SEM.

4.3.8. rHDL reduces phosphorylation of FOXO1 and enhances its transcription factor activity in high glucose and hypoxia

In the absence of a change in HIF-1α with rHDL, we next examined FOXO1, a transcription factor which interacts with the PDK4 promoter and plays a role in the regulation of angiogenesis. In hypoxia under normal glucose conditions, FOXO1 phosphorylation was increased (100 ±4 to 149 ±18 %, 49% increase, $P<0.05$, Figure 4.9A-C), compared to the normoxia control. In hypoxia under high glucose, rHDL treatment decreased the phosphorylation of FOXO1 (193 ±13 to 138 ±15 %, 29% decrease, $P<0.05$), compared to PBS and high glucose-treated cells, returning it to the level observed under normal glucose conditions. A chromatin immunoprecipitation assay (ChIP) assessed FOXO1 interaction with a known site within the PDK4 promoter region (Figure 4.10A). High glucose exposure reduced the amount of FOXO1-bound to the PDK4 promoter compared to the normal glucose control (100 ±4 to 8.7 ±1 %, 91% decrease, $P<0.0001$, Figure 4.10B). Hypoxia exposure significantly reduced FOXO1-bound PDK4 promoter compared to the normoxia control (100 ±4 to 39 ±5 %, 62% decrease, $P<0.01$). rHDL treatment under high glucose and hypoxic conditions enhanced the amount of FOXO1-bound PDK4 promoter sequence (34 ±3 to 61 ±13 %, 79% increase, $P<0.05$). In summary, rHDL enhanced the transcription factor activity of FOXO1 on the PDK4 promoter region.

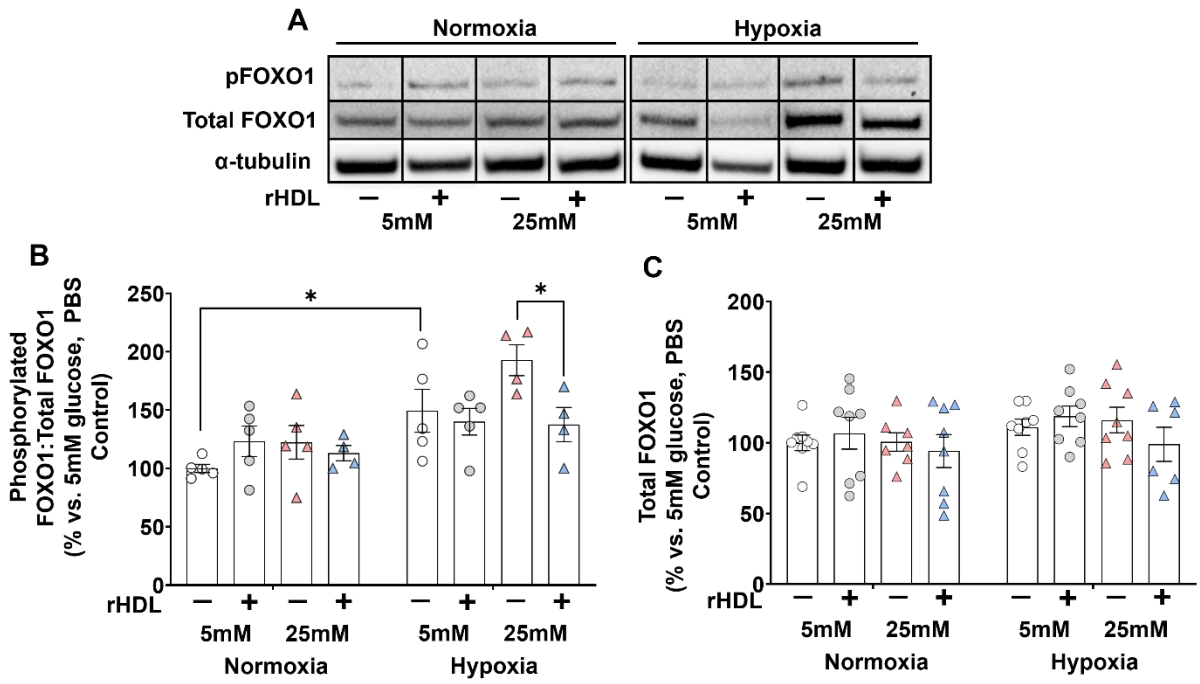

Figure 4.9. rHDL reduces FOXO1 phosphorylation in high glucose and hypoxia.

HCAECs were incubated with rHDL (20 µM) or PBS (vehicle control) for 18 h, then exposed to normal (5 mmol/L) or high (25 mmol/L) glucose conditions for 72 h. Cells were exposed to normoxia or hypoxia (1.2% O^2) for 6 h. (A) Representative Western blot images of phosphorylated FOXO1 (pFOXO1) and total FOXO1 levels (B) Graphed densitometry analyses of pFOXO1:Total FOXO1, and (C) total FOXO1 with data normalized to α-tubulin (N=4-8, data are representative of 4-8 technical replicates across 3 independent experiments). **P*<0.05 by two-way ANOVA. Data are expressed as mean±SEM.

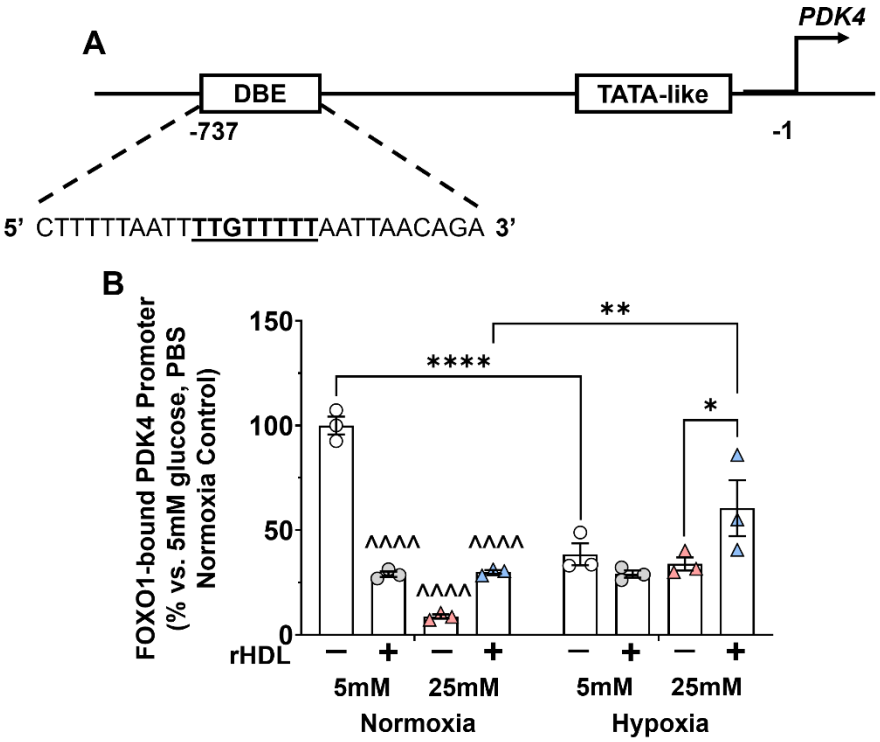

Figure 4.10. rHDL increases FOXO1 binding to the PDK4 promoter in high glucose and hypoxia.

HCAECs were incubated with rHDL (20 µM) or PBS (vehicle control) for 18 h, then exposed to normal (5 mmol/L) or high (25 mmol/L) glucose conditions for 72 h. Cells were exposed to normoxia or hypoxia (1.2% O^2) for 6 h. (A) A schematic showing the FOXO1 binding site sequence (underlined) in the PDK4 gene promoter region that was targeted by the chromatin immunoprecipitation assay (ChIP). (B) FOXO1 binding to this known site in the PDK4 promoter was measured using ChIP (N=3, data are representative of 3 technical replicates from 1 independent experiment). **P*<0.05, ***P*<0.01, *****P*<0.0001 vs. controls by two-way ANOVA. ^^^^*P*<0.0001 vs 5mM glucose, PBS control by two-way ANOVA. Data are expressed as mean±SEM.

4.4. Discussion

Diabetes impairs ischemia-driven angiogenesis, which contributes to the development of diabetic vascular complications such as chronic wounds [35]. Endothelial cell metabolic reprogramming in response to hypoxia is an important part of preserving EC function. The PDK4/PDC axis is central to the regulation of metabolic reprogramming [74, 115], and disruption of this axis may contribute to the impairment of angiogenesis in diabetes. We hypothesised that rHDL may correct this impairment, since it has pro-angiogenic effects in high glucose and diabetic mouse models [45, 85, 86, 111]. We now report the following important findings. Firstly diabetes impairs metabolic reprogramming responses to wound ischemia *in vivo*. rHDL rescues this, while also rescuing impaired wound healing and enhancing neovascularization. High glucose impairs EC metabolic reprogramming responses to hypoxia, with rHDL incubation returning the regulation of the PDK4/PDC axis to that seen in normal glucose. rHDL rescues high glucose-impaired *in vitro* angiogenic functions, and siRNA knockdown of PDK4 ameliorates these effects of rHDL on angiogenesis. Finally, the mechanism underlying the metabolic effects of rHDL may be elicited by activation of FOXO1 activity and binding to the PDK4 promoter. Taken together, we show diabetes impairs metabolic reprogramming responses to hypoxia and demonstrate a new mechanism by which rHDL rescues diabetes-impaired angiogenesis.

We observed a striking impairment to the induction of PDK4 and pPDC in diabetic mice in the early stages post-wounding (Figure 4.1). This result indicates that control of mitochondrial respiration is perturbed in diabetic wound tissue, and may contribute to impaired endothelial cell function and wound neovascularisation.

The known effect of diabetes on PDK4 expression and activity varies depending upon the tissue. For example, *PDK4* mRNA expression is elevated in muscle tissue from diabetic mice,

which is likely connected to the fact that diabetes causes impaired glucose utilisation [116]. Other studies have shown that general cellular metabolism is perturbed in different ways across diabetic tissues [117]. This variation is expected, since different tissues display unique metabolic phenotypes that support their function. Our findings highlight the clear effect of diabetes on metabolic reprogramming in murine wound tissue, but also the importance of the PDK4/PDC axis in the early response to wound ischaemia. A strength of this study is the measurement of key metabolic *in vivo* markers in separate cohorts of mice over time post-wound ischemia, providing a clear demonstration of their expression patterns through the different phases of healing. We identified that the axis plays a lesser role in the later stages of wound healing. The tissue-specific and temporal elements must both be considered in the translation of these findings.

rHDL enhanced PDK4 and pPDC levels in the wound tissue of diabetic mice (Figure 4.1), and enhanced both neovascularization and healing (Figure 4.2), suggesting a potential association between the PDK4/PDC axis and neovascularisation. Our *in vitro* findings in HCAECs confirmed this with siRNA-mediated knockdown of PDK4 causing a reduction in rHDL-induced tubulogenesis (Figure 4.7).

We demonstrated that hypoxia exposure increased *PDK4* mRNA expression and pPDC, highlighting the importance of this mechanism in the EC hypoxia response (Figure 4.3). Importantly, exposure to high glucose in hypoxia did not elicit an additional stepwise induction in PDK4 expression and pPDC, and increased mitochondrial respiration (Figure 4.4). This demonstrated that high glucose negatively affects the cells' ability to suppress respiration. In parallel, high glucose negatively impacted angiogenic functions in response to hypoxia (Figure 4.5, 4.6), suggesting that aberrant metabolic responses to hypoxia contribute to the impairment of angiogenesis in high glucose.

Preincubation with rHDL rescued high glucose-impaired metabolic reprogramming responses to hypoxia (Figure 4.3). In high glucose and hypoxia, rHDL elevated PDK4 and PDC phosphorylation, reduced mitochondrial respiration (Figure 4.4) and rescued *in vitro* angiogenic functions (Figure 4.5, 4.6). When PDK4 was knocked down these effects of rHDL on angiogenesis were attenuated, demonstrating the importance of PDK4 in mediating the pro-angiogenic properties of rHDL (Figure 4.7). Overall, our data demonstrate that rHDL corrects impaired metabolic reprogramming responses to hypoxia and rescues impaired angiogenesis.

The question of how rHDL elicits changes in PDK4 transcription was central to this study. In the absence of an effect on the central hypoxia transcription factor HIF-1α (Figure 4.8), we investigated the transcription factor FOXO1 as it is known to interact with the PDK4 promoter region [118]. When FOXO1 is phosphorylated, it is excluded from the nucleus and its transcriptional activity is abrogated [118]. A role for FOXO1 in angiogenesis and EC function has previously been identified [49]. Wilhelm et al. demonstrated that deletion of FOXO1 in mice caused an increase in vessel sprouting. Conversely, its overexpression severely restricted angiogenesis and led to vessel thinning. The angiogenic role of FOXO1 in response to hypoxia was not examined. We observed that phosphorylation of FOXO1 was increased under hypoxic conditions, indicating a decrease in its nuclear activity (Figure 4.9). With high glucose exposure, phosphorylation was further increased, potentially pushing its activity below acceptable levels which may explain the impairment to PDK4 expression. rHDL significantly decreased FOXO1 phosphorylation, restoring its levels to those seen in the normal glucose control. This finding was supported by ChIP which showed that rHDL treatment increased the binding of FOXO1 to the PDK4 promoter (Figure 4.10), thereby presenting a mechanism to explain our observed increases in PDK4 expression by rHDL (Figure 4.11).

In conclusion, we have demonstrated that diabetes impairs metabolic reprogramming and angiogenic responses to hypoxia, which are rescued by rHDL *in vitro* and *in vivo*. These findings provide further mechanistic support for the effects of rHDL on diabetes-impaired angiogenesis and may lead to the translation of HDL as a topical therapeutic agent for diabetic wound healing for the prevention of diabetic vascular complications.

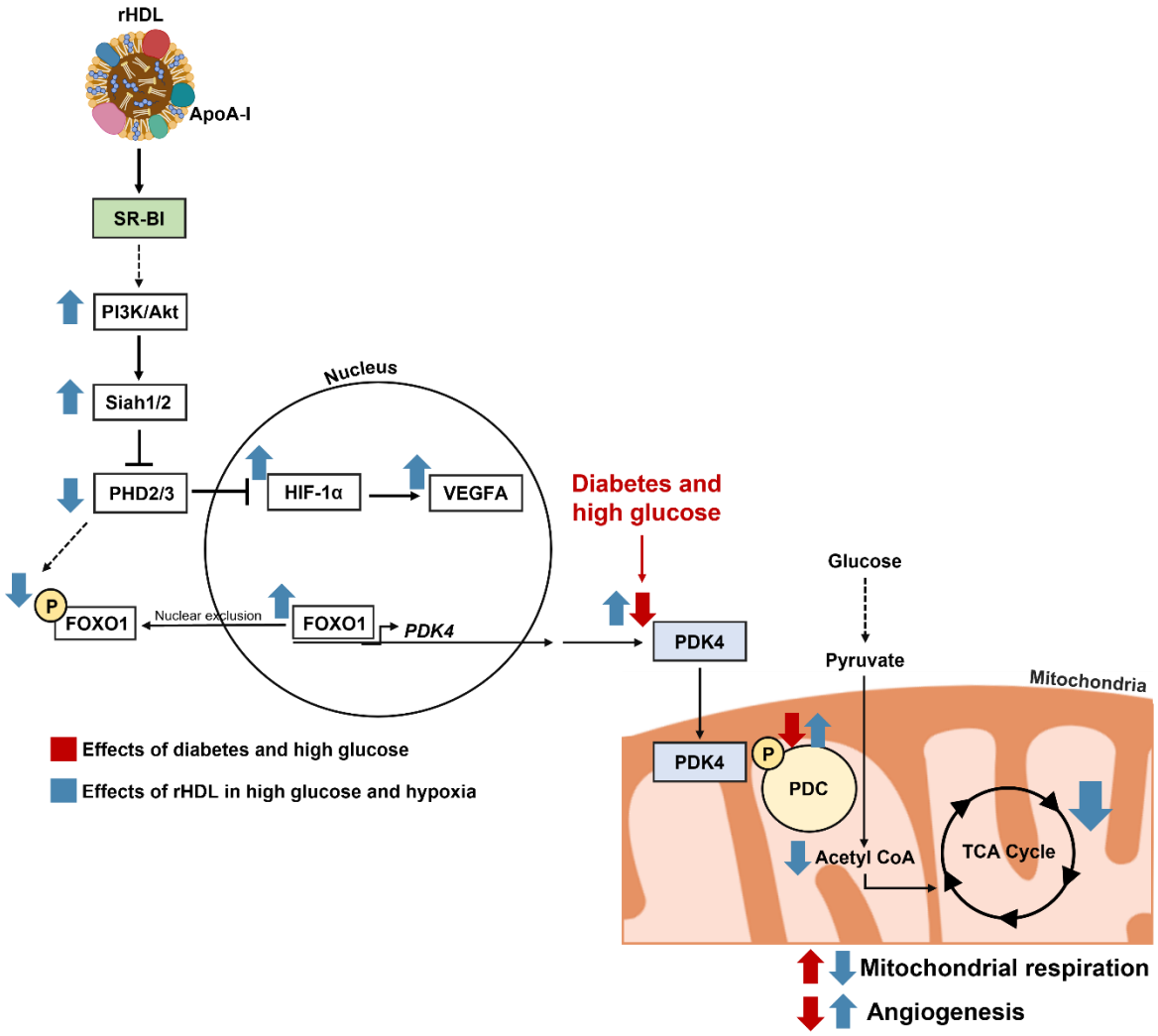

Figure 4.11. Proposed mechanism of impairment to the PDK4/PDC axis by diabetes and its regulation by rHDL.

Diabetes impairs the induction of the PDK4/PDC axis in response to hypoxia, which is associated with aberrant metabolic responses and an impairment to EC function. In an SR-BI-dependent manner, rHDL decreases expression of the PHD proteins, which may affect phosphorylation of FOXO1. Decreased phosphorylation of FOXO1 leads to increased transcription factor activity, which increases binding of FOXO1 to the PDK4 promoter region and the transcription of PDK4. Increased PDK4 is associated with an increase in inactivation of the PDC, which would lead to a decrease in the amount of glucose-derived acetyl CoA available to fuel the TCA cycle. Overall mitochondrial respiration is decreased, improving cell survival in high glucose and hypoxia and preserving hypoxia-induced angiogenesis.

5. Endothelial-specific, inducible overexpression of PDK4 using a novel lentiviral vector

5.1. Introduction

Cellular metabolism is central to every function a cell performs. It provides energy in the form of ATP, but also building blocks like amino acids and metabolic intermediates with their own roles in intracellular signalling [119]. Because of this, the type of metabolism a cell performs and the way it is regulated is often as unique as its specific function. For example, myocytes oxidise large quantities of glucose to produce enough ATP for muscle contraction and must continue to do so in diabetes to protect against hyperglycaemia [116, 120]. Other cells may preferentially metabolise fatty acids, or rely heavily on glutamine metabolism.

Endothelial cells are unique in that they preferentially suppress mitochondrial respiration in response to hypoxia and rely on glycolysis to produce energy to conserve oxygen consumption [41, 109]. Because of the uniqueness of each cell's metabolic phenotype, therapies aimed at altering cellular metabolism must be targeted to that specific cell type so as not to perturb the metabolism of other cells in a negative way.

The previous chapter demonstrated that rHDL rescues diabetes-impaired angiogenesis and wound healing, in part through the improvement of endothelial cell metabolic reprogramming in hypoxia. rHDL has limitations as a targeted approach to altering endothelial metabolism as it has exhibits pleiotropic effects and lacks cell-specificity due to the presence of ABCAI, ABCGI and SR-B1 on many cells [79, 121]. In the present study, we have therefore taken a different approach to targeting PDK4 in endothelial cells. We developed and employed an endothelial-specific, doxycycline-inducible gene expression system packaged into a lentiviral vector.

The latest generation of lentiviral vectors have recently demonstrated dramatically improved safety and therapeutic efficacy in clinical trials [122]. This technology may represent the future of medical therapy as it can be engineered to enable an exquisite level of regulatory control

and cell-targeted specificity of transgene expression. The benefits of this are immense, in particular because the therapy can be focused precisely at the site and in the cell type where transgene expression will be effective, substantially limiting off-target effects. Lentiviruses, unlike many other viral vectors, also integrate their DNA stably into the host genome and have been shown to elicit limited immune activation following their transduction [89]. They also possess a higher capacity for larger transgenes than other viruses [92]. These factors indicate that lentiviral gene transfer is the only approach capable of achieving the level of precision that we believe is required for augmentation of PDK4 expression in a clinical setting.

To create this vector, we used a plasmid with two distinct expression cassettes. In the first, expression of a doxycycline-inducible transactivator protein, rtTA2S-M2, is controlled by the endothelial lineage-specific, murine vascular endothelial cadherin (VEcad) promoter. In the second, expression of a transgene, in our case the open reading frame of PDK4, is driven by an inducible promoter TREalb, which is induced by rtTA2S-M2 [101]. This plasmid was packaged into a lentiviral vector, used to transduce target endothelial cells and 'switch on' the expression of the transgene PDK4 with the addition of doxycycline. Not only is the cell-targeting specificity of PDK4 overexpression important but so too is the doxycycline-inducible on/off control of this vector. This temporal regulation will allow the PDK4 transgene to be activated at the optimal experimentally-determined time in a disease or healing process. For example, wound healing is a highly regulated process with distinct stages, including the inflammatory, proliferative, and remodelling phases [31]. Activating PDK4 overexpression too early could interrupt the inflammatory phase, and activating PDK4 expression during the remodelling phase could disrupt the maturation of a newly-formed vascular network. Being able to switch off transgene expression will also mean that there is no disruption of cell function in normal, healthy tissue.

The aims of the present study were to: i) create an inducible endothelial cell specific PDK4-overexpression lentiviral vector (lentiVEcad-PDK4) in parallel with a CopGFP control lentivirus (lentiVEcad-GFP); ii) validate the inducibility and cell-specificity of the gene expression of these lentiviruses *in vitro* and iii) determine whether transduction of lentiVEcad-PDK4 improves wound angiogenesis and healing in diabetic mice. We hypothesised that endothelial-specific overexpression of PDK4 would enhance wound angiogenesis, and that this would promote healing in the diabetic mice.

5.2. Methods

5.2.1. Generation of lentivirus expressing PDK4

A gene expression system which enables endothelial-specific and doxycycline-inducible expression of a transgene was obtained [101]. Briefly, the vector contained the endothelial-specific promotor of the VE-cadherin gene, which drives the expression of the Tet-responsive transactivator protein (rtTA). The rtTA protein, in the presence of doxycycline, interacts with a Tet-responsive albumin promoter (TREalb) to drive expression of a transgene. The pVEcad vector was provided to our group by the Qian Group (University of Navarra, Spain). This vector contained green fluorescent protein (GFP), was denoted "pVEcad-GFP" and was used as our control lentivirus. To generate pVEcad-PDK4 we excised the open reading frame of GFP and replaced it with murine *Pdk4.*

5.2.1.1. Bacterial cell culture and transformation

Library Efficiency™ DH5α Competent Cells (Thermo Fisher Scientific) were used for all relevant applications. Cells were cultured in sterile lysogeny broth (1L deionised H_2O, 10g tryptone, 5g yeast extract, 10g NaCl, pH 7.4.) in various volumes depending on the quantity of DNA required.

Bacterial transformation was achieved using the heat shock method as follows. 1-5µl of DNA was added to 50µL of competent cells in an Eppendorf tube and gently mixed, then incubated on ice for 20 minutes. The heat shock was conducted by placing the tube in a thermocycler set to exactly 42°C for 45 seconds. Tubes were then placed back on ice for 2 minutes. 950µL of SOC medium was added and tubes were incubated while shaking at 37°C for at least 1 hour. 100µL of the bacterial culture was plated on 10cm LB agar plates containing ampicillin at a concentration of 100mg/mL, then incubated overnight at 37°C.

5.2.1.2. DNA preparation

To extract DNA from bacterial cultures, the Qiagen Maxi- or Mini-prep kits were used. Briefly, bacterial cultures were pelleted by centrifugation at 2500rpm for 15 minutes at 4°C then resuspended in Buffer P1. Buffer P2 was then added and mixed vigorously, then incubated at room temperature for 5 minutes. Prechilled Buffer P3 was added and again mixed vigorously, then incubated on ice for up to 20 minutes. The solution was centrifuged between 14000 to 21000 rpm for at least 30 minutes at 4°C, and the supernatant was applied to an equilibrated QIAGEN-tip column. The column was then washed with Buffer QC, and DNA was eluted into a clean vessel using Buffer QF. To precipitate the DNA, room temperature isopropanol was added and centrifuged at 14000 rpm for 30 minutes at 4°C. Supernatant was discarded, and the DNA pellet was washed with room temperature 70% ethanol, and centrifuged at 14000 rpm for 10 minutes. Supernatant was discarded and pellet was air dried until no ethanol remained, then dissolved into an appropriate quantity of TE buffer.

5.2.1.3. DNA product size and quality assessment

DNA samples were run on 1% (w/v) agarose gels. To make these gels, agarose powder was added to the appropriate volume of TAE buffer. The TAE buffer was prepared by dissolving 242 g Tris base in water, adding 57.1 ml glacial acetic acid and 100 ml of 500 mM EDTA, then bringing the final volume to 1 litre. This solution was then diluted 1:50 in water to make a 1X working buffer. The agarose powder in TAE buffer was then microwaved at 100% power for 1 minute, mixed, and then microwaved again until all the agarose powder was dissolved. GelRed® Nucleic Acid Stain (Sigma Aldrich) was added to the molten agarose in a 1:10000 dilution. Molten agarose was poured into a gel mould and allowed to set at room temperature. To prepare samples to be run on these agarose gels, DNA samples were combined with 6X Blue/Orange Loading Dye (Promega) and nuclease-free water to the appropriate final volume.

To determine DNA fragment size, samples were run alongside 2µL of the Promega 1kb or 100bp DNA ladder. Gels were visualised using the GelDoc system (Bio-Rad).

5.2.1.4. Generating the Pdk4 PCR product

A plasmid containing the murine *Pdk4* sequence was obtained (Origene). Primers complementary to the *Pdk4* sequence and containing SalI sites were designed, and a PCR product was produced that contained SalI restriction enzyme sites flanking each side of the open reading frame of *Pdk4* using the reagents described in Table 5.1. The cycling conditions described in Table 5.2 were run using the T100 Thermal Cycler (BioRad).

Table 5.1. Reaction components for production of PDK4 insert

Component	**Volume (uL)**
5x GoTaq Flexi Buffer	10.0
dNTPs	1.0
Forward primer, 10µM	5.0
Reverse primer, 10µM	5.0
Plasmid template, 500ng	0.625
$MgCL_2$, 2mM final conc.	4.0
GoTaq DNA polymerase	1.0
Nuclease-free H_2O	23.375
Total	50.0

Table 5.2. Cycling conditions for generation of PCR product

Stage	**Temperature**	**Time**
Denaturation	98°C	30 seconds
Annealing, 35x cycles	98°C	10 seconds
	67°C	30 seconds
	72°C	1 minute
Final extension	72°C	2 minutes
Hold	10°C	Indefinitely

The resultant PCR product was run on a 1% (w/v) agarose gel for at least 30 minutes at 50-100V as outlined in the previous section and gel-extracted using the Qiagen Gel Extraction kit to ensure removal of residual plasmid. The extracted DNA was quantified using a NanoDrop 8000 spectrophotometer (Thermo Fisher Scientific).

5.2.1.5. TA cloning using the pGEM T-Easy system

The newly generated *Pdk4* PCR product was ligated first into the TA cloning vector pGEM T-easy using the reaction mix in Table 5.3. The ligation was performed at room temperature for at least 3 hours before bacterial transformation. Insertion of the *Pdk4* PCR product into pGEM T-easy enables complete digestion of the SalI sites, which enhances the chances of successful *Pdk4* PCR product insertion into the VEcad lentiviral transfer vector.

Table 5.3. Reaction mix for pGEM T-easy ligation

Component	**Volume (uL)**
10X Ligation buffer	1.0
pGEM vector, 50ng total	1.0
PCR product, 3:1 molar ratio	1.2
T4 DNA ligase	1.0
Nuclease-free H_2O	5.8
Total	10.0

To excise the *Pdk4* PCR product from the pGEM vector, a SalI digestion was performed using 1µL of enzyme for 1µg of plasmid DNA. The incubation was completed at 37°C for at least 3 hours, and the digested fragment was gel extracted using the Qiagen Gel Extraction kit.

5.2.1.6. Preparation of pVEcad vector

The plasmid containing the VE-cadherin promoter gene expression system (pVEcad) was linearised by digestion with the SalI restriction enzyme, using 1µL of enzyme for each 1µg of plasmid DNA. The incubation was completed at 37°C for at least 3 hours.

The digested vector was run on a 1% (w/v) agarose gel for at least 30 minutes at 50-100V and gel extracted using the Qiagen Gel Extraction kit. The extracted DNA was quantified using a NanoDrop 8000 spectrophotometer (Thermo Fisher Scientific).

5.2.1.7. Ligation of Pdk4 PCR product with pVEcad

The following reaction mix was used to ligate the *Pdk4* PCR product with the linearised pVEcad vector. The ligation was performed at room temperature for at least 3 hours before bacterial transformation.

Table 5.4. Reaction mix for Pdk4 PCR product, pVEcad ligation

Component	**Volume (µL)**
10X Ligation buffer	1.2
pVEcad vector, 30ng total	6.0
PCR product, 3:1 molar	3.0
T4 DNA ligase	1.0
Nuclease-free H_2O	0.8
Total	12.0

The ligation product was used for bacterial transformation as described in 2.2.6.1.

5.2.2. Large-scale lentivirus production

To generate lentiviral particles, HEK293T cells were first cultured as described in section 2.2.1 Once at 70-80% confluency, the cells were transfected with the gene transfer plasmid and the third-generation packaging plasmids in the following quantities.

Table 5.5. Plasmid quantities for lentivirus production

Plasmid	**Quantity (µg)**
pVEcad (GFP or PDK4)	80.0
pMDL g/pRRE	40.0
pRSV-Rev	20.0
pMD2.G	20.0

For transfection of two T175 flasks of HEK293T cells, the following reagents were added to a 15mL Falcon tube: 1.2mL Opti-MEM media, all the plasmid DNA as outlined above, and 400uL of FuGENE (Promega). The FuGENE was added carefully such that it did not come into contact with the plastic of the Falcon tube. This mixture was incubated at room temperature for 15 minutes. 24mL of DMEM containing 10% FBS was added to the transfection mix, then split between the two T175 flasks. 24 hours later, media was replaced with fresh DMEM.

48 hours later, media was collected from the flasks and cellular debris removed by centrifugation at 2000rpm for 5 minutes. Media was then filtered through a 0.45µM low-retention filter and stored at -80°C. Media was replaced on cells and left to incubate for a further 72 hours, then collected and processed again.

To purify the lentivirus particles, the media was thawed on ice and then layered over 5mL of 20% sucrose in PBS into 33mL Beckman Coulter ultracentrifugation tubes. Media was then ultracentrifuged in an SW28Ti rotor for 2 hours at 26000rpm at 4°C. The supernatant was carefully poured off, and 100uL of PBS containing 1% BSA was carefully added to the tube,

then left to rest undisturbed at 4°C overnight. 24 hours later, the virus particles were aliquoted into 20µL samples and stored at -80°C.

5.2.3. Quantification of lentiviral titre

To determine the concentration of the virus samples, the Lenti-X™ qRT-PCR Titration Kit (Takara Bio) was used. Firstly, viral RNA was isolated using the NucleoSpin® RNA Virus Kit (Takara Bio). Briefly, 600µL Buffer RAV1 containing Carrier RNA was added to the sample to lyse the viral particles. 600µL ethanol (96–100 %) was added to the clear lysis solution. To bind the viral RNA, the lysed solution was added to a NucleoSpin® columns and centrifuged for 1 minute at 8000rpm. The silica membrane was washed with 500µL of Buffer RAW, then 600µL Buffer RAV3. Viral RNA was eluted using 50µL RNase-free H_2O

For qRT-PCR Amplification of Lentiviral Genomic RNA, the following reaction mix was used.

Table 5.6. Master reaction mix for qRT-PCR amplification of lentiviral genomic RNA, per well.

Reagent	**Volume (µL)**
RNase-free water	8.5
2X Quant-X buffer	12.5
Lenti-X Forward primer,	0.5
Lenti-X Reverse primer,	0.5
Quant-X enzyme	0.5
RT enzyme mix	0.5
Total	23.0

The control template and the lentiviral RNA samples were serially diluted, and 2µL of each sample was added to a 96-well plate, followed by 23µL of the master reaction mix. The plate was centrifuged at 800rpm for 1 minute to remove any bubbles. The following cycling conditions were used to analyse the viral RNA content.

Table 5.7. Cycling conditions for qRT-PCR amplification of lentiviral genomic RNA

Stage	**Temperature**	**Time**
RT reaction	42°C	5 minutes
	95°C	10 seconds
qPCR 40X cycles	95°C	5 seconds
	60°C	30 seconds
Dissociation curve	95°C	15 seconds
	60°C	30 seconds
	All (60°C-95°C)	Variable

5.2.4. Cell culture

Human coronary artery endothelial cells (HCAECs), human aortic smooth muscle cells (HAoSMCs), and human dermal fibroblasts (HDFs) were cultured as per section 2.2.1.

5.2.5. In vitro lentiviral transduction

For overexpression of PDK4 using the doxycycline-inducible, endothelial cell-specific lentiviral vector, HCAECs, HAoSMCs and HDFs were seeded in 6-well tissue culture plates at 5 x 10^4 cells/well. Cells were cultured in MesoEndo for 24 hours at 37ºC in 5% CO2. Media was then replaced with 800µL of MesoEndo containing 8µg/mL polybrene. The PDK4 or GFP control lentivirus was added to each well at a multiplicity of infection (MOI) of 5 or 10. For this cell density, an MOI of 5 is equivalent to a concentration of 1 x 10^7 transforming units (TU)/mL and an MOI of 10 is equivalent to a concentration of 2 x 10^7 TU/mL. After 24 hours, media was replaced with 2mL MesoEndo. 48 hours after lentiviral transduction, doxycycline hyclate was added to the cell media at a concentration of 4µg/uL or 8µg/uL to activate gene expression. After a further 48 hours cells either underwent exposure to additional conditions or were processed for gene expression or protein analysis.

5.2.1. RNA extraction and analysis

RNA extraction and qRT-PCR analysis of cell mRNA expression was conducted as described in section 2.2.2.1 onward.

5.2.2. Protein extraction and analysis

Protein extraction and western blotting or ELISA analysis of cell protein expression was conducted as described in sections 2.2.2.5 onward.

5.2.3. In vivo methodology

5.2.3.1. Lentiviral transduction in the murine diabetic wound healing model

To assess the effect of PDK4 overexpression by lentiviral gene transfer on wound angiogenesis and healing, the lentiVEcad-PDK4 or lentiVEcad-GFP control viruses were injected into the wound tissue at a single site at the time of surgery. 25µL of lentivirus particles were injected into each wound at a concentration of 2×10^8 TU/mL.

5.2.3.2. Doxycycline administration

Doxycycline hyclate was administered in the drinking water of the mice at a concentration of 1mg/mL, in light-protected water bottles two days prior to lentiviral transduction. Water was changed every 48 hours.

5.2.3.3. Murine diabetic wound healing model

The diabetic murine wound healing model was conducted as described in section 2.3.2. Briefly, mice were rendered diabetic by a bolus intraperitoneal injection of streptozotocin (165mg/g). At least two weeks post-injection, mice were anaesthetised, and two full-thickness excisional wounds were created either side of the dorsal midline. A silicone splint was secured, and to

assess the effect of PDK4 overexpression by lentiviral gene transfer on wound angiogenesis and healing, the lentiVEcad-PDK4 or lentiVEcad-GFP control virus was administered as described in section 5.2.3.1. Wound closure was measured daily, and laser Doppler perfusion imaging assessed wound blood flow perfusion. Histological analysis of the wound was also conducted as described in section 2.3.9.

5.3. Results

5.3.1. Cloning murine Pdk4 into the pVEcad-GFP vector

We first aimed to replace the GFP coding sequence in the pVEcad vector with the PDK4 coding sequence. To achieve this, a PCR product encoding murine *Pdk4* was generated. Agarose gel electrophoresis analysis confirmed the correct size of the DNA product (Lane 3, Figure5.1A). Sanger sequencing of a pGEM-T Easy intermediate vector containing the *Pdk4* product confirmed the correct sequence (Figure 5.1B), except for a single base pair mismatch at position 1155bp, which replaced a thymine with a cytosine (Figure 5.1C). Both the correct codon (CAT) and the variant codon (CAC) encode the amino acid histidine.

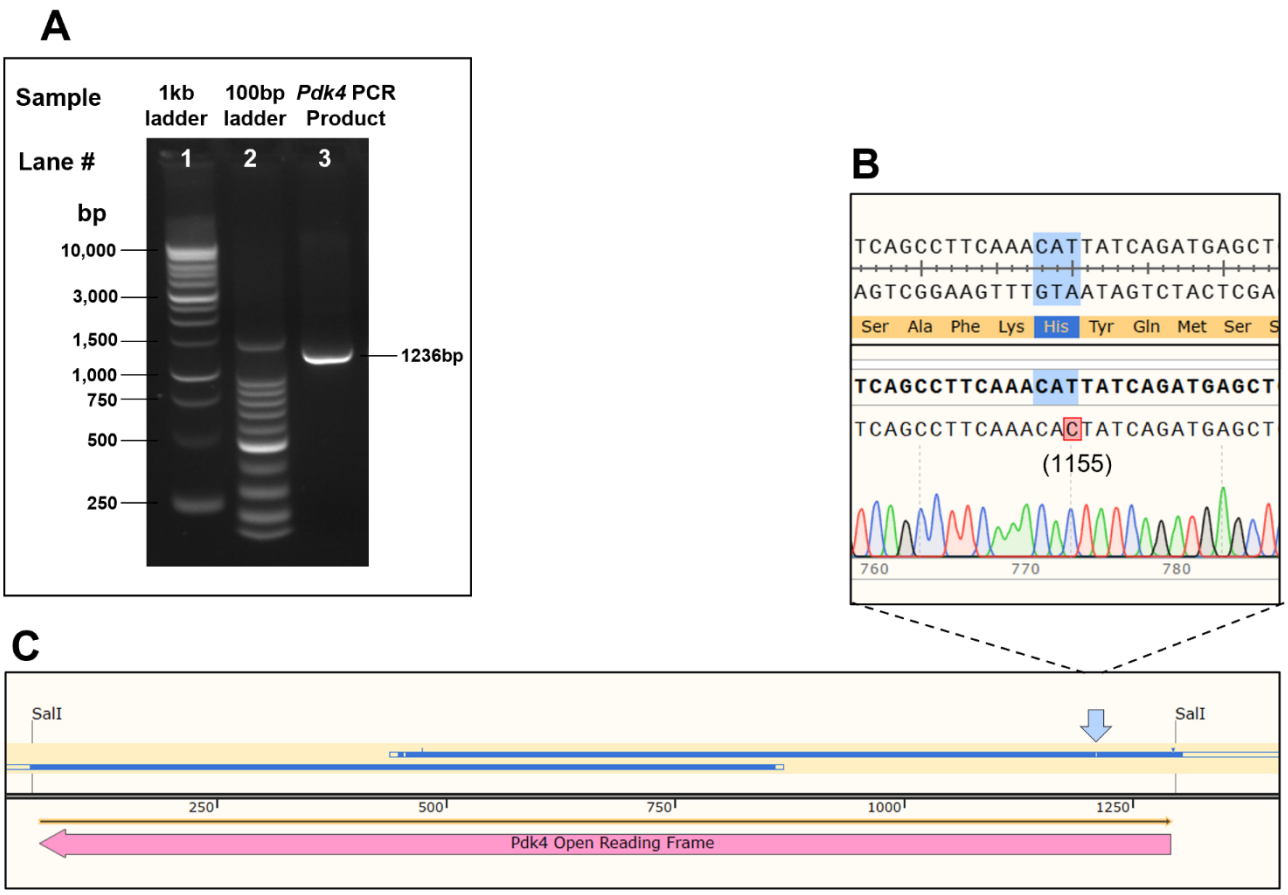

Figure 5.1. *Pdk4* PCR product.

A PCR product encoding murine *Pdk4* was produced using *Taq* polymerase. (A) The PCR product size was analysed by agarose gel electrophoresis. (B-C) Sanger sequencing confirmed the sequence of the PCR product and identified a single base pair mismatch depicted in the inset panel and indicated by the light blue arrow. Sequencing data was visualised using Snapgene software.

5.3.2. The sequence, features and linearisation of the pVEcad-GFP vector

The features of the lentiviral transfer vector, pVEcad-GFP are depicted in Figure 5.2B. pVEcad-GFP was analysed by agarose gel electrophoresis to confirm the correct size. A typical pattern of two bands for circular plasmids can be seen in lane 2 (Figure 5.2A), which contains the undigested pVEcad-GFP plasmid. After digestion with the SalI restriction enzyme, to linearise pVEcad-GFP in preparation for the insertion of the *Pdk4* PCR product, a single band can be seen at approximately 8000bp in lane 3, and a second band at approximately 800bp represents the excised CopGFP sequence.

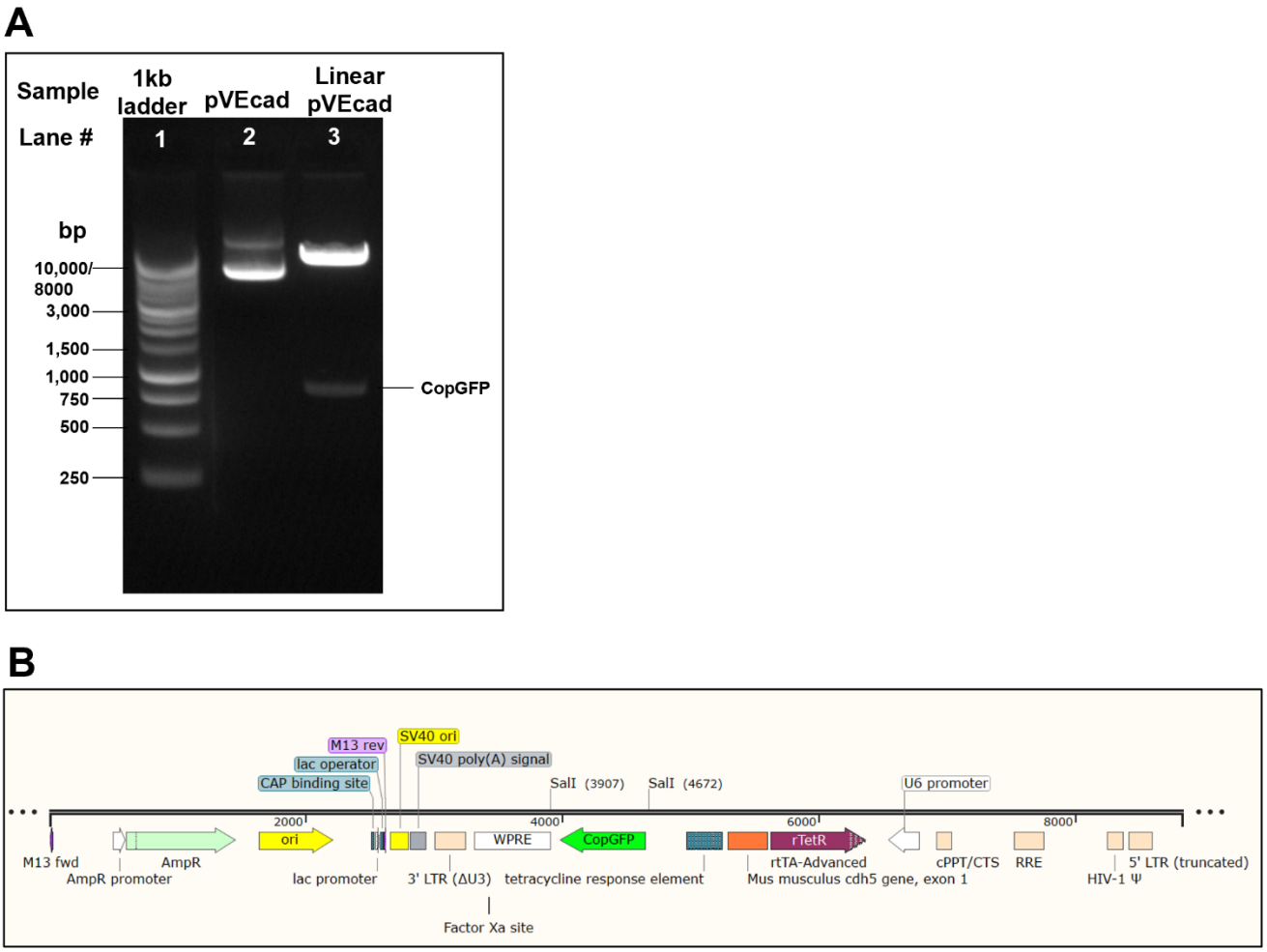

Figure 5.2. Features and linearisation of pVEcad-GFP

(A) Undigested and linearised pVEcad-GFP were analysed by agarose gel electrophoresis to confirm the size and complete digestion, including excision of the open reading frame of CopGFP using digestion with the SalI restriction enzyme. (B) Features of pVEcad-GFP were identified and visualised using Snapgene software.

5.3.3. Successful ligation of the Pdk4 PCR product into linearised pVEcad

The features of the newly-created pVEcad-PDK4 vector are depicted in Figure 5.3. The *Pdk4* PCR product was ligated into the linearised pVEcad vector. The ligation product was digested with SalI and analysed by agarose gel electrophoresis to confirm the presence of the *Pdk4* insert (Figure 5.3A). After SalI digestion, the linear VEcad plasmid can be seen in lane 5 at approximately 8000bp, and the Pdk4 PCR product can be seen at approximately 1200bp. The pVEcad-PDK4 vector also underwent Sanger sequencing to confirm the correct DNA sequence (Figure 5.3B-C).

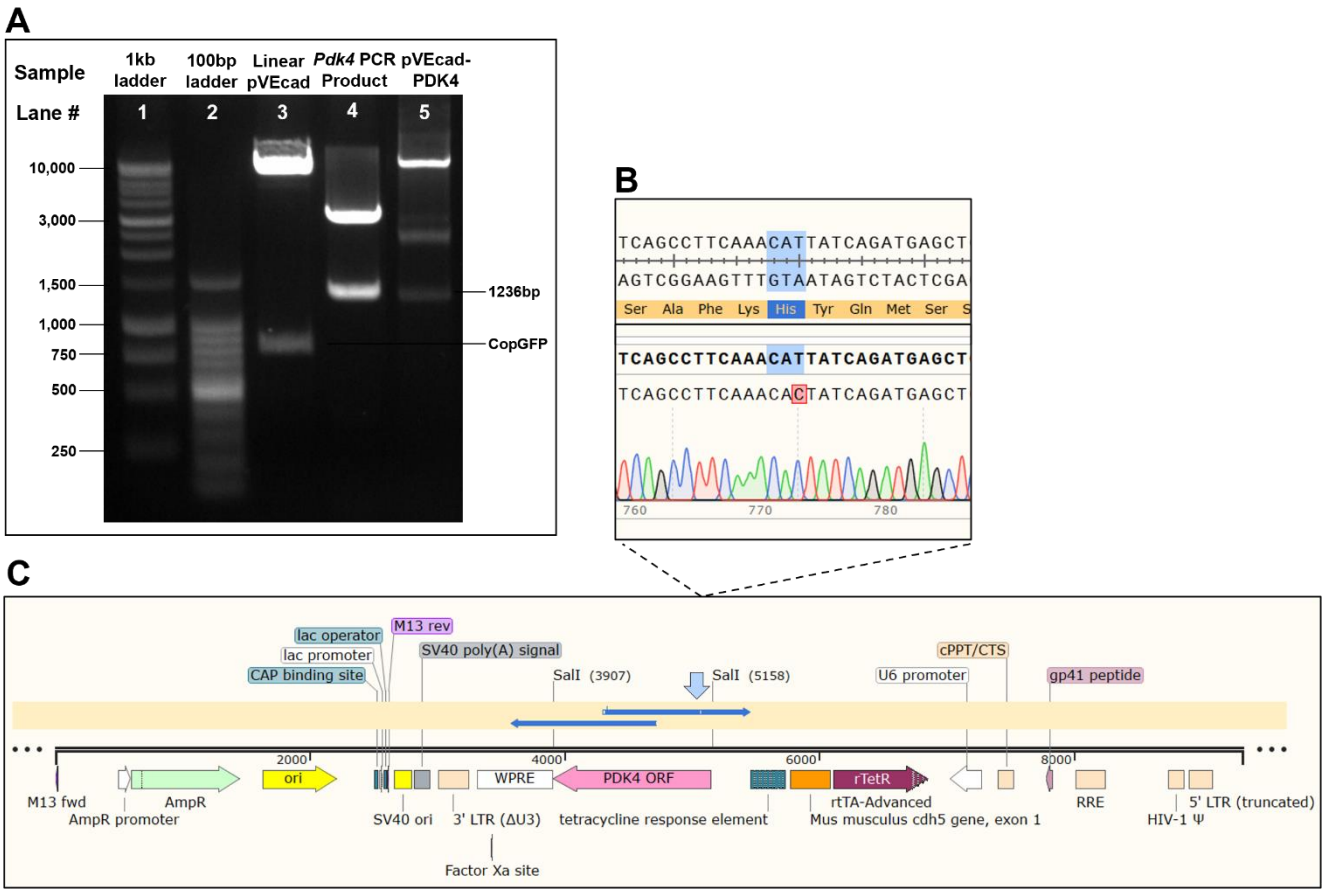

Figure 5.3. Features of the newly-created pVEcad-PDK4 vector.

(A) Agarose gel analysis of pVEcad-PDK4 size and presence of the Pdk4 insert. (B-C) Sanger sequencing of the pVEcad-PDK4 ligation product confirmed the presence and correct orientation of the PDK4 transgene. The single base pair mismatch was also identified and is indicated by the light blue arrow. Sequencing data was visualised using the Snapgene software.

5.3.4. Inducible GFP expression using the lentiVEcad-GFP lentiviral vector

This experiment aimed to characterise the GFP expression elicited by the lentiVEcad-GFP vector at two different MOIs in the presence or absence of doxycycline. In HCAECs, transduction with the lentiVEcad-GFP lentiviral vector at MOI5 and MOI10 induced GFP expression at very low, though non-zero, levels in the absence of doxycycline. At MOI5, GFP expression was significantly induced with doxycycline treatment at 8µg/mL (321.0 ± 35.8 vs. 26.7 ± 4.7 fluorescent cells, $P<0.05$; Figure 5.4A). At MOI10, GFP expression was significantly increased with doxycycline treatment at 4µg/mL (459.3 ± 123.8 vs. 50.7 ± 0.3 fluorescent cells, $P<0.01$), and further increased at 8µg/mL (799.7 ± 10.0 vs. 459.3 ± 123.8 fluorescent cells, $P<0.0001$).

In human aortic smooth muscle cells (HAoSMCs) and human dermal fibroblasts (HDFs), no GFP expression was able to be detected, either in the presence or absence of doxycycline. In summary, the lentiVEcad-GFP vector exhibited endothelial cell-specific and inducible expression of GFP.

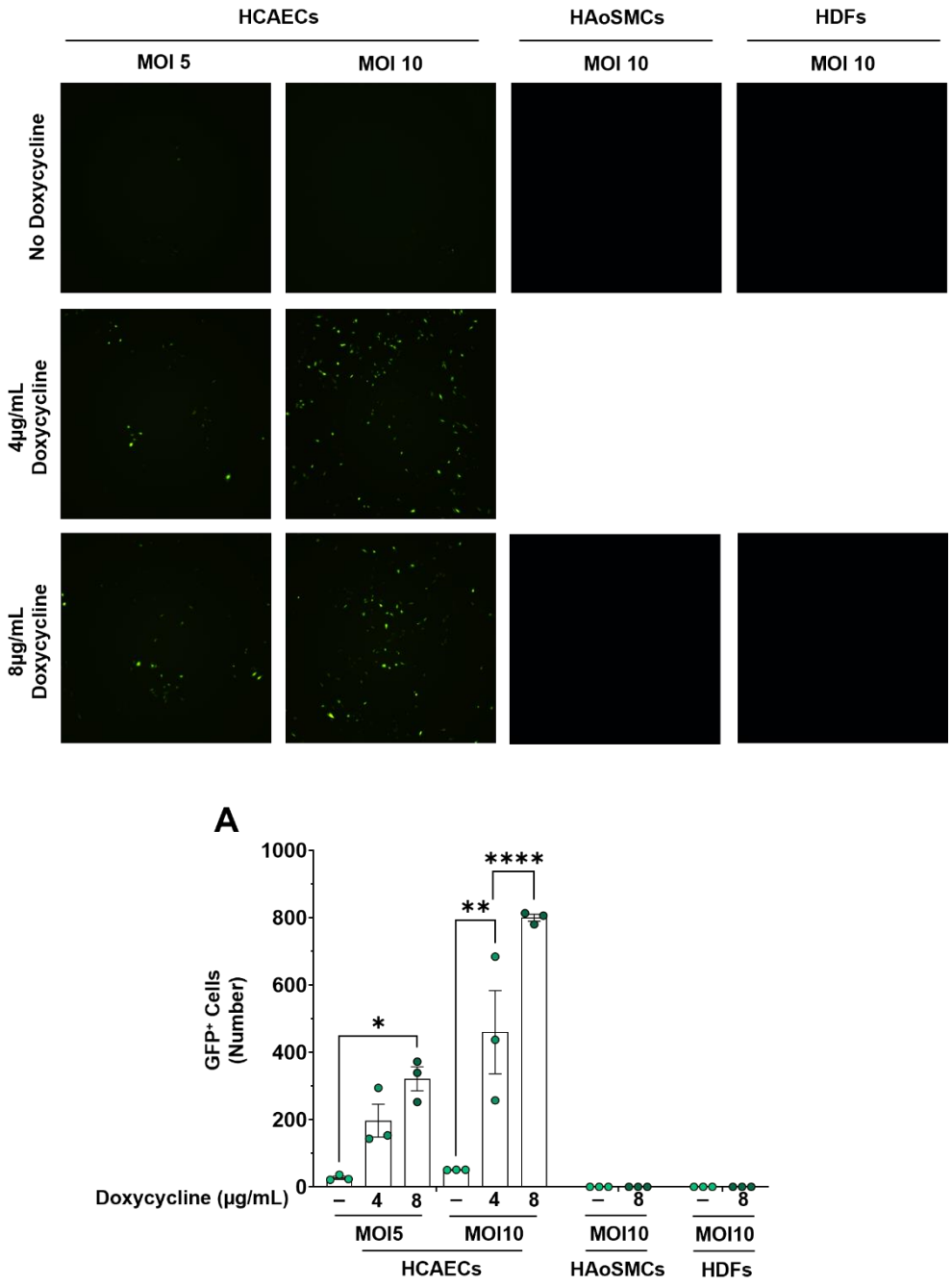

Figure 5.4. Inducible GFP expression using the lentiVEcad-GFP lentiviral vector *in vitro*.

HCAECs, HAoSMCs, and HDFs were transduced with the lentiVEcad-GFP lentivirus at MOI5 or MOI10 for 48 h, then exposed to doxycycline at 4µg/mL or 8µg/mL for a further 48 h. Cells were visualised using fluorescence microscopy at 5X magnification and images analysed using ImageJ. **P*<0.05, ***P*<0.01, *****P*<0.0001 by two way ANOVA. *N*=3, data are representative of 3 technical replicates from 1 independent experiment. Data are presented as mean ± SEM.

5.3.5. Inducible Pdk4 expression using the lentiVEcad-PDK4 vector

This experiment aimed to characterise the PDK4 expression elicited by the lentiVEcad-PDK4 vector in the presence or absence of doxycycline. In HCAECs, transduction with the lentiVEcad-PDK4 vector significantly induced *Pdk4* mRNA expression in the absence of doxycycline (3536.1 ± 198.5 vs. 100.0 ± 7.2 %, $P<0.0001$; Figure 5.5A/B). In the presence of doxycycline, *Pdk4* mRNA was significantly increased compared to both the lentiVEcad-GFP control (20650.8 ± 3262.8 vs. 163.2 ± 18.3 %, $P<0.0001$) and compared to the no-doxycycline control (20650.8 ± 3262.8 vs. 3536.1 ± 198.5, $P<0.01$).

In HAoSMCs and HDFs, neither the GFP nor PDK4 lentivirus treatment or exposure to doxycycline had any significant effect on the amount of *Pdk4* mRNA that was able to be detected (Figure 5.5A/C, D). In summary, *Pdk4* mRNA expression was induced by the lentiVEcad-PDK4 vector in the presence and absence of doxycycline in endothelial cells only.

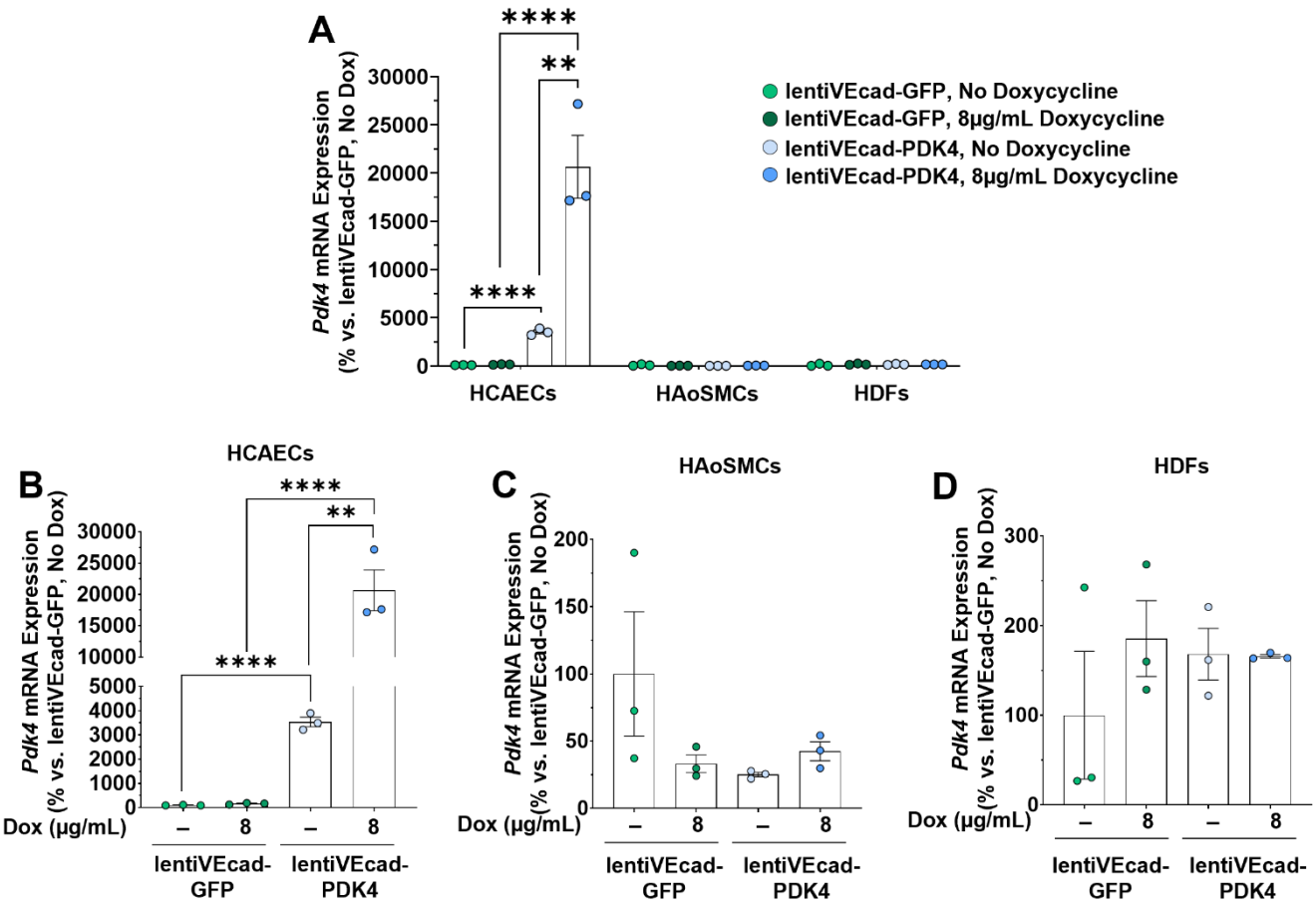

Figure 5.5. Inducible *Pdk4* expression using the lentiVEcad-PDK4 vector *in vitro*

HCAECs, HAoSMCs, and HDFs were transduced with the lentiVEcad-GFP and lentiVEcad-PDK4 lentiviruses at MOI10 for 48 h, then exposed to doxycycline at 8µg/mL for a further 48 h. Cells were harvested and RNA extracted, and *Pdk4* mRNA was measured using qPCR, with gene expression normalised using the $^{\Delta\Delta}$Ct method to human *18S*. ***P*<0.01, *****P*<0.0001 by two way ANOVA. *N*=3, data are representative of 3 technical replicates from 1 independent experiment. Data are presented as mean ± SEM.

5.3.6. No changes in body weight and blood glucose levels between lentiVEcad-GFP- and lentiVEcad-PDK4-treated mice

To identify any potential phenotypic differences that may develop between the mice treated with the different lentiviral vectors, mouse body weights were monitored pre- and post-operatively throughout the study, and blood glucose levels were monitored weekly. Dermal injection of lentiVEcad-GFP and lentiVEcad-PDK4 vectors caused no significant differences in mouse body weights (Table 5.8) or blood glucose levels (Table 5.9) either at time of surgery or at completion of the experiment.

Body Weights (g)	Time of Surgery	Study Endpoint
lentiVEcad-GFP, No doxycycline	24.5 ± 0.0	23.1 ± 0.0
lentiVEcad-PDK4, No doxycycline	22.6 ± 0.7	22.1 ± 0.7
lentiVEcad-GFP, Doxycycline	22.6 ± 0.8	22.2 ± 1.0
lentiVEcad-PDK4, Doxycycline	23.8 ± 0.5	23.6 ± 0.7

Table 5.8. Body weights

In the murine diabetic wound healing model, mouse weights were measured immediately pre-operatively (time of surgery), and at the conclusion of the 9-day wound healing study (study endpoint). LentiVEcad-GFP, no doxycycline (N=1), lentiVEcad-PDK4, no doxycycline (N=2), lentiVEcad-GFP, doxycycline (N=5), lentiVEcad-PDK4, doxycycline (N=5). Data are presented as mean ± SEM.

Blood Glucose Levels (mmol/L)	Time of Surgery	Study Endpoint
lentiVEcad-GFP, No doxycycline	26.6 ± 0.0	29.0 ± 0.0
lentiVEcad-PDK4, No doxycycline	30.5 ± 2.5	30.9 ± 2.2
lentiVEcad-GFP, Doxycycline	27.0 ± 2.9	29.0 ± 3.1
lentiVEcad-PDK4, Doxycycline	21.9 ± 3.2	24.5 ± 2.9

Table 5.9 Blood glucose levels

In the murine diabetic wound healing model, mouse blood glucose levels were measured pre-operatively (time of surgery), and at the conclusion of the 9-day wound healing study (study endpoint). LentiVEcad-GFP, no doxycycline (N=1), lentiVEcad-PDK4, no doxycycline (N=2), lentiVEcad-GFP, doxycycline (N=5), lentiVEcad-PDK4, doxycycline (N=5). Data are presented as mean ± SEM.

5.3.7. lentiVEcad-PDK4 lentiviral gene transfer increases wound blood flow reperfusion in diabetic mice

This experiment aimed to determine how transduction with the lentiVEcad-PDK4 vector affected wound blood flow reperfusion in diabetic mice. In diabetic mice that received doxycycline in their drinking water, treatment with the lentiVEcad-PDK4 lentivirus increased wound blood flow reperfusion compared to the lentiVEcad-GFP vector at day 4 (925.0 ± 96.1 vs. 604.1 ± 58.5 LDPI units, $P<0.01$; Figure 5.7A) and at day 7 (803.5 ± 27.2 vs. 491.9 ± 55.3 LDPI units, $P<0.01$).

In diabetic mice that did not receive doxycycline in their drinking water, treatment with the lentiVEcad-PDK4 lentiviral vector also increased blood flow reperfusion at day 4, but only compared to the mice that received the lentiVEcad-GFP treatment and doxycycline (957.2 ± 93.3 vs. 604.1 ± 58.5 LDPI units).

Furthermore, in only the mice that received the lentiVEcad-PDK4 lentiviral treatment, there was no significant difference in blood flow reperfusion between the mice that received doxycycline and those that did not at any time point. In summary, transduction with the lentiVEcad-PDK4 vector increased wound blood flow reperfusion in both the presence and absence of doxycycline.

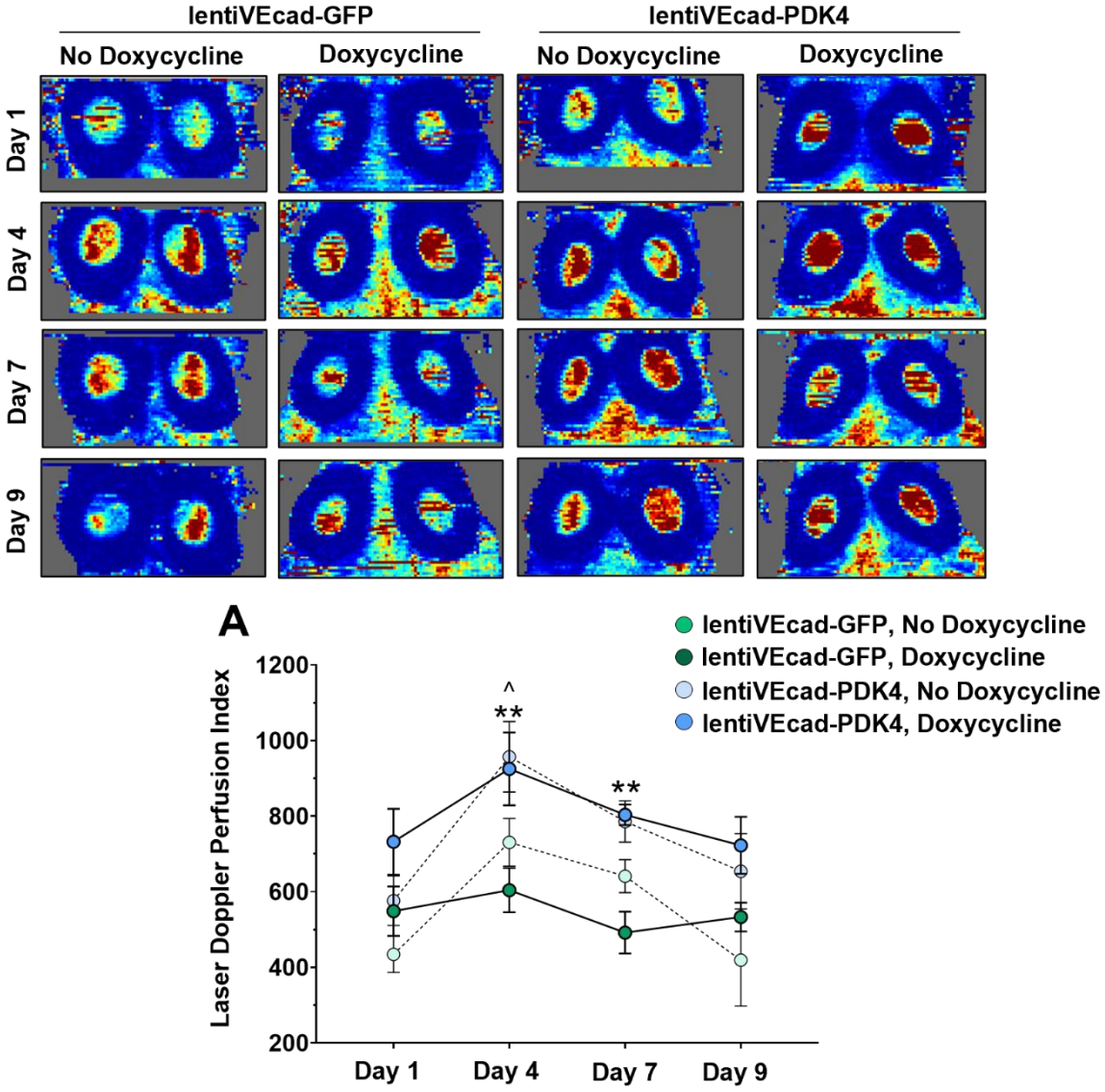

Figure 5.7. The effect of lentiVEcad-PDK4 on blood flow reperfusion in diabetic mice

In the murine diabetic wound healing model, wound blood flow was measured using laser Doppler perfusion imaging. Images represent high (red) to low (blue) blood flow from day 1-9 in diabetic mice. ***P*<0.01 vs. lentiVEcad-GFP, doxycycline by two-way ANOVA. ^*P*<0.05 vs. lentiVEcad-GFP, doxycycline by two-way ANOVA. *N*=2-10, data are representative of 2-10 independent wounds. Data are presented as mean ± SEM.

5.3.8. The effect of lentiVEcad-PDK4 on wound closure in diabetic mice

This experiment aimed to determine how transduction with the lentiVEcad-PDK4 vector affected wound closure in diabetic mice. In diabetic mice that received doxycycline in their drinking water, treatment with the lentiVEcad-PDK4 lentivirus increased wound closure compared to the lentiVEcad-GFP control, reaching significance at day 9 (34.0 ± 7.5 vs. 20.7 ± 3.9 % closure, $P<0.01$; Figure 5.8A, C).

In diabetic mice that did not receive doxycycline in their drinking water, treatment with the lentiVEcad-PDK4 lentiviral vector increased wound closure compared to the mice that received the lentiVEcad-GFP treatment without doxycycline (30.8 ± 4.4 vs. 4.2 ± 2.5 % closure, $P<0.01$; Figure 5.8B).

In the mice that received the lentiVEcad-PDK4 lentiviral treatment, there was no significant difference in wound closure between the mice that received doxycycline and those that did not at any time point (Figure 5.8D). In summary, transduction with the lentiVEcad-PDK4 vector increased wound closure in both the presence and absence of doxycycline.

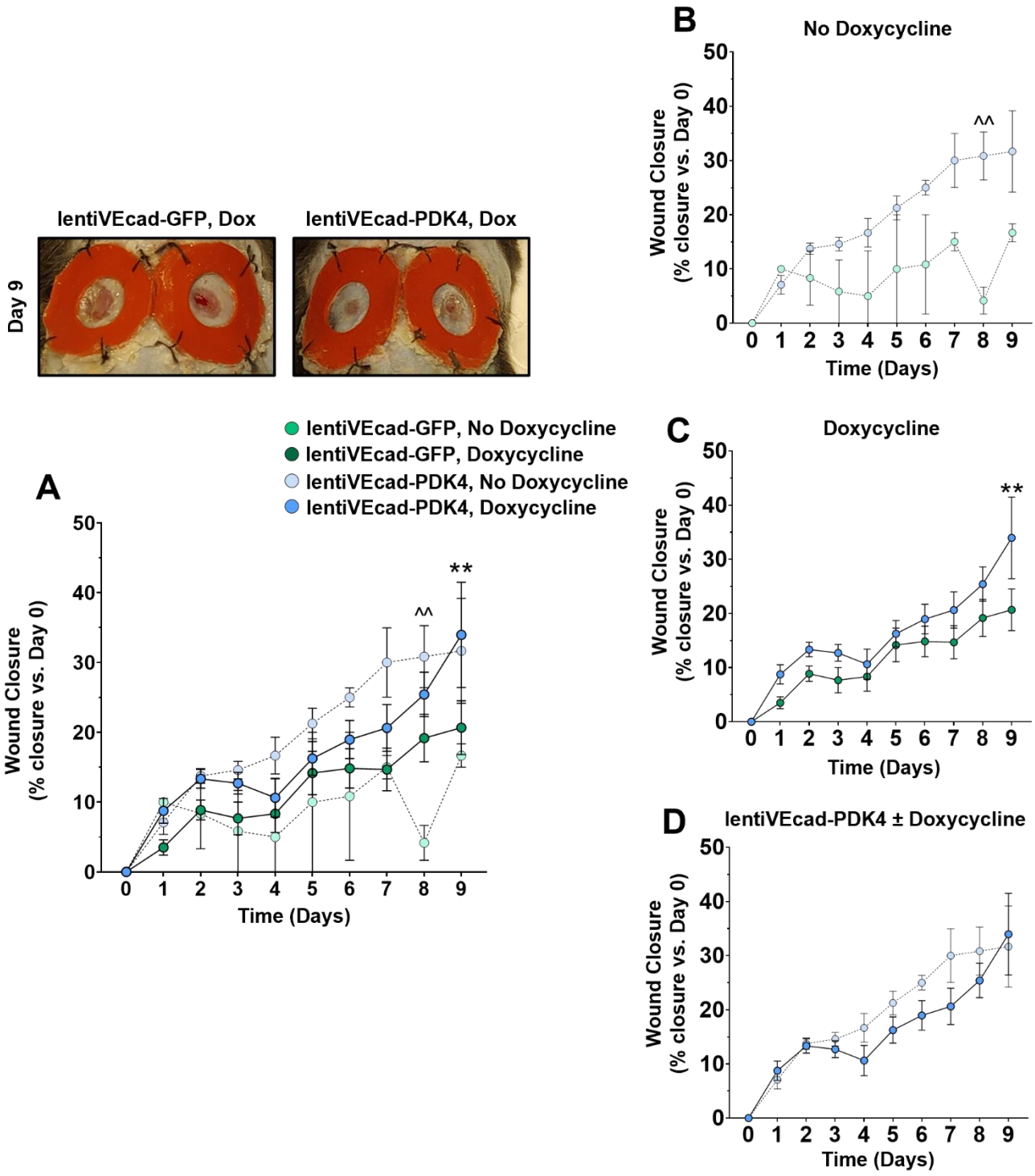

Figure 5.8. The effect of lentiVEcad-PDK4 on wound closure in diabetic mice

In the murine diabetic wound healing model, wound closure was measured daily using microcalipers. Measurements are expressed as percent closure vs. initial measurement. ***P*<0.01 vs. lentiVEcad-GFP, doxycycline by two-way ANOVA. ^^*P*<0.05 vs. pVEcad-GFP, no doxycycline by two-way ANOVA. *N*=2-10, data are representative of 2-10 independent wounds. Data are presented as mean ± SEM.

5.4. Discussion

Lentiviruses are a subclass of retrovirus which stably integrate their DNA into the host cell's genome. Researchers can use this feature to achieve permanent transgene expression that can be passed through cell generations. This, combined with their capacity for large transgenes and the limited immune response elicited by their integration, makes lentiviruses a popular choice of gene therapy vector [89, 92]. In particular, their capacity for large transgenes or gene expression systems means they can be readily engineered to contain expression systems with in-built regulatory mechanisms. These regulatory mechanisms can confer temporal regulation and cell-specific transgene expression, and therefore make the lentiviral vector system an ideal choice for targeting endothelial cell metabolism through PDK4 expression. Because regulation of cellular metabolism is unique and specific to a particular cell type and its function, alterations to metabolic regulation must be limited to the target cell type to avoid disturbing important metabolic functions in other cells.

We therefore created a novel lentiviral vector that allowed for endothelial cell-specific and inducible overexpression of PDK4, and tested the hypothesis that this specific overexpression would enhance wound angiogenesis and improve wound healing. We found that the vector did indeed provide inducible, endothelial cell-specific *Pdk4* expression *in vitro,* and had significant effects on wound angiogenesis and healing *in vivo*.

The original vector, which contained CopGFP as a protein expression control, was obtained from Yang *et al.* [101]. Yang *et al.* developed and tested different versions of the gene expression system in different cell types *in vitro.* These different versions involved the insertion of a "stuffer" DNA sequence between the two expression cassettes, and inversion of one of the expression cassettes, both with the goal of reducing gene expression leak from the system. The specific vector that we utilised in our studies was referred to in the original paper as "SindLuc-

A1", and contained the two expression cassettes oriented in the antisense direction with respect to the vector RNA.

Yang *et al.* also characterised the efficacy and specificity of the different lentiviral vectors in a murine model of gastrointestinal cancer and demonstrated endothelial cell-specificity through both luciferase activity measurement and detection of luciferase protein in tumour tissue using immunohistochemistry. To our knowledge, this is the only lentiviral vector in the literature that provides inducible endothelial cell-specific overexpression.

Yang *et al.* determined that the optimal time post-transduction of their VEcad lentivirus for maximal transgene expression was 48 hours, and that maximal transgene expression was reached with 4µg/mL or higher concentrations of doxycycline. Our *in vitro* findings align with this, as we also observed significant induction of transgene expression with 4µg/mL of doxycycline (Figure 5.4). However, we observed more consistent and stable induction of transgene expression with 8µg/mL doxycycline.

We also observed excellent cell-specificity when measuring *Pdk4* expression following transduction with the lentiVEcad-PDK4 vector *in vitro* (Figure 5.5). We were able to detect *Pdk4* mRNA levels in the HAoSMCs and fibroblasts, likely to be endogenous *Pdk4* as it is known to be expressed in many cell types [72, 73, 123]. Interestingly, we observed that transduction with the lentiVEcad-PDK4 vector elevated *Pdk4* mRNA levels even in the absence of doxycycline (Figure 5.5). While the *Pdk4* mRNA levels were much higher in the presence of doxycycline, this nevertheless indicates that the "Tet on" gene expression system includes a degree of "leakiness". Leakiness of the Tet-On system is a well-known challenge with regards to inducible gene expression, and has been identified in the literature. For example, a study by Costello *et al.* aimed to use the Tet-On system to conditionally knock

down specific miRNAs, but observed that leaky basal transgene expression in the uninduced state was sufficient to knock down their miRNA of interest [124].

This leakiness effect was not reported in the original study by Yang *et al.*, though it is important to note that they measured transgene expression through luciferase protein expression, meaning that there may have been gene expression leakiness exhibited at the mRNA level which did not translate to leakiness in protein expression. In our study, it is possible that the significant increase in *Pdk4* mRNA levels that we observed with the uninduced vector might not translate to an increase in protein expression, or an effect on PDC phosphorylation. In support of this, with the lentiVEcad-GFP signal we detected *in vitro*, we were detecting functional protein expression and observed very little system leakiness in the absence of doxycycline (Figure 5.4). It will be important moving forward to characterise the effect of the lentiVEcad-PDK4 vector on PDK4 protein expression, PDC phosphorylation and cellular metabolism using the Seahorse Bioanalyser system, since this will provide insight into any potential protein expression leak from the uninduced vector. There is also an opportunity to test different concentrations of the lentivirus, as well as further concentrations of doxycycline and determine whether transgene expression leak can be minimised in that way.

While we investigated the ability of doxycycline to induce transgene expression *in vitro*, we did not examine the possibility for switching transgene expression off by removal of doxycycline from the system. The original study conducted by Yang *et al.* also did not investigate this property of the expression system. This will be essential to characterise moving forward to fully capitalise on the temporal regulation that the Tet-On system allows.

In our *in vivo* study of the lentiVEcad vectors, we did not observe that either lentiviral treatments elicited weight loss in the mice. Future studies should test the toxicity of the

lentiviral vectors more comprehensively and measure changes in local tissue inflammation and immune cells, as well as lentivirus accumulation or potential transgene expression in the liver.

Our *in vivo* study also displayed signs of gene expression leakage influencing wound angiogenesis and healing in mice not treated with doxycycline. In our laser Doppler perfusion imaging findings, the lentiVEcad-PDK4 transduction with doxycycline treatment significantly increased wound angiogenesis compared to the lentiVEcad-GFP control vector (Figure 5.7). However, the lentiVEcad-PDK4 vector without doxycycline also elicited increased wound angiogenesis, and there was no difference in the effect of the lentiVEcad-PDK4 vector with either of the doxycycline conditions. Taking our *in vitro* findings into account, we hypothesise that the degree of leaky gene expression which comes from the uninduced vector may be sufficient to elicit the positive effect on angiogenesis in the wound. We observed a similar effect when examining wound closure, where the induced lentiVEcad-PDK4 vector does significantly increase closure compared to the induced lentiVEcad-GFP control, but the uninduced lentiVEcad-PDK4 vector elicits a similar if not more striking effect (Figure 5.8). This raises the question of the optimal level of overexpression, and will require further investigation to understand this mechanism. It may be that a more modest lentiviral particle number of lentiVEcad-PDK4 will be more beneficial than the much higher dose which comes from the induced vector.

In future studies, it will also be essential to measure *Pdk4* expression in the individual wound cell types that contribute to the healing process. Important cell types to investigate include keratinocytes, fibroblasts, and immune cells such as macrophages. Individual cell types can be sorted from wound tissue using their cell surface marker phenotype and flow-assisted cell sorting, but maintaining the quality of the RNA and protein that is extracted from sorted cells can be extremely challenging, in our experience. As mentioned regarding the *in vitro* findings,

it must also be determined whether transgene expression can be "switched off" in an *in vivo* model. Wound healing is a highly regulated process, and progresses through distinct stages. We hypothesise that there will be an optimal time period for PDK4 overexpression that likely will not extend beyond the proliferative phase of wound healing, since that phase is when angiogenesis is most critical. Aberrantly prolonging the suppression of endothelial cell mitochondrial respiration is likely to ultimately impede wound healing rather than enhance it. The optimal "window" for PDK4 overexpression therefore needs to be determined precisely.

In conclusion, we have created a novel gene expression system that allows for endothelial-specific and inducible PDK4 overexpression *in vitro*, but that requires further refinement *in vivo*. *In vitro*, the vector demonstrated significant cell-specificity and inducibility, albeit with some transgene expression leak from the uninduced vector. The vector showed no toxicity *in vivo*, and PDK4 overexpression significantly enhanced wound angiogenesis and healing. Interestingly, the mice not treated with doxycycline displayed evidence of leakiness of the transfection lentiviral PDK4 vector in that wound healing was also enhanced, when compared to lentiVEcad-GFP transduced control mice. These promising results present a novel strategy for improving endothelial cell function in the diabetic wound environment and enhancing wound angiogenesis and healing.

6. General Discussion

6.1. Introduction

An impairment to ischaemia-driven angiogenesis underpins the development of more severe vascular complications in patients with diabetes compared to patients without diabetes. In patients with occlusive atherosclerotic disease, the body's natural response is to initiate new vessel growth and maturation to reoxygenate ischaemic tissue. Similarly, in the process of wound healing, angiogenesis is a central process which provides oxygen and nutrients, carried in the blood, to the healing tissue.

Patients with diabetes exhibit a less extensive collateral circulation associated with occlusive disease, and their chronic, non-healing wounds exhibit insufficient angiogenesis [20, 22, 33, 35]. Because of this observation, angiogenesis has long been a target of study in the context of diabetic vascular complications, and many attempts have been made to therapeutically target angiogenesis to reduce the burden these complications place upon individuals and the broader healthcare system. These attempts have largely been unsuccessful, and there are no pro-angiogenic therapies routinely used in clinical practice with regard to diabetic vascular complications. To develop new therapies that can more effectively support endothelial cell function and stimulate angiogenesis in the diabetic context, we need to understand more about how endothelial cells are affected by diabetes, and which components of their biology are fundamental to their angiogenic capacity.

Strict regulation of metabolic pathways, particularly of those which involve breakdown of glucose, has emerged as a central requirement for the maintenance of angiogenic capacity in endothelial cells. As has been discussed in previous sections, glycolysis has been the primary focus of study thus far, and has been identified as a critical process for endothelial cell angiogenesis. The role of mitochondrial respiration in endothelial cell function has been studied far less, and its significance as described in the literature changes depending on the context it

has been studied in. The PDK4/PDC axis represents one critical point at which mitochondrial respiration can be regulated, and couples glycolysis to mitochondrial respiration, but little is known about its role in angiogenesis.

6.1.1. Hypothesis and aims

The overarching aim of this thesis was to characterise the role of the PDK4/PDC axis in endothelial cell angiogenesis, the effect of diabetes upon the axis, and determine the efficacy of targeting the axis as a potential therapeutic strategy for diabetic vascular complications. This work was conducted with the goal of identifying new, effective ways of supporting endothelial cell function and enhancing angiogenesis in the diabetic context.

6.1.2. Summary of findings

Centrally, this thesis has identified a highly context-specific role for the PDK4/PDC axis and mitochondrial respiration in endothelial cell angiogenic function.

Under normoxic and normal glucose conditions, knocking down PDK4 using siRNA induced a compensatory increase in PDC phosphorylation and a reduction in mitochondrial respiration, which was associated with impaired tubulogenesis. This indicates that reduced mitochondrial respiration can be negative for endothelial cell function under these conditions. PDK4 knockdown under high glucose conditions also impaired tubulogenesis, but the exact effect on mitochondrial respiration under these conditions remains to be determined. Lentiviral-mediated PDK4 overexpression prevented a high glucose-induced impairment to PDC phosphorylation and suppressed mitochondrial respiration. This suppression of respiration was associated with the rescue of high glucose-impaired angiogenic functions, but only under hypoxic and high glucose conditions. PDK4 overexpression had no effect under normoxic, normal glucose conditions.

Similarly, we observed that rHDL rescued high glucose-impaired angiogenic functions *in vitro*, and enhanced wound angiogenesis and closure *in vivo*, but these effects were also highly context-specific in that rHDL had very little effect on the PDK4/PDC axis under normoxic, normal glucose conditions. We found that PDK4 was essential for the pro-angiogenic effects of rHDL, and we identified FOXO1 as the transcription factor which may be driving PDK4 expression in response to rHDL treatment.

We developed a novel lentiviral vector which allowed for endothelial cell-specific and doxycycline-inducible expression of murine PDK4 *in vitro*. The specificity and inducibility of the vector *in vitro* was striking, but it did exhibit some leak of *Pdk4* mRNA expression in the uninduced state. This expression leak may explain why, in our *in vivo* diabetic wound healing model, the uninduced pVEcad-PDK4 vector elicited an increase in wound angiogenesis and closure, alongside the strong increases elicited by the induced vector. The effects of the pVEcad-PDK4 vector on wound angiogenesis and closure highlight a very promising strategy for rescuing diabetes-impaired wound angiogenesis and healing.

6.2. The role of the PDK4/PDC axis in endothelial cell angiogenesis *in vitro*

The data obtained from our PDK4 knockdown and overexpression studies clearly suggests a context-specific role for mitochondrial respiration in endothelial cell angiogenesis, and highlights that targeting endothelial cell metabolism ought to be done in a strictly regulated way. One of our first findings was that a simple decrease in mitochondrial respiration under normoxic and normal glucose conditions was associated with an impairment to endothelial cell function, indicating that maintenance of respiration is essential for EC function under baseline conditions. As mentioned in Chapter 3, this increase in PDC phosphorylation occurred via an unknown compensatory response following PDK4 knockdown, which we initially expected to decrease PDC phosphorylation. This effect should be investigated further by knocking down

the other PDKs and PDPs to determine which enzyme responded in a compensatory manner, as discussed more comprehensively in Chapter 3. Regardless, this relationship between mitochondrial respiration and EC function aligns with findings from Govar *et al.*, Diebold *et al.*, and Zou *et al.* who all noted that a decrease in mitochondrial respiration impaired endothelial cell function under "baseline" conditions, or that an increase in mitochondrial respiration could be protective in the pathological context of ischaemia/reperfusion injury [56-58]. In particular, these studies noted impairments to EC proliferation more than any other function, and Diebold *et al.* hypothesised that mitochondria may primarily serve as biosynthetic organelles for endothelial cell proliferation. They postulated this based on the idea that the tricarboxylic acid cycle produces essential metabolic intermediates required for biosynthesis of macromolecules, and that flux through the electron transport chain replenishes mitochondrial NAD^+, supporting continuous flux through the TCA cycle and NAD^+ utilisation in other important areas [57]. In contrast, our data show that inhibiting mitochondrial respiration under hypoxic and high glucose conditions by PDK4 overexpression has a significant positive effect on endothelial cell tubulogenesis and migration. We had initially hypothesised that suppression of mitochondrial respiration would be beneficial generally, and under any conditions, but these findings highlight the context-specificity of this effect. Importantly, we did not specifically measure proliferation in our *in vitro* studies, and it would be of interest to study proliferation specifically and determine whether modulating PDK4 expression affected this function under different conditions. Additionally, we could measure the levels of macromolecules like amino acids and TCA cycle intermediates to determine if an insufficiency in these factors is elicited by a decrease in mitochondrial respiration through PDK4 overexpression.

It would also be of interest to examine the role of oxidative stress in this system. Our initial hypothesis was that inhibition of mitochondrial respiration would be beneficial for endothelial

cell function under hypoxic and high glucose conditions because it would reduce cellular reliance on oxygen-consuming pathways and preserve cellular function for participation in angiogenesis. However, we did not specifically hypothesise that the inhibition of mitochondrial respiration would reduce oxidative stress under these conditions. It is possible that, under the combination of high glucose and hypoxic conditions, oxidative stress reaches a critical level in the endothelial cells and causes an impairment to their angiogenic function. Hyperglycaemia is well-documented to exacerbate oxidative stress in endothelial cells through increased mitochondrial superoxide production [125-127]. At a critical level, the negative consequences of enhanced oxidative stress may outweigh the benefit of increased macromolecules for proliferation, meaning that inhibiting mitochondrial respiration and oxygen consumption would become beneficial.

There are several additional avenues that ought to be pursued to further characterise the role of the PDK4/PDC axis in endothelial cell function. Firstly, it would be of interest to examine the relative roles of all the PDKs and PDPs in the regulation of mitochondrial respiration in multiple types of endothelial cells *in vitro*, or in mouse models *in vivo*. Endothelial-specific PDK or PDP knockout mice could be generated using the Cre-loxP system, with expression of the Cre recombinase protein driven by endothelial-specific promoters of genes like Tie2, VE-cadherin, or Flk-1. Deleting each PDK or PDP gene would allow researchers to examine the relative contribution of each gene to endothelial cell function, and possibly discern the degree to which the genes compensate for each other in various disease contexts. In particular, comparing the role of each enzyme in ischaemic and non-ischaemic environments would be useful.

Secondly, it is essential that new methods are employed to measure PDC phosphorylation and metabolic flux through central pathways. Measuring PDC phosphorylation by western blotting

was effective under baseline conditions, but lacked the sensitivity to detect potentially rapid changes under more complex conditions. Mass spectrometry can provide a higher-resolution method of detecting protein phosphorylation, and can be used to track glucose metabolism through various pathways using C^{13}-labelled substrates. We will expand on the use of mass spectrometry for analysis of cellular metabolism in later sections, as it applies to the entirety of this thesis.

In combination with a higher-resolution method of measuring protein phosphorylation, additional methods of inhibiting the PDKs could be used. Dichloroacetate is a pharmacological inhibitor of the PDKs, and does not discriminate between isoforms of the enzyme. This would not allow us to differentiate between the relative contribution of each isoform, but pharmacological inhibition as opposed to siRNA-mediated knockdown might more effectively allow us to determine how the PDKs affect PDC phosphorylation and mitochondrial respiration under the combined conditions of high glucose and hypoxia.

These additional methods of characterising the role of PDK4 in this context could be combined with further study of the effect of diabetes upon the PDK4/PDC axis.

6.3. The effect of diabetes upon endothelial cell metabolic reprogramming

In Chapter 3 we observed that high glucose exposure reduced PDC phosphorylation. In Chapter 4, we determined that high glucose exposure elicited an increase in basal mitochondrial respiration, and in our *in vivo* diabetic wound healing model hyperglycaemia impaired the induction of PDK4 expression and PDC phosphorylation in response to wound ischaemia. These responses were associated with a significant impairment to all measured endothelial cell functions *in vitro* and impaired wound angiogenesis and healing *in vivo*.

These findings highlight that high glucose exposure and hyperglycaemia impair the induction of the PDK4/PDC axis in response to hypoxia, and overstimulate mitochondrial respiration. This identifies a link between an impairment of the PDK4/PDC axis and diabetes-impaired angiogenesis.

The relationship between diabetes and the PDK4/PDC axis ought to be further characterised in a number of ways. In particular, it would be of interest to understand more about exactly how diabetes overstimulates mitochondrial respiration in endothelial cells, and what features of overstimulated mitochondrial respiration in diabetes contribute to impaired endothelial cell function. We observed that diabetes impaired the induction of PDK4 expression in response to hypoxia, but the question remains about how exactly this occurs. Because we observe an impairment at the mRNA level, this suggests an impairment to the transcriptional regulation of PDK4. HIF-1α is a central transcription factor which regulates many genes that are important for cellular function in hypoxic conditions. PDK4 is known to be a downstream target of HIF-1α [74], and we observed in Chapter 4 that high glucose exposure significantly reduced HIF-1α expression under hypoxic conditions. We hypothesise that under high glucose and hypoxic conditions, the impairment to HIF-1α stabilisation also impairs PDK4 expression induction in response to hypoxia. This could be tested in a number of ways. Firstly, by supplementing HIF-1α protein expression under high glucose and hypoxic conditions and determining whether PDK4 expression is restored. Secondly, a chromatin immunoprecipitation assay could be used to confirm that high glucose exposure does decrease the amount of HIF-1α bound to the PDK4 promoter. High glucose exposure may clearly reduce HIF-1α expression, but it would be useful to confirm that this was also associated with a reduction in the interaction between HIF-1α and PDK4.

Another important question involves the exact mechanism by which overstimulated mitochondrial respiration has a negative impact upon endothelial cell angiogenic function. Hyperglycaemia is known to exacerbate oxidative stress through the following mechanism. If excess glucose overstimulates flux through the TCA cycle, higher quantities of NADH and $FADH_2$ will be produced and will shuttle electrons to the electron transport chain. If the proton gradient across the inner mitochondrial membrane reaches a critical threshold, coenzyme Q will donate electrons one at a time to molecular oxygen, thereby producing superoxide and subsequent reactive oxygen species (ROS) will be generated by various enzymes such as superoxide dismutase (SOD). Part of this increased ROS production could be attributed to the impairment of PDK4/PDC axis induction that we observed, and its inability to prevent overstimulation of mitochondrial respiration. While we did not measure the production of ROS due to both the inherent complexity involved with quantifying ROS and the limited scope of this study, it would be of interest to investigate how the PDK4/PDC axis might affect mitochondrial ROS production under hypoxic and high glucose conditions. We would hypothesise that PDK4 overexpression under these conditions would suppress mitochondrial ROS production, which could explain the rescue of endothelial cell function.

Finally, it would also be of interest to examine how the PDK4/PDC axis was affected in other diabetic murine models, including genetic and diet-based models. This concept also applies to the entirety of this project, and will be discussed further in a later section.

6.4. The effect of reconstituted high-density lipoproteins on the PDK4/PDC axis and diabetes-impaired angiogenesis

The data presented in Chapter 4 highlighted the context-specific nature of the effects of rHDL upon the PDK4/PDC axis.

Similar to the questions posed in the previous section, we can also ask exactly how the enhancement of PDK4 expression by rHDL rescues endothelial cell function. The decrease in mitochondrial respiration that we observed with rHDL treatment could lead to a decrease in oxidative stress, or it may allow for additional upregulation of glycolysis. In particular, rHDL has been shown to reduce oxidative stress through a number of antioxidant pathways [121, 128, 129], so this avenue holds promise. These effects could be studied in more detail by quantifying the production of ROS, or using mass spectrometry to assess flux through metabolic pathways more comprehensively.

Another avenue for discussion involves the use of an additional negative control throughout the rHDL studies. In particular, it would be of interest to attenuate the biological effects of rHDL by either glycating or oxidising the rHDL particle, which can be performed by incubating the rHDL with high concentrations of glucose or an oxidising agent like myeloperoxidase (MPO)[130]. If the effects upon the PDK4/PDC axis were also attenuated by this modification of the rHDL particle, it would confirm that the effects are mediated by functional apoA-I.

This may also give us some insight into the relationship between endogenous HDL and endothelial function in diabetic patients. In this study we did not hypothesise that dysfunctional HDL in diabetes was a causative factor for the impaired induction of the PDK4/PDC axis in response to hypoxia. Rather, we approached this study in the context of understanding the mechanisms behind the rescue of diabetes-impaired angiogenesis by rHDL to further develop it as a topical therapeutic agent for diabetic vascular complications. Regardless, it would be of interest to examine HDL functionality and integrity in diabetic patients, and determine whether there was some relationship with PDK4 expression in the endothelial cells of diabetic patients. To our knowledge, PDK4 expression has never been examined in the endothelial cells from diabetic patients. We could speculate that there is some relationship between higher levels of

HDL functionality and better endothelial function, and preparedness to participate in angiogenesis. This may not necessarily be a causative relationship, but perhaps some factor such as diet, exercise, or an underlying genetic component underpins this potential relationship. In support of this idea, unpublished studies conducted by our group have assessed the relationship between HDL functionality and the rate of wound closure in non-diabetic and diabetic patients who have received a ray amputation. We have found that the HDL which is isolated from diabetic patients exhibits significantly reduced functionality, including reductions in its cholesterol efflux capacity, anti-inflammatory effects, and pro-angiogenic effects. This reduced HDL functionality was associated with a slower rate of wound closure in the diabetic patients. Understanding the fundamental biology related to both HDL functionality and endothelial cell angiogenic function may allow us to better predict which patients will respond best to revascularisation procedures, or which patients are most likely to develop a non-healing wound or other vascular complication.

6.5. The effect of endothelial-specific, inducible overexpression of PDK4 on the PDK4/PDC axis and diabetes-impaired angiogenesis

The development of the novel lentivirus which allows for endothelial-specific, inducible overexpression of PDK4 provided us with some of the most promising effects observed throughout this study, but also requires additional characterisation.

In particular, the observed gene expression leak from the uninduced pVEcad-PDK4 vector requires further investigation and fine-tuning. Leakiness of the Tet-on system is a known factor that must be contended with [124, 131], and researchers may employ various strategies to mitigate it. For example, inserting elements which destabilise the mRNA as demonstrated by Pham *et al.* [132], or by identifying mutant versions of the rtTA protein that are more sensitive to doxycycline [133]. Rather than modifying the vector, we could initially address this question

by optimising the administered concentration of virus and dosage of doxycycline. As mentioned in the discussion of Chapter 5, it would also be essential to quantify the protein expression elicited by the pVEcad-PDK4 vector as opposed to just the mRNA expression, since the leaky mRNA expression may not actually translate to leak of protein expression and effects upon downstream targets. It will also be essential to characterise and optimise the effect had upon PDC phosphorylation and mitochondrial respiration, either using the methods employed earlier in this study, or by employing new methods such as mass spectrometry and metabolic flux analysis. Importantly, all these effects must be examined specifically in endothelial cells as opposed to whole wound tissue, and any potential off-target effects on other cell types should be screened for. Once this effect is further characterised, we can begin to ask questions about the mechanism by which PDK4 overexpression improves endothelial cell function, alongside the studies described earlier in this chapter with regards to oxidative stress.

Finally, the ideal context and timing for delivery of this vector ought to be determined. Throughout this chapter we have raised important questions about the context-specific role of mitochondrial respiration in endothelial cells, and highlighted that enhancing or disrupting mitochondrial respiration can have negative consequences if the context is not suitable for that modulation. We need to understand a great deal more about the microenvironment in which angiogenesis is taking place if we aim to affect endothelial cell metabolism in order to support their participation in angiogenesis. For example, we must determine whether a particular chronic, non-healing wound is truly ischaemic, and characterise to what degree an individual patient experiences hyperglycaemia. This could be determined by quantifying the level of HIF-1α expression in an ischaemic wound, which is something our lab has previously conducted to confirm that the wounds created in our murine diabetic wound healing model are truly experiencing hypoxia. We find that HIF-1α is significantly upregulated immediately post-creation of the wound environment. This, along with other similar measures could provide

thorough characterisation of a patient's wound environment and determine their suitability for gene therapy. Importantly, there would be no use in enhancing PDK4 expression to suppress mitochondrial respiration in endothelial cells unless we are certain that they are being exposed to an ischaemic environment, and if we are certain that they risk mitochondrial overstimulation by hyperglycaemia. We must also determine the ideal timing for stimulation of PDK4 expression within the complicated and highly temporally regulated process of wound healing. The current data and future studies outlined throughout this chapter will allow us to better understand these contexts, and be confident that we can apply technology like our novel lentiviral vector appropriately such that unintended negative consequences are less likely to occur.

6.6. Future Directions

While avenues for further study have been mentioned throughout this chapter, there are several areas that apply to the entire thesis and thus can be discussed more centrally.

Firstly is the use of mass spectrometry and metabolic flux analysis to further interrogate how PDK4 affects mitochondrial respiration and other metabolic pathways. As described in the late 90s and early 2000s, combining mass spectrometry with "tracer" experiments which use C^{13}-labelled substrates can be a powerful tool for determining metabolic flux [134, 135]. The technology has advanced significantly in the past 20 years – not just the mass spectrometry technology but also the computational technology required to model metabolic flux mathematically. Briefly, these experiments involve the incubation of cells *in vitro* or treatment of mice *in vivo* with glucose or another substrate which contains a C^{13} isotope at a specific position in the molecule. Once the cells or tissues have been processed appropriately, the C^{13} can be detected using mass spectrometry, and the metabolic fate of the original molecule inferred. The data collected from these experiments can undergo modelling to allow for

quantification and visualisation of the flux through various pathways. This approach includes many challenges – the treatment with the C^{13}-labelled substrate must be highly optimised, as must the method of cell or tissue processing. In addition, modelling the data requires a comprehensive understanding of certain mathematical principles and computational biology techniques. Regardless, this powerful approach can allow researchers to gain a detailed understanding of a cell's metabolic pathways, and would be very useful for studying the role of the PDK4/PDC axis, and the effects that diabetes has upon it.

Secondly, it will be essential to characterise this system in other preclinical models of diabetes, including in female mice, and ideally also in patients with diabetes. We have studied the effects of hyperglycaemia using a streptozotocin-induced diabetic model, but this approach does not allow us to examine the diet-based effects of diabetes, such as increased systemic inflammation or elevated triglyceride levels. It would be of interest to examine how the PDK4/PDC axis and endothelial cell function was affected in a *db/db* or *ob/ob* genetic model, in which the mice are genetically modified to overeat, and are then fed a high-fat diet and develop obesity and insulin resistance as a result [136]. These mice experience vascular dysfunction [137-139], but it is possible that the effects of obesity, systemic inflammation, and the presence of elevated triglycerides may also affect endothelial cell regulation of metabolic pathways such as fatty acid oxidation, which would have an impact on mitochondrial respiration. Examining the PDK4/PDC axis in endothelial cells derived from diabetic patients will also provide critical information, and confirm whether the context-specific effects we have observed under hyperglycaemic conditions hold true, or are altered in a more complex disease phenotype.

6.7. Summary and Conclusions

In summary, the studies conducted in this thesis have characterised, for the first time, a highly context-specific and essential role for the PDK4/PDC axis and mitochondrial respiration in

diabetes-impaired angiogenesis. Disruption of the axis by siRNA-mediated PDK4 knockdown impaired endothelial cell function, and further characterisation of this effect under high glucose conditions would be useful. High glucose exposure *in vitro* and hyperglycaemia *in vivo* impaired the induction of the PDK4/PDC axis in response to hypoxia, while overexpression of PDK4 and suppression of mitochondrial respiration rescued high glucose-impaired endothelial cell function. rHDL rescued diabetes-impaired angiogenesis, and the PDK4/PDC axis was found to be essential for these pro-angiogenic effects. In line with the *in vitro* PDK4 overexpression experiments, endothelial-specific, inducible overexpression of PDK4 by lentiviral gene transfer *in vivo* significantly enhanced wound angiogenesis and healing, though this effect also requires fine-tuning. Collectively, these data support our hypothesis that the PDK4/PDC axis plays a critical role in endothelial cell angiogenesis, and that diabetes impairs the integrity of the axis. Restoration of the PDK4/PDC axis did indeed improve endothelial cell angiogenesis *in vitro* in high glucose and wound healing in diabetic mice.

These promising findings form the basis for further examination of endothelial cell metabolic reprogramming in diabetic vascular complications, and could inform the development of new therapies that target endothelial cell metabolism to enhance ischaemia-driven angiogenesis in the diabetic context. Our approach to addressing this research question is unique, in that we have focussed directly on correcting cellular metabolism, which is a central cause of the impairment to angiogenesis in ischaemia which contributes to diabetic vascular complications. In particular, our lentiviral gene transfer approach has the potential to be personalised to the needs of individual patients through the Tet-On “on/off” switch, which is a level of regulation that has never previously been investigated in this context. Taken together, we believe that the development of this new lentiviral vector will ultimately prove

to be more effective than current non-specific, non-inducible approaches for the prevention of diabetic vascular complications.

7. Bibliography

1. Federation, I.D., *IDF Diabetes Atlas*. 8 ed. 2017.

2. Zimmet, P., K.G.M.M. Alberti, and J. Shaw, *Global and societal implications of the diabetes epidemic.* Nature, 2001. **414**(6865): p. 782-787.

3. Chen, L., D.J. Magliano, and P.Z. Zimmet, *The worldwide epidemiology of type 2 diabetes mellitus—present and future perspectives.* Nature Reviews Endocrinology, 2012. **8**(4): p. 228-236.

4. Lusis, A.J., *Atherosclerosis.* Nature, 2000. **407**(6801): p. 233-41.

5. Lee, R.T. and P. Libby, *The Unstable Atheroma.* 1997. **17**(10): p. 1859-1867.

6. Hoffmann, R., et al., *Impact of the Metabolic Syndrome on Angiographic and Clinical Events After Coronary Intervention Using Bare-Metal or Sirolimus-Eluting Stents.* The American Journal of Cardiology, 2007. **100**(9): p. 1347-1352.

7. Meier, P., et al., *The impact of the coronary collateral circulation on mortality: a meta-analysis.* European Heart Journal, 2011. **33**(5): p. 614-621.

8. Koerselman, J., et al., *Coronary Collaterals.* Circulation, 2003. **107**(19): p. 2507-2511.

9. Juguilon, C., et al., *Endothelial Cell Sprouting in Coronary Collateral Growth.* 2022. **36**(S1).

10. Abacı, A., et al., *Effect of Diabetes Mellitus on Formation of Coronary Collateral Vessels.* Circulation, 1999. **99**(17): p. 2239-2242.

11. Mouquet, F., et al., *Metabolic syndrome and collateral vessel formation in patients with documented occluded coronary arteries: association with hyperglycaemia, insulin-resistance, adiponectin and plasminogen activator inhibitor-1.* Eur Heart J, 2009. **30**(7): p. 840-9.

12. Zbinden, R., et al., *Coronary collateral flow and peripheral blood monocyte concentration in patients treated with granulocyte-macrophage colony stimulating factor.* Heart, 2004. **90**(8): p. 945-6.

13. Gloekler, S., et al., *Coronary collateral growth by external counterpulsation: a randomised controlled trial.* Heart, 2010. **96**(3): p. 202-7.

14. Rubanyi, G.M., *Mechanistic, Technical, and Clinical Perspectives in Therapeutic Stimulation of Coronary Collateral Development by Angiogenic Growth Factors.* Molecular Therapy, 2013. **21**(4): p. 725-738.

15. Henry, T.D., et al., *The VIVA Trial.* Circulation, 2003. **107**(10): p. 1359-1365.

16. Ahimastos, A.A., et al., *A meta-analysis of the outcome of endovascular and noninvasive therapies in the treatment of intermittent claudication.* J Vasc Surg, 2011. **54**(5): p. 1511-21.

17. Aitken, S., *Peripheral artery disease in the lower limbs: The importance of secondary risk prevention for improved long-term prognosis.* Australian Journal of General Practice, 2020. **49**(5): p. 239-244.

18. Thiruvoipati, T., *Peripheral artery disease in patients with diabetes: Epidemiology, mechanisms, and outcomes.* World Journal of Diabetes, 2015. **6**(7): p. 961.

19. Au, T.B., et al., *Peripheral arterial disease - diagnosis and management in general practice.* Aust Fam Physician, 2013. **42**(6): p. 397-400.

20. De Vivo, S., et al., *Risk factors for poor collateral development in claudication.* Vasc Endovascular Surg, 2005. **39**(6): p. 519-24.

21. Ziegler, M.A., et al., *Marvels, Mysteries, and Misconceptions of Vascular Compensation to Peripheral Artery Occlusion.* Microcirculation, 2010. **17**(1): p. 3-20.

22. McDermott, M.M., et al., *Collateral vessel number, plaque burden, and functional decline in peripheral artery disease.* Vascular Medicine, 2014. **19**(4): p. 281-288.

23. McDermott, M.M., et al., *Proximal Superficial Femoral Artery Occlusion, Collateral Vessels, and Walking Performance in Peripheral Artery Disease.* JACC: Cardiovascular Imaging, 2013. **6**(6): p. 687-694.

24. Raiter, A., et al., *Angiogenic peptides improve blood flow and promote capillary growth in a diabetic and ischaemic mouse model.* Eur J Vasc Endovasc Surg, 2010. **40**(3): p. 381-8.

25. Yan, J., et al., *Recovery from hind limb ischemia is less effective in type 2 than in type 1 diabetic mice: Roles of endothelial nitric oxide synthase and endothelial progenitor cells.* Journal of Vascular Surgery, 2009. **50**(6): p. 1412-1422.

26. Guo, S. and L.A. Dipietro, *Factors affecting wound healing.* J Dent Res, 2010. **89**(3): p. 219-29.

27. Okonkwo, U. and L. Dipietro, *Diabetes and Wound Angiogenesis.* International Journal of Molecular Sciences, 2017. **18**(7): p. 1419.

28. Vas, P., et al., *Effectiveness of interventions to enhance healing of chronic foot ulcers in diabetes: a systematic review.* Diabetes Metab Res Rev, 2019. **36**: p. 3284.

29. Rayman, G., et al., *Guidelines on use of interventions to enhance healing of chronic foot ulcers in diabetes (IWGDF 2019 update).* Diabetes Metab Res Rev, 2019. **36**.

30. Bhutani, S. and G. Vishwanath, *Hyperbaric oxygen and wound healing.* Indian Journal of Plastic Surgery, 2012. **45**(02): p. 316-324.

31. Gosain, A. and L.A. Dipietro, *Aging and Wound Healing.* World Journal of Surgery, 2004. **28**(3): p. 321-326.

32. Maruyama, K., et al., *Decreased Macrophage Number and Activation Lead to Reduced Lymphatic Vessel Formation and Contribute to Impaired Diabetic Wound Healing.* The American journal of pathology, 2007. **170**(4): p. 1178-1191.

33. Okonkwo, U.A. and L.A. DiPietro, *Diabetes and Wound Angiogenesis.* Int J Mol Sci, 2017. **18**(7): p. 45-60.

34. Smola, H., G. Thiekötter, and N.E. Fusenig, *Mutual induction of growth factor gene expression by epidermal-dermal cell interaction.* J Cell Biol, 1993. **122**(2): p. 417-29.

35. Brem, H. and M. Tomic-Canic, *Cellular and molecular basis of wound healing in diabetes.* J Clin Invest, 2007. **117**(5): p. 1219-22.

36. Galiano, R.D., et al., *Topical Vascular Endothelial Growth Factor Accelerates Diabetic Wound Healing through Increased Angiogenesis and by Mobilizing and Recruiting Bone Marrow-Derived Cells.* The American Journal of Pathology, 2004. **164**(6): p. 1935-1947.

37. Klein, S.A., et al., *Angiogenesis inhibitor TNP-470 inhibits murine cutaneous wound healing.* J Surg Res, 1999. **82**(2): p. 268-274.

38. Porporato, P.E., et al., *Lactate stimulates angiogenesis and accelerates the healing of superficial and ischemic wounds in mice.* Angiogenesis, 2012. **15**(4): p. 581-92.

39. Lin, C.J., et al., *Expression of miR-217 and HIF-1α/VEGF pathway in patients with diabetic foot ulcer and its effect on angiogenesis of diabetic foot ulcer rats.* Journal of Endocrinological Investigation, 2019. **42**(11): p. 1307-1317.

40. Roman, C.D., et al., *Vascular endothelial growth factor-mediated angiogenesis inhibition and postoperative wound healing in rats.* J Surg Res, 2002. **105**(1): p. 43-47.

41. De Bock, K., et al., *Role of PFKFB3-driven glycolysis in vessel sprouting.* Cell, 2013. **154**(3): p. 651-63.

42. Appelhoff, R.J., et al., *Differential Function of the Prolyl Hydroxylases PHD1, PHD2, and PHD3 in the Regulation of Hypoxia-inducible Factor.* J Biol Chem, 2004. **279**: p. 38458-38465.

43. Jiang, B.H., et al., *Transactivation and Inhibitory Domains of Hypoxia-inducible Factor 1α MODULATION OF TRANSCRIPTIONAL ACTIVITY BY OXYGEN TENSION.* J Biol Chem, 1997. **272**: p. 19253-19260.

44. Forsythe, J.A., et al., *Activation of vascular endothelial growth factor gene transcription by hypoxia-inducible factor 1.* Mol Cell Biol, 1996. **16**(9): p. 4604-4613.

45. Tan, J.T., et al., *High-Density Lipoproteins Rescue Diabetes-Impaired Angiogenesis via Scavenger Receptor Class B Type I.* Diabetes, 2016. **65**(10): p. 3091-103.

46. Yamakawa, M., et al., *Hypoxia-inducible factor-1 mediates activation of cultured vascular endothelial cells by inducing multiple angiogenic factors.* Circ Res, 2003. **93**(7): p. 664-73.

47. Ornitz, D.M. and N. Itoh, *The Fibroblast Growth Factor signaling pathway.* WIREs Dev Biol, 2015. **4**: p. 215-266.

48. Yu, P., et al., *FGF-dependent metabolic control of vascular development.* Nature, 2017. **545**: p. 224-228.

49. Wilhelm, K., et al., *FOXO1 couples metabolic activity and growth state in the vascular endothelium.* Nature, 2016. **529**(7585): p. 216-20.

50. Arany, Z., et al., *HIF-independent regulation of VEGF and angiogenesis by the transcriptional coactivator PGC-1a.* Nature, 2008. **451**.

51. Sawada, N., et al., *Endothelial PGC-1α Mediates Vascular Dysfunction in Diabetes.* 2014. **19**(2): p. 246-258.

52. Kim, B., et al., *Endothelial pyruvate kinase M2 maintains vascular integrity.* J Clin Invest, 2018. **128**: p. 4543–4556.

53. Boros, L.G., et al., *Nonoxidative pentose phosphate pathways and their direct role in ribose synthesis in tumors: is cancer a disease of cellular glucose metabolism?* 1998. **50**(1): p. 55-59.

54. Prasai, P.K., et al., *Decreases in GSH:GSSG activate vascular endothelial growth factor receptor 2 (VEGFR2) in human aortic endothelial cells.* Redox Biol, 2018. **19**: p. 22-27.

55. Forbes, N.S., et al., *Estradiol stimulates the biosynthetic pathways of breast cancer cells: Detection by metabolic flux analysis.* Metabolic Engineering, 2006. **8**(6): p. 639-652.

56. Abdollahi Govar, A., et al., *3-Mercaptopyruvate sulfurtransferase supports endothelial cell angiogenesis and bioenergetics.* British Journal of Pharmacology, 2020. **177**(4): p. 866-883.

57. Diebold, L.P., et al., *Mitochondrial complex III is necessary for endothelial cell proliferation during angiogenesis.* Nature Metabolism, 2019. **1**(1): p. 158-171.

58. Zou, R., et al., *Empagliflozin attenuates cardiac microvascular ischemia/reperfusion injury through improving mitochondrial homeostasis.* Cardiovascular Diabetology, 2022. **21**(1).

59. Fisslthaler, B. and I. Fleming, *Activation and signaling by the AMP-activated protein kinase in endothelial cells.* Circ Res, 2009. **105**(2): p. 114-27.

60. Dagher, Z., et al., *Acute Regulation of Fatty Acid Oxidation and AMP-Activated Protein Kinase in Human Umbilical Vein Endothelial Cells.* Circulation Research, 2001. **88**: p. 1276-1282.

61. Kalucka, J., et al., *Quiescent Endothelial Cells Upregulate Fatty Acid β-Oxidation for Vasculoprotection via Redox Homeostasis.* Cell Metabolism, 2018. **28**(6): p. 881-894.e13.

62. Schoors, S., et al., *Fatty acid carbon is essential for dNTP synthesis in endothelial cells.* Nature, 2015. **520**(7546): p. 192-197.

63. Wynn, R.M., et al., *Pyruvate dehydrogenase kinase-4 structures reveal a metastable open conformation fostering robust core-free basal activity.* J Biol Chem, 2008. **283**(37): p. 25305-15.

64. Patel, K.P., et al., *The spectrum of pyruvate dehydrogenase complex deficiency: clinical, biochemical and genetic features in 371 patients.* Mol Genet Metab, 2012. **106**(3): p. 385-94.

65. Randle, P.J., et al., *The glucose fatty-acid cycle its role in insulin sensitivity and the metabolic disturbances of diabetes mellitus.* The Lancet, 1963. **281**(7285): p. 785-789.

66. Chien, H.-C., P.L. Greenhaff, and D. Constantin-Teodosiu, *PPARδ and FOXO1 Mediate Palmitate-Induced Inhibition of Muscle Pyruvate Dehydrogenase Complex and CHO Oxidation, Events Reversed by Electrical Pulse Stimulation.* International Journal of Molecular Sciences, 2020. **21**(16): p. 5942.

67. Park, J.M., et al., *Hyperpolarized NMR study of the impact of pyruvate dehydrogenase kinase inhibition on the pyruvate dehydrogenase and TCA flux in type 2 diabetic rat muscle.* Pflügers Archiv - European Journal of Physiology, 2021. **473**(11): p. 1761-1773.

68. Schoonjans, C.A., et al., *Targeting Endothelial Cell Metabolism by Inhibition of Pyruvate Dehydrogenase Kinase and Glutaminase-1*. Journal of Clinical Medicine, 2020. **9**(10): p. 3308.

69. Stacpoole, P.W., *Therapeutic Targeting of the Pyruvate Dehydrogenase Complex/Pyruvate Dehydrogenase Kinase (PDC/PDK) Axis in Cancer.* J Natl Cancer Inst, 2017. **109**(11): p. 101-115.

70. Rardin, M.J., et al., *Monitoring phosphorylation of the pyruvate dehydrogenase complex.* Analytical Biochemistry, 2009. **389**(2): p. 157-164.

71. Korotchkina, L.G. and M.S. Patel, *Site Specificity of Four Pyruvate Dehydrogenase Kinase Isoenzymes toward the Three Phosphorylation Sites of Human Pyruvate Dehydrogenase.* Journal of Biological Chemistry, 2001. **276**(40): p. 37223-37229.

72. Bowker-Kinley, M.M., et al., *Evidence for existence of tissue-specific regulation of the mammalian pyruvate dehydrogenase complex.* Biochemical Journal, 1998. **329**(1): p. 191-196.

73. Klyuyeva, A., et al., *Tissue-specific kinase expression and activity regulate flux through the pyruvate dehydrogenase complex.* Journal of Biological Chemistry, 2019. **294**(3): p. 838-851.

74. Lee, J.H., et al., *Hypoxia induces PDK4 gene expression through induction of the orphan nuclear receptor ERRgamma.* PLoS One, 2012. **7**(9): p. 115-125.

75. Kim, J.W., et al., *HIF-1-mediated expression of pyruvate dehydrogenase kinase: a metabolic switch required for cellular adaptation to hypoxia.* Cell Metab, 2006. **3**(3): p. 177-85.

76. Quintela, A.M., et al., *PPARbeta activation restores the high glucose-induced impairment of insulin signalling in endothelial cells.* Br J Pharmacol, 2014. **171**(12): p. 3089-102.

77. Morales-Cano, D., et al., *Activation of PPARβ/δ prevents hyperglycaemia-induced impairment of Kv7 channels and cAMP-mediated relaxation in rat coronary arteries.* Clin Sci (Lond), 2016. **130**(20): p. 1823-36.

78. Davidson, W.S., *HDL-C vs HDL-P: How Changing One Letter Could Make a Difference in Understanding the Role of High-Density Lipoprotein in Disease.* Clinical Chemistry, 2014. **60**(11): p. e1-e3.

79. Acton, S., et al., *Identification of scavenger receptor SR-BI as a high density lipoprotein receptor.* Science, 1996. **271**(5248): p. 518-20.

80. Terasaka, N., et al., *ABCG1 and HDL protect against endothelial dysfunction in mice fed a high-cholesterol diet.* J Clin Invest, 2008. **118**(11): p. 3701–3713.

81. Prosser, H.C., M.K.C. Ng, and C.A. Bursill, *The role of cholesterol efflux in mechanisms of endothelial protection by HDL.* Curr Opin Lipidology, 2012. **23**(3): p. 182-189.

82. Sumi, M., et al., *Reconstituted High-Density Lipoprotein Stimulates Differentiation of Endothelial Progenitor Cells and Enhances Ischemia-Induced Angiogenesis.* Arteriosclerosis, Thrombosis, and Vascular Biology, 2007. **27**(4): p. 813-818.

83. Nieuwdorp, M., et al., *Reconstituted HDL infusion restores endothelial function in patients with type 2 diabetes mellitus.* Diabetologia, 2008. **51**(6): p. 1081-4.

84. Van Oostrom, O., et al., *Reconstituted HDL Increases Circulating Endothelial Progenitor Cells in Patients With Type 2 Diabetes.* 2007. **27**(8): p. 1864-1865.

85. Prosser, H.C., et al., *Multifunctional regulation of angiogenesis by high-density lipoproteins.* Cardiovasc Res, 2014. **101**(1): p. 145-54.

86. Tan, J.T., et al., *High-density lipoproteins augment hypoxia-induced angiogenesis via regulation of post-translational modulation of hypoxia-inducible factor 1alpha.* FASEB J, 2014. **28**(1): p. 206-17.

87. Goff, S.P. and P. Berg, *Construction of hybrid viruses containing SV40 and λ phage DNA segments and their propagation in cultured monkey cells.* Cell, 1976. **9**(4, Part 2): p. 695-705.

88. Administration, U.S.F.D., *FDA approves CAR-T cell therapy to treat adults with certain types of large B-cell lymphoma.* 2017.

89. Bulcha, J.T., et al., *Viral vector platforms within the gene therapy landscape.* Signal Transduction and Targeted Therapy, 2021. **6**(1): p. 53.

90. Usman, N. and M. Suarez, *Adenoviruses*, in *StatPearls*. 2022, StatPearls Publishing

Copyright © 2022, StatPearls Publishing LLC.: Treasure Island (FL).

91. Naso, M.F., et al., *Adeno-Associated Virus (AAV) as a Vector for Gene Therapy.* BioDrugs, 2017. **31**(4): p. 317-334.

92. Munis, A.M., *Gene Therapy Applications of Non-Human Lentiviral Vectors.* Viruses, 2020. **12**(10).

93. Dull, T., et al., *A third-generation lentivirus vector with a conditional packaging system.* J Virol, 1998. **72**(11): p. 8463-71.

94. Merten, O.W., M. Hebben, and C. Bovolenta, *Production of lentiviral vectors.* Mol Ther Methods Clin Dev, 2016. **3**: p. 16017.

95. Mackenzie, T.C., et al., *Efficient Transduction of Liver and Muscle after in Utero Injection of Lentiviral Vectors with Different Pseudotypes.* Molecular Therapy, 2002. **6**(3): p. 349-358.

96. Witting, S.R., P. Vallanda, and A.L. Gamble, *Characterization of a third generation lentiviral vector pseudotyped with Nipah virus envelope proteins for endothelial cell transduction.* Gene Therapy, 2013. **20**(10): p. 997-1005.

97. Qian, Z., et al., *Targeting Vascular Injury Using Hantavirus-Pseudotyped Lentiviral Vectors.* Molecular Therapy, 2006. **13**(4): p. 694-704.

98. Marodon, G., et al., *Specific transgene expression in human and mouse CD4+cells using lentiviral vectors with regulatory sequences from theCD4 gene.* Blood, 2003. **101**(9): p. 3416-3423.

99. Nicklin, S.A., et al., *Analysis of Cell-Specific Promoters for Viral Gene Therapy Targeted at the Vascular Endothelium.* Hypertension, 2001. **38**(1): p. 65-70.

100. Gory, S., et al., *The Vascular Endothelial-Cadherin Promoter Directs Endothelial-Specific Expression in Transgenic Mice.* Blood, 1999. **93**(1): p. 184-192.

101. Yang, G., et al., *Development of Endothelial-Specific Single Inducible Lentiviral Vectors for Genetic Engineering of Endothelial Progenitor Cells.* Scientific Reports, 2015. **5**(1): p. 17166.

102. Vigna, E., et al., *Robust and efficient regulation of transgene expression in vivo by improved tetracycline-dependent lentiviral vectors.* Mol Ther, 2002. **5**(3): p. 252-61.

103. Stahlhut, M., et al., *Comparison of Tetracycline-regulated Promoters in Lentiviral-based Vectors in Murine Transplantation Studies.* Curr Gene Ther, 2016. **16**(4): p. 242-248.

104. Hacein-Bey-Abina, S., et al., *Insertional oncogenesis in 4 patients after retrovirus-mediated gene therapy of SCID-X1.* J Clin Invest, 2008. **118**(9): p. 3132-42.

105. Emery, D.W., *The use of chromatin insulators to improve the expression and safety of integrating gene transfer vectors.* Hum Gene Ther, 2011. **22**(6): p. 761-74.

106. Dunn, L., et al., *Murine model of wound healing.* J Vis Exp, 2013(75): p. e50265.

107. Song, Q., et al., *Hyperglycemia attenuates angiogenic capability of survivin in endothelial cells.* Microvasc Res, 2009. **78**(3): p. 257-64.

108. Taniguchi, C.M., et al., *Cross-talk between hypoxia and insulin signaling through Phd3 regulates hepatic glucose and lipid metabolism and ameliorates diabetes.* Nature Medicine, 2013. **19**(10): p. 1325-1330.

109. Zlacká, J., et al., *Synthesis of Glycolysis Inhibitor PFK15 and Its Synergistic Action with an Approved Multikinase Antiangiogenic Drug on Human Endothelial Cell Migration and Proliferation.* International Journal of Molecular Sciences, 2022. **23**(22): p. 14295.

110. Assmann, G. and A.M. Gotto, *HDL Cholesterol and Protective Factors in Atherosclerosis.* 2004. **109**: p. 8-14.

111. Theofilatos, D., et al., *HDL-apoA-I induces the expression of angiopoietin like 4 (ANGPTL4) in endothelial cells via a PI3K/AKT/FOXO1 signaling pathway.* Metabolism - Clinical and Experimental, 2018. **87**: p. 36-47.

112. Connaughton, S., et al., *Regulation of pyruvate dehydrogenase kinase isoform 4 (PDK4) gene expression by glucocorticoids and insulin.* Molecular and Cellular Endocrinology, 2010. **315**(1-2): p. 159-167.

113. Jeoung, N.H. and R.A. Harris, *Role of pyruvate dehydrogenase kinase 4 in regulation of blood glucose levels.* Korean Diabetes J, 2010. **34**(5): p. 274-83.

114. Lee, I.K., *The role of pyruvate dehydrogenase kinase in diabetes and obesity.* Diabetes Metab J, 2014. **38**(3): p. 181-6.

115. Xie, Y., et al., *Farnesoid X receptor activation promotes cell proliferation via PDK4-controlled metabolic reprogramming.* 2016. **6**: p. 18751.

116. Kim, Y.I., et al., *Insulin Regulation of Skeletal Muscle PDK4 mRNA Expression Is Impaired in Acute Insulin-Resistant States.* Diabetes, 2006. **55**(8): p. 2311-2317.

117. Sas, K.M., et al., *Tissue-specific metabolic reprogramming drives nutrient flux in diabetic complications.* JCI Insight, 2016. **1**(15).

118. Gopal, K., et al., *FoxO1 regulates myocardial glucose oxidation rates via transcriptional control of pyruvate dehydrogenase kinase 4 expression.* American Journal of Physiology-Heart and Circulatory Physiology, 2017. **313**(3): p. H479-H490.

119. Wong, B.W., et al., *Endothelial cell metabolism in health and disease: impact of hypoxia.* EMBO J, 2017. **36**(15): p. 2187-2203.

120. Dyar, K.A., et al., *Muscle insulin sensitivity and glucose metabolism are controlled by the intrinsic muscle clock.* Mol Metab, 2014. **3**(1): p. 29-41.

121. Tabet, F. and K.A. Rye, *High-density lipoproteins, inflammation and oxidative stress.* Clin Sci (Lond), 2009. **116**(2): p. 87-98.

122. Milone, M.C. and U. O'Doherty, *Clinical use of lentiviral vectors.* Leukemia, 2018. **32**(7): p. 1529-1541.

123. Connaughton, S., et al., *Regulation of pyruvate dehydrogenase kinase isoform 4 (PDK4) gene expression by glucocorticoids and insulin.* Mol Cell Endocrinol, 2010. **315**(1-2): p. 159-67.

124. Costello, A., et al., *Leaky Expression of the TET-On System Hinders Control of Endogenous miRNA Abundance.* 2019. **14**(3): p. 1800219.

125. Baynes, J.W. and S.R. Thorpe, *Role of oxidative stress in diabetic complications: A new perspective on an old paradigm.* Diabetes, 1999. **48**: p. 1-9.

126. Cohen, R.A. and X. Tong, *Vascular oxidative stress: the common link in hypertensive and diabetic vascular disease.* J Cardiovasc. Pharmacol., 2010. **55**(1): p. 308-316.

127. Domingueti, C.P., et al., *Diabetes mellitus: The linkage between oxidative stress, inflammation, hypercoagulability and vascular complications.* J Diabetes Complications, 2016. **30**(4): p. 738-45.

128. Suc, I., et al., *HDL and ApoA prevent cell death of endothelial cells induced by oxidized LDL.* Arterioscler Thromb Vasc Biol, 1997. **17**(10): p. 2158-66.

129. Kontush, A., S. Chantepie, and M.J. Chapman, *Small, Dense HDL Particles Exert Potent Protection of Atherogenic LDL Against Oxidative Stress.* Arteriosclerosis, Thrombosis, and Vascular Biology, 2003. **23**(10): p. 1881-1888.

130. Shao, B., et al., *Myeloperoxidase: an oxidative pathway for generating dysfunctional high-density lipoprotein.* Chem Res Toxicol, 2010. **23**(3): p. 447-54.

131. Zhou, Y., C. Lei, and Z. Zhu, *A low-background Tet-On system based on post-transcriptional regulation using Csy4.* PLOS ONE, 2020. **15**(12): p. e0244732.

132. Pham, D.H., et al., *Attenuation of leakiness in doxycycline-inducible expression via incorporation of 3′ AU-rich mRNA destabilizing elements.* BioTechniques, 2008. **45**(2): p. 155-162.

133. Zhou, X., et al., *Optimization of the Tet-On system for regulated gene expression through viral evolution.* Gene Therapy, 2006. **13**(19): p. 1382-1390.

134. Wittmann, C. and E. Heinzle, *Mass spectrometry for metabolic flux analysis.* Biotechnol Bioeng, 1999. **62**(6): p. 739-750.

135. Wittmann, C., *Metabolic Flux Analysis Using Mass Spectrometry*. 2002, Springer Berlin Heidelberg. p. 39-64.

136. Suriano, F., et al., *Novel insights into the genetically obese (ob/ob) and diabetic (db/db) mice: two sides of the same coin.* Microbiome, 2021. **9**(1).

137. Nguyen Dinh Cat, A., et al., *Vascular dysfunction in obese diabetic db/db mice involves the interplay between aldosterone/mineralocorticoid receptor and Rho kinase signaling.* Sci Rep, 2018. **8**(1): p. 2952.

138. Katare, R., et al., *Progressive Decrease in Coronary Vascular Function Associated With Type 2 Diabetic Heart Disease.* 2018. **9**.

139. Lemmey, H.A.L., et al., *Hyperglycaemia disrupts conducted vasodilation in the resistance vasculature of db/db mice.* Vascular Pharmacology, 2018. **103-105**: p. 29-35.